

## Enclosure 3

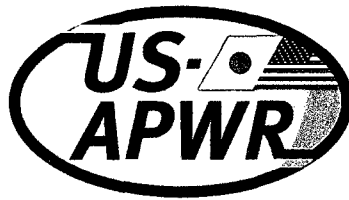
MHI Topical Report: MUAP-07009-NP, Rev.0

### **Thermal Design Methodology**

May 2007  
(Non-Proprietary Version)

This is a non-proprietary version of MHI Topical Report, MUAP-07009-NP, Rev.0, with all proprietary information removed.

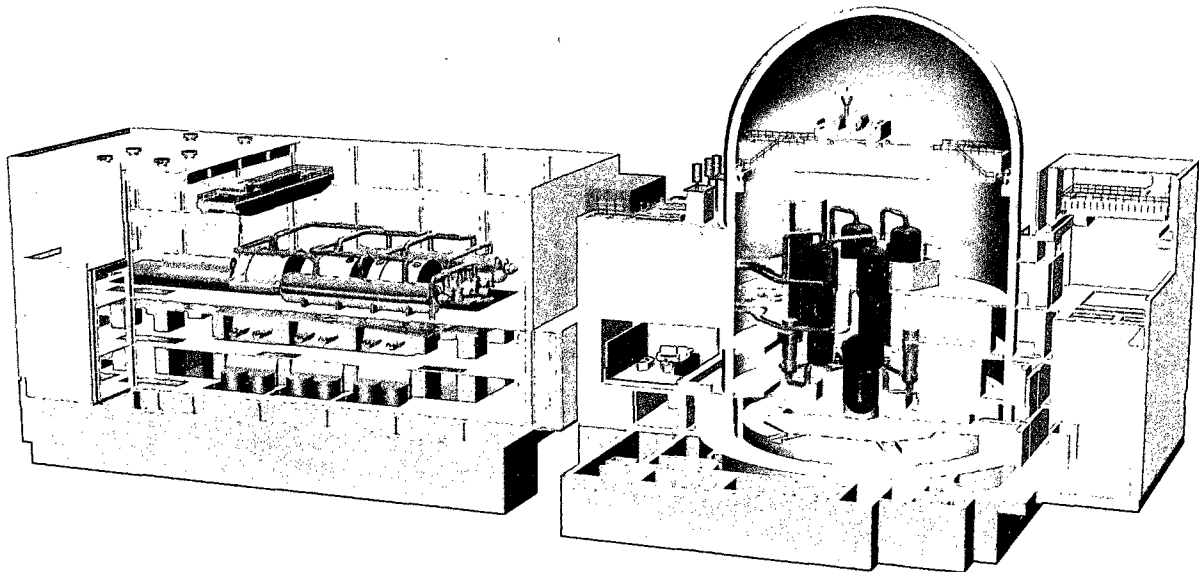
Portions of the report where proprietary information has been removed are identified by the designation "[ ]".



Non-Proprietary

# US-APWR Topical Report

## Thermal Design Methodology



Doc. Number :  
MUAP-07009-NP R0

May 2007



**MITSUBISHI HEAVY INDUSTRIES, LTD.**

©2007  
Mitsubishi Heavy Industries, Ltd.  
All Rights Reserved

# **THERMAL DESIGN METHODOLOGY**

**Non-Proprietary Version**

**May 2007**

**© 2007 Mitsubishi Heavy Industries, Ltd.  
All Rights Reserved**

**Revision History**

Revision	Page	Description
0	All	Original issued

© 2007  
MITSUBISHI HEAVY INDUSTRIES, LTD.  
All Rights Reserved

This document has been prepared by Mitsubishi Heavy Industries, Ltd. (MHI) in connection with MHI's request to the U.S. Nuclear Regulatory Commission (NRC) for a pre-application review of the US-APWR nuclear power plant design. This document contains MHI's technical information and intellectual property and it is delivered on the express condition that it not be disclosed, copied or reproduced in whole or in part, or used for the benefit of anyone other than MHI without the written permission of MHI, except for the purpose for which it is delivered.

This document is protected by the copyright laws of Japan and the U.S., international treaties and conventions as well as the applicable laws of any country where it is used.

Mitsubishi Heavy Industries, Ltd.  
16-5, Konan 2-chome, Minato-ku  
Tokyo 108-8215 Japan

**ABSTRACT**

This topical report is prepared for review by the United States Nuclear Regulatory Commission (NRC) of the Mitsubishi thermal-hydraulic design code, VIPRE-01M, and its design applicability to Light Water Pressurized Water Reactor cores.

VIPRE-01M is an MHI version of the VIPRE-01 code. VIPRE-01 was developed by Electric Power research Institute (EPRI) and has been generically approved by NRC for PWR licensing applications. MHI has added specific DNB correlations and implemented some minor modifications that enable enhanced design application flexibility to the code. MHI demonstrates VIPRE-01M's applicability to PWR cores via sensitivity studies, comparison with other qualified codes, and calculation of measured to predicted heat flux ratio (M/P) of published DNB tests.

With DNB test data, MHI also demonstrates VIPRE-01M's applicability to PWR cores in which MHI-designed fuel assemblies are used.

## Table of Contents

List of Tables	iv
List of Figures	v
List of Acronyms	viii
<b>1.0 INTRODUCTION</b>	<b>1-1</b>
<b>2.0 DESCRIPTION OF THERMAL DESIGN METHODOLOGY</b>	
2.1 Design Basis	2-1
2.2 Thermal Design Methodology	2-1
<b>3.0 VIPRE-01M DESCRIPTION</b>	
3.1 VIPRE-01M Features	3-1
3.2 Compliance with VIPRE-01 SER	3-2
<b>4.0 CORE MODELING</b>	
4.1 Nodalization	4-1
4.2 Turbulent Mixing	4-2
4.3 Hydraulic Resistance	4-3
4.4 Two-Phase Flow Model	4-4
4.5 Engineering Factors	4-4
4.6 Core Inlet Flow Distribution	4-5
4.7 Boundary Conditions	4-5
4.8 Calculation Control Parameters	4-5
<b>5.0 DNB CORRELATIONS</b>	
5.1 DNB Correlations for Design Analysis	5-1
5.2 Qualification of DNB Correlations with VIPRE-01M	5-1
5.3 Applicability of DNB Correlations for Mitsubishi Fuels	5-1
<b>6.0 TRANSIENT FUEL ROD MODELING</b>	
6.1 Nodalization	6-1
6.2 Thermal Properties	6-1
6.3 Power Distribution	6-1
6.4 Gap Conductance	6-1
6.5 Heat Transfer Coefficient	6-2
6.6 Zr-Water Reaction	6-2
<b>7.0 QUALIFICATION FOR DESIGN APPLICATION</b>	
7.1 Steady State Analysis	7-1
7.1.1 Thermal-Hydraulic Characteristics	7-1
7.1.2 DNBR	7-1
7.2 Transient Analysis	7-1
7.2.1 Initial Rod Temperature	7-1
7.2.2 Heat Flux and DNBR	7-2
7.2.3 Peak Cladding Temperature	7-2
<b>8.0 CONCLUSION</b>	<b>8-1</b>
<b>9.0 REFERENCES</b>	<b>9-1</b>

**APPENDIX A: SENSITIVITY STUDIES**

**APPENDIX B: QUALIFICATION OF WRB-1/2 CORRELATIONS WITH VIPRE-01M**

**APPENDIX C: APPLICABILITY OF WRB-1/2 CORRELATIONS FOR MITSUBISHI  
FUELS**

**APPENDIX D: FUEL THERMAL PROPERTIES**

## List of Tables

Table 5-1	Statistical Results of DNB Test Analyses using WRB-1 Correlation	5-2
Table 5-2	Statistical Results of DNB Test Analyses using WRB-2 Correlation	5-2
Table 5-3	Statistical Results of Z2 DNB Test Analyses using WRB-1 Correlation	5-3
Table 5-4	Statistical Results of Z3 DNB Test Analyses using WRB-1 Correlation	5-3
Table 5-5	Statistical Results of Z2 DNB Test Analyses using WRB-2 Correlation	5-3
Table 5-6	Statistical Results of Z3 DNB Test Analyses using WRB-2 Correlation	5-3
Table 7-1	Analyzed Cases and Results of Benchmarking with THINC-IV	7-4
Table 7-2	DNBR Results of Transient and Steady State Analyses	7-4
Table A.1-1	Sensitivity Study on Radial Nodalization	A-1
Table A.1-2	Sensitivity Study on Axial Nodalization	A-2
Table A.2-1	Sensitivity Study on Turbulent Mixing Parameter ABETA	A-10
Table A.3-1	Sensitivity Study on Axial Friction Factor	A-13
Table A.3-2	Sensitivity Study on Radial Loss Coefficient	A-13
Table A.5-1	Sensitivity Study on Core Inlet Flow Distribution	A-15
Table A.6-1	Sensitivity Study on Time Step Size	A-18
Table B.3-1	Data Base for WRB-1/VIPRE-01M Analyses	B-3
Table B.3-2	Data Base for WRB-2/VIPRE-01M Analyses	B-3
Table B.3-3	Data Analyses for WRB-1 Data Base	B-8
Table B.3-4	Data Analyses for WRB-2 Data Base	B-8
Table B.3-5	Statistical Procedure for Limit DNBR based on WRB-1 Data Base	B-9
Table B.3-6	Statistical Procedure for Limit DNBR based on WRB-2 Data Base	B-9
Table C.2-1	DNB Test Section Geometry	C-1
Table C.3-1	M/P Statistical Result for Z2 based on WRB-1/VIPRE-01M	C-9
Table C.3-2	M/P Statistical Result for Z3 based on WRB-1/VIPRE-01M	C-9
Table C.3-3	M/P Statistical Result for Z2 based on WRB-2/VIPRE-01M	C-9
Table C.3-4	M/P Statistical Result for Z3 based on WRB-2/VIPRE-01M	C-9
Table C.3-5	Statistical Procedure for Z2 Limit DNBR based on WRB-1	C-10
Table C.3-6	Statistical Procedure for Z3 Limit DNBR based on WRB-1	C-10
Table C.3-7	Statistical Procedure for Z2 Limit DNBR based on WRB-2	C-11
Table C.3-8	Statistical Procedure for Z3 Limit DNBR based on WRB-2	C-11
Table C-(a)-1	Z2-1 DNB DATA BASE (WRB-1/VIPRE-01M)	C-30
Table C-(a)-2	Z2-1 DNB DATA BASE (WRB-2/VIPRE-01M)	C-32
Table C-(b)-1	Z2-2 DNB DATA BASE (WRB-1/VIPRE-01M)	C-34
Table C-(b)-2	Z2-2 DNB DATA BASE (WRB-2/VIPRE-01M)	C-36
Table C-(c)-1	Z3-1 DNB DATA BASE (WRB-1/VIPRE-01M)	C-38
Table C-(c)-2	Z3-1 DNB DATA BASE (WRB-2/VIPRE-01M)	C-40
Table C-(d)-1	Z3-2 DNB DATA BASE (WRB-1/VIPRE-01M)	C-42
Table C-(d)-2	Z3-2 DNB DATA BASE (WRB-2/VIPRE-01M)	C-44



## List of Figures

Figure 2-1	Framework of Thermal Design Methodology	2-3
Figure 4-1	Typical Modeling for VIPRE-01M 1/8 Core Analysis (17x17-257FA Core, 4-Loop Plant)	4-7
Figure 5-1	Mitsubishi Grid Spacers, Z2 and Z3	5-4
Figure 7-1	Comparison between VIPRE-01M and THINC-IV (Case-1 Typical Cell)	7-5
Figure 7-2	Comparison between VIPRE-01M and THINC-IV (Case-1 Thimble Cell)	7-6
Figure 7-3	Comparison between VIPRE-01M and THINC-IV (Case-2 Typical Cell)	7-7
Figure 7-4	Comparison between VIPRE-01M and THINC-IV (Case-2 Thimble Cell)	7-8
Figure 7-5	Comparison between VIPRE-01M and THINC-IV (Case-3 Typical Cell)	7-9
Figure 7-6	Comparison between VIPRE-01M and THINC-IV (Case-3 Thimble Cell)	7-10
Figure 7-7	Comparison between VIPRE-01M and THINC-IV (Case-4 Typical Cell)	7-11
Figure 7-8	Comparison between VIPRE-01M and THINC-IV (Case-4 Thimble Cell)	7-12
Figure 7-9	Comparison between VIPRE-01M and THINC-IV (Case-5 Typical Cell)	7-13
Figure 7-10	Comparison between VIPRE-01M and THINC-IV (Case-5 Thimble Cell)	7-14
Figure 7-11	Comparison between VIPRE-01M and THINC-IV (Case-6 Typical Cell)	7-15
Figure 7-12	Comparison between VIPRE-01M and THINC-IV (Case-6 Thimble Cell)	7-16
Figure 7-13	Comparison between VIPRE-01M and THINC-IV (Case-7 Typical Cell)	7-17
Figure 7-14	Comparison between VIPRE-01M and THINC-IV (Case-7 Thimble Cell)	7-18
Figure 7-15	Comparison between VIPRE-01M and THINC-IV (Case-8 Typical Cell)	7-19
Figure 7-16	Comparison between VIPRE-01M and THINC-IV (Case-8 Thimble Cell)	7-20
Figure 7-17	Comparison of Fuel Temperature between VIPRE-01M and FINE (14x14 fuel - BOL)	7-21
Figure 7-18	Comparison of Fuel Temperature between VIPRE-01M and FINE (14x14 fuel - EOL (71GWd/t))	7-22
Figure 7-19	Comparison of Fuel Temperature Distribution between VIPRE-01M and FINE	7-23
Figure 7-20	System Transient Conditions for Loss of Flow Analysis	7-24
Figure 7-21	Comparison of the DNBR Analysis Results between VIPRE-01M and FACTRAN/THINC-III	7-25
Figure 7-22	System Transient Conditions for Locked Rotor Analysis	7-26

Figure 7-23 Comparison of Peak Cladding Temperature Analysis between VIPRE-01M and FACTRAN	7-27
Figure A.1-1 Sensitivity Study Cases for Radial Nodalization	A-3
Figure A.1-2 Sensitivity Study on Radial Nodalization (Over Power Condition, Typical Cell)	A-4
Figure A.1-3 Sensitivity Study on Radial Nodalization (Over Power Condition, Thimble Cell)	A-5
Figure A.1-4 Sensitivity Study Cases for Axial Nodalization	A-6
Figure A.1-5 Sensitivity Study on Axial Nodalization (Over Power Condition, Typical Cell)	A-7
Figure A.1-6 Sensitivity Study on Axial Nodalization (Over Power Condition, Thimble Cell)	A-8
Figure A.1-7 Sensitivity Study on Axial Nodalization (DNBR)	A-9
Figure A.2-1 Sensitivity Study on Turbulent Mixing Parameter ABETA (Over Power Condition, Typical Cell)	A-11
Figure A.2-2 Sensitivity Study on Turbulent Mixing Parameter ABETA (Over Power Condition, Thimble Cell)	A-12
Figure A.5-1 Sensitivity Study on Hot Assembly Inlet Flow (Over Power Condition, Typical cell)	A-16
Figure A.5-2 Sensitivity Study on Hot Assembly Inlet Flow (Over Power Condition, Thimble cell)	A-17
Figure B.3-1 VIPRE-01M Modeling for 5x5 Test Geometries	B-5
Figure B.3-2 VIPRE-01M Modeling for 4x4 Test Geometries	B-6
Figure B.3-3 Measured vs. Predicted DNB Heat Flux based on WRB-1/VIPRE-01M	B-10
Figure B.3-4 M/P vs. Local Mass Flux based on WRB-1/VIPRE-01M	B-11
Figure B.3-5 M/P vs. System Pressure based on WRB-1/VIPRE-01M	B-12
Figure B.3-6 M/P vs. Local Quality based on WRB-1/VIPRE-01M	B-13
Figure B.3-7 Measured vs. Predicted DNB Heat Flux based on WRB-2/VIPRE-01M	B-14
Figure B.3-8 M/P vs. Local Mass Flux based on WRB-2/VIPRE-01M	B-15
Figure B.3-9 M/P vs. System Pressure based on WRB-2/VIPRE-01M	B-16
Figure B.3-10 M/P vs. Local Quality based on WRB-2/VIPRE-01M	B-17
Figure C.2-1 Radial Geometry and Power Distribution for Z2-1	C-2
Figure C.2-2 Radial Geometry and Power Distribution for Z2-2	C-2
Figure C.2-3 Radial Geometry and Power Distribution for Z3-1	C-3
Figure C.2-4 Radial Geometry and Power Distribution for Z3-2	C-3
Figure C.2-5 Axial Geometry for Z2-1	C-4
Figure C.2-6 Axial Geometry for Z2-2	C-5
Figure C.2-7 Axial Geometry for Z3-1	C-6
Figure C.2-8 Axial Geometry for Z3-2	C-7
Figure C.3-1 Measured vs. Predicted DNB Heat Flux for Z2 based on WRB-1/VIPRE-01M	C-13
Figure C.3-2 Measured vs. Predicted DNB Heat Flux for Z3 based on WRB-1/VIPRE-01M	C-14
Figure C.3-3 M/P vs. Local Mass Flux for Z2 based on WRB-1/VIPRE-01M	C-15
Figure C.3-4 M/P vs. Local Mass Flux for Z3 based on WRB-1/VIPRE-01M	C-16

---

Figure C.3-5 M/P vs. System Pressure for Z2 based on WRB-1/VIPRE-01M	C-17
Figure C.3-6 M/P vs. System Pressure for Z3 based on WRB-1/VIPRE-01M	C-18
Figure C.3-7 M/P vs. Local Quality for Z2 based on WRB-1/VIPRE-01M	C-19
Figure C.3-8 M/P vs. Local Quality for Z3 based on WRB-1/VIPRE-01M	C-20
Figure C.3-9 Measured vs. Predicted DNB Heat Flux for Z2 based on WRB-2/VIPRE-01M	C-21
Figure C.3-10 Measured vs. Predicted DNB Heat Flux for Z3 based on WRB-2/VIPRE-01M	C-22
Figure C.3-11 M/P vs. Local Mass Flux for Z2 based on WRB-2/VIPRE-01M	C-23
Figure C.3-12 M/P vs. Local Mass Flux for Z3 based on WRB-2/VIPRE-01M	C-24
Figure C.3-13 M/P vs. System Pressure for Z2 based on WRB-2/VIPRE-01M	C-25
Figure C.3-14 M/P vs. System Pressure for Z3 based on WRB-2/VIPRE-01M	C-26
Figure C.3-15 M/P vs. Local Quality for Z2 based on WRB-2/VIPRE-01M	C-27
Figure C.3-16 M/P vs. Local Quality for Z3 based on WRB-2/VIPRE-01M	C-28
Figure D.2-1 Thermal Conductivity of $\text{UO}_2$ Fuel	D-3
Figure D.2-2 Specific Heat of $\text{UO}_2$ Fuel	D-3
Figure D.3-1 Thermal Conductivity of Zircaloy-4	D-6
Figure D.3-2 Specific Heat of Zircaloy-4 and ZIRLO™	D-6
Figure D.4-1 Thermal Conductivity of $\text{ZrO}_2$	D-9
Figure D.4-2 Specific Heat of $\text{ZrO}_2$	D-9

## **List of Acronyms**

ANS	American Nuclear Society
AOO	Anticipated Operational Occurrence
APWR	Advanced Pressurized Water Reactor
BOL	Beginning of Life
CHF	Critical Heat Flux
DL	Design Limit (for DNBR)
DNB	Departure from Nucleate Boiling
DNBR	Departure from Nucleate Boiling Ratio
EOL	End of Life
EPRI	Electric Power Research Institute
FA	Fuel Assembly
LOCA	Loss of Coolant Accident
M/P	Measured to Predicted ratio
MHI	Mitsubishi Heavy Industries, Ltd.
NRC	U.S. Nuclear Regulatory Commission
PWR	Pressurized Water Reactor
PCT	Peak Cladding Temperature
QAP	Quality Assurance Program
RTDP	Revised Thermal Design Procedure
SER	Safety Evaluation Report
SL	Safety Analysis Limit (for DNBR)
TDC	Thermal Diffusion Coefficient

## 1.0 INTRODUCTION

The objective of this topical report is to present a comprehensive thermal design methodology utilized by Mitsubishi Heavy Industries, Ltd. (MHI) for analyzing the thermal-hydraulic conditions in the MHI-designed Pressurized Water Reactor cores.

For the PWR core thermal-hydraulic analysis, the major design criterion is, as stated in the next chapter, to prevent a Departure from Nucleate Boiling (DNB) from happening in the core during normal operation and operational transients (former ANS Condition I events) and events of faults of moderate frequency (former ANS Conditions II events) for already-built nuclear power plants, or during Anticipated Operational Occurrence (AOO) events termed in Appendix A to 10 CFR Part 50 (Rev. 1) for new plant design. Departure from Nucleate Boiling Ratio (DNBR) could also be used as a conservative measure for some Condition III events. For certain Condition IV or Postulated Accident (Non-LOCA) transients, a conservative criterion on Peak Cladding Temperature (PCT) is imposed. The PCT criterion will prevent cladding embrittlement from occurring.

This topical report will delineate the overall process used to perform the core thermal-hydraulic analysis and highlight the features of the computer tool, VIPRE-01M, which includes the DNB correlations that will be used for Mitsubishi PWR core design and safety analysis, and the fuel rod model that will have significant impact on the heat flux transient and/or PCT.

Section 2 of the report describes the design bases that are used for the core thermal-hydraulic analyses and the thermal analysis process involved in the Mitsubishi methodology. Section 3 highlights the features of the VIPRE-01M code, which is essentially identical to the EPRI VIPRE-01 [Ref. 1-5] except for the addition of DNB correlations and certain enhancements for more flexible design applications. As indicated in the Section, the VIPRE-01M code complies with the NRC-issued Safety Evaluation Report (SER) of the EPRI VIPRE-01. Section 4 explains how VIPRE-01M will be used to model the reactor core geometry and the selection of noding and time step size. The additional options for constitutive models, such as flow resistance, turbulent mixing factors and subcooled boiling correlation are described. Section 5 elaborates on the DNBR related subjects. Mitsubishi added WRB-1 [Ref.6] and WRB-2 [Ref.7] correlations to the VIPRE-01M code for DNBR calculation purposes. Comprehensive data base is analyzed and presented in the section to demonstrate the compatibility of WRB-1 and WRB-2 with the VIPRE-01M code for Mitsubishi fuel designs.

Transient Fuel Rod Modeling, another key capability of the VIPRE-01M, is discussed in Section 6. Section 7 demonstrates that VIPRE-01M is qualified to be a design code for PWR cores. The section includes examples of design applications and comparisons with other qualified codes such as THINC [Ref.8] for core DNBRs; FINE [Ref.9] for steady state fuel rod analysis; FACTRAN [Ref.10] for transient fuel rod analysis.

---

## 2.0 DESCRIPTION OF THERMAL DESIGN METHODOLOGY

### 2.1 Design Basis

For PWR core thermal design in already-built power plants, the major design criterion for the Conditions I & II events was established to prevent DNB phenomena from happening in the core. The limitation on DNB is expressed in the "DNBR limit value" during safety analyses and is reflected in "Core Thermal Limits" that lead to the setpoints determination such as Over-Temperature  $\Delta T$  and Over-Power  $\Delta T$ .

The design basis for generating the DNBR limit value and core thermal limits is that DNB phenomena will not occur on the most limiting fuel rods with at least a 95% probability at a 95% confidence level during Condition I and Conditions II events.

The same design basis will be required for the AOOs in new nuclear power plant designs. AOOs are defined in Appendix A to 10 CFR Part 50 (Rev. 1) as those conditions of off-normal operation that are expected to occur one or more times during the life of the nuclear power plant. In Regulatory Guide 1.70 and draft Regulatory Guide 1.206, AOOs are referred to as the conditions of the events that are categorized as incidents of moderate frequency and infrequent events, which were also referred to in the former American Nuclear Society (ANS) standards as Condition II and Condition III events, respectively. While Condition I and Condition II are still used for elaboration purposes above, Conditions I through IV definitions are no longer used as safety analysis categorizations in new nuclear power plant designs.

### 2.2 Thermal Design Methodology

Figure 2-1 shows the framework of two cascading flow paths of procedures which the thermal design (or DNB design) analysis follows.

DNBR is defined as the ratio of DNB heat flux,  $q''_{DNB}$ , and actual local heat flux,  $q''_{local}$ .

$$DNBR = \frac{q''_{DNB}}{q''_{local}}$$

"Min. DNBR" is the minimum value of the DNBRs determined in the core.

DNB heat flux is predicted by the adopted DNB correlation as the function of local coolant conditions and fuel geometry such as equivalent diameter of hydraulic channel, rod diameter, grid locations and so on. Mitsubishi uses either the WRB-1 or WRB-2 correlation for the core thermal designs of different fuel grids and features.

The local thermal-hydraulic parameters that are needed by the DNB correlations are generated by VIPRE-01M, the Mitsubishi subchannel analysis code. VIPRE-01 (EPRI version) is a subchannel analysis code that has been reviewed and approved by the NRC. An SER has been issued in 1986 [Ref. 1]. The WRB-1 and WRB-2 correlations are NRC-approved DNB correlations that are applicable to Westinghouse-like fuel bundles. Detailed discussions of VIPRE-01M and the compatibility between VIPRE-01M and WRB-1/WRB-2, as well as their applicability to the Mitsubishi fuel designs, are described in Sections 5 and 7.

The left path of the framework in Figure 2-1 shows the process to derive the limiting DNBR in accordance with the above-mentioned design basis. The Revised Thermal Design Procedure (RTDP) [Ref. 11] is used for deriving the Design Limit DNBR. RTDP is a Westinghouse-developed statistical thermal design procedure. It has been approved by the NRC in 1989 [Ref. 12]. The application of the RTDP will follow the guidelines prescribed in the SER issued by NRC.

The Design Limit (DL) of DNBR is obtained by considering the uncertainties of certain major input parameters and the uncertainty of the selected DNB correlation on a 95% probability at 95% confidence level basis.

The Safety Analysis Limit (SL) of DNBR is determined after accommodating the DNBR penalties incurred by rod bows, transition core geometry and/or reserving more core operational flexibilities.

The right path of the framework in Figure 2-1 shows the process of deriving the Min. DNBR of the most limiting fuel rods.

For the Min. DNBR analysis, parameters of which uncertainties are considered in the DL determination in the RTDP are input to VIPRE-01M as nominal values. The nominal DNBR value, obtained through such process, should be greater than the SL that is determined for each specific core.

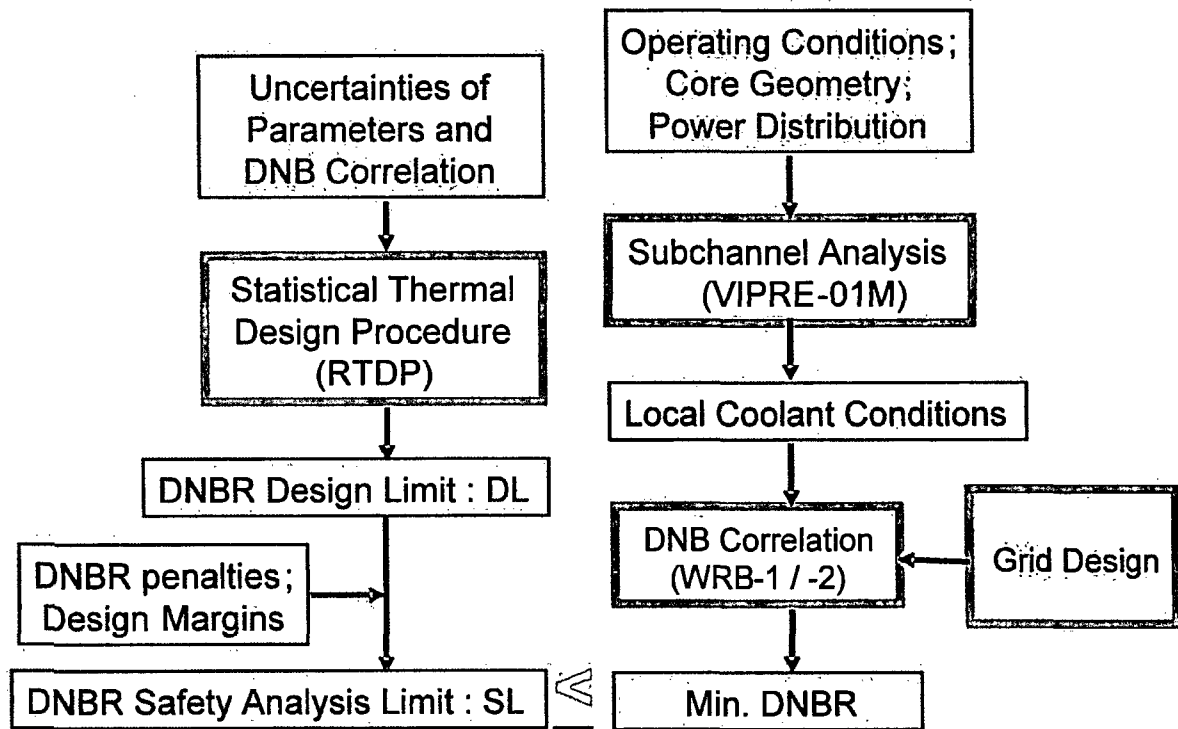


Figure 2-1 Framework of Thermal Design Methodology



### 3.0 VIPRE-01M DESCRIPTION

#### 3.1 VIPRE-01M Features

VIPRE-01M is the Mitsubishi version of VIPRE-01, which is a subchannel analysis code developed to perform thermal-hydraulic analyses in reactor cores. Using the original VIPRE-01 code as the basis, Mitsubishi incorporates certain added functions for more flexible design applications. VIPRE-01M is used to evaluate reactor core thermal limits related to the Min. DNBR, reactor core coolant conditions, and fuel temperature and heat flux in normal and off-normal conditions.

The original version of VIPRE-01 was developed by Battelle Pacific Northwest Laboratories, under the sponsorship of Electric Power Research Institute (EPRI). Its basic components are from the well-known COBRA code series [Ref. 12-15]. VIPRE-01 divides the reactor core into a number of flow channels. The size of each flow channel could be as small as the flow area surrounded by four rods (fuel rods and/or control rod guide thimble) situated on a square lattice, or be formed by a number of fuel rod bundles. Conservation equations of mass, momentum (in axial and lateral directions), and energy are solved to determine axial mass flux distributions, lateral flow rate per unit length, and enthalpy distributions. Fluid properties are functions of the local enthalpy and a uniform but time-varying system pressure. Transient thermal behavior of the fuel rod is also analyzed in association with the determined thermal-hydraulic analysis results.

Specific constitutive models which prescribe optional flow resistance, turbulent mixing, and subcooled as well as saturated boiling, are selected in VIPRE-01M analyses to provide adequate results for the purposes of the applications.

VIPRE-01M has incorporated the following features into the original VIPRE-01.

(1) DNB correlations for design applications

WRB-1 and WRB-2 are incorporated into the VIPRE-01M code for the purpose of design analysis of Mitsubishi fuel core. Regarding W-3 correlation [Ref. 16], some options were added to allow its use without spacer factor for the safety analysis of low pressure events

(2) Fuel thermal properties for design applications

Fuel thermal properties used in the Mitsubishi fuel performance code and safety analysis codes are introduced. They accommodate the degradation effect of thermal conductivity of  $\text{UO}_2$  with burnup.

(3) Options for hot spot PCT analysis

The VIPRE-01M code may be used for hot spot PCT analysis for condition III or condition IV events (Non-LOCA), as the replacement of the FACTRAN code. For this purpose, new options for forced film boiling at the hot spot and the Zr-Water reaction model involving the heat generation within fuel cladding are added in VIPRE-01M.

#### (4) More user-friendly interfaces

To be more user-friendly and have better Quality Assurance, the following optimized code interfaces with the user are implemented in VIPRE-01M:

- Free format input style like NAMELIST has been introduced for user's convenience and reducing input errors.
- Dynamic memory allocation has been introduced for the calculation efficiency and reliable administration of executable modules.
- New interface for reading the results of system transient code MARVEL [Ref.17] and printing DNBR and rod temperature summaries have been added.

The modifications mentioned above only add "bells and whistles" to the design applications. The original solution methods and constitutive models are not changed at all. Therefore, the VIPRE-01M code is virtually identical to the original VIPRE-01. The conclusion of verification for the original VIPRE-01 code by EPRI still remains valid.

### 3.2 Compliance with VIPRE-01 SER

The original VIPRE-01 code has been approved generically by the NRC for PWR core design applications [Ref.1]. Several conditions were imposed by the SER if specific applications are desired.

For applications to PWR core analyses, the NRC staff requires that VIPRE-01 be limited to PWR licensing calculations with heat transfer regime up to CHF.

Since the intent of the Mitsubishi applications of the VIPRE-01M is for normal and off-normal core operating conditions (excluding LOCA calculations) with heat transfer regime up to Departure from Nucleate Boiling, the VIPRE-01M is within the bounds specified in the SER. When VIPRE-01M is used to calculate the limiting hot spot PCT, it will be applied in a conservative manner similar to that used in the FACTRAN analysis. The comprehensive analytical method will be presented later in this report.

The SER prescribes that the use of a steady state CHF correlation with VIPRE-01 is acceptable for reactor transient analysis provided that the CHF correlation and its DNBR limit have been reviewed and approved by the NRC and that the application is within the range of applicability of the correlation including fuel assembly geometry, spacer grid design, pressure, coolant mass velocity, quality, etc. Use of any CHF correlation which has not been approved will require the submittal of a separate topical report for staff review and approval. The use of a CHF correlation which has been previously approved for application in connection with another thermal-hydraulic code other than VIPRE-01 will require an analysis showing that, given the correlation data base, VIPRE-01 gives the same or a conservative safety limit, or a new higher DNBR limit must be used, based on the analysis results.

Mitsubishi intends to use WRB-1 and WRB-2 correlations for PWR core DNB analyses. Since both correlations were approved in conjunction with the THINC code by the NRC, Mitsubishi will demonstrate their compatibility with the VIPRE-01M code and their applicability in PWR core design applications per the guidelines prescribed in the SER. All the support documents along with the relevant correlation limits in the PWR core applications are presented in Sections 5 and 7 of this topical report.

The SER emphasizes that "Each organization using VIPRE-01 for licensing calculations should submit separate documentation describing how they intend to use VIPRE-01 and providing justification for their specific modeling assumptions, choice of particular two-phase flow models and correlations, heat transfer correlations, CHF correlation and DNBR limit, input values of plant specific data such as turbulent mixing coefficient, slip ratio, grid loss coefficient, etc., including defaults".

In this topical report, Mitsubishi thoroughly describes the modeling assumptions, choices of constitutive models, and DNB correlation options. Other plant specific input data will be shown in the plant application.

Relevant time step size will be selected to ensure numerical stability and accuracy. Specifically, Courant number will be kept greater than 1, if the profile fit subcooled void model is used, in accordance with the requirement of SER.

SER requires that the user abide by the quality assurance procedures described in Section 2.6 of itself, by which EPRI maintain the program versions certainly. Mitsubishi closely keeps track of the latest program status and code error notification from EPRI per its quality assurance procedures. Mitsubishi will maintain its code version under Mitsubishi's Quality Assurance Program (QAP) [Ref.18] and commits to inform EPRI of any modifications made to the approved version, in accordance with the license agreement with EPRI.

## 4.0 CORE MODELING

VIPRE-01M has a rather efficient way to model the reactor core. The conventional way of modeling the PWR cores by other subchannel analysis codes, such as THINC, is by way of multi-pass or successive stage approaches. Such codes are first set up to determine the core-wide thermal-hydraulic parameters which are subject to the over-all boundary conditions (including the core power level, radial and axial power distributions, reactor pressure, core inlet temperature, and core inlet flow distribution, etc.) imposed on the core. The subchannel code will determine the detailed thermal-hydraulic information for the inter-fuel assembly configuration and for each fuel assembly as a flow channel. The successive stage is then to determine the thermal-hydraulic conditions within the focused fuel assembly, that is, the hot assembly. This subchannel analysis during the successive stage will determine the desired thermal-hydraulic design information such as enthalpy distribution, axial and lateral mass flow rate, local pressure, and the Min. DNBRs associated with the hot assembly.

VIPRE-01M modeling of a PWR core is based on the one-pass modeling approach, which treats hot channels (the subchannels with the highest enthalpy rise) and their immediate surrounding channels in great detail, while the rest of the core is modeled on a relatively coarse mesh. No separate computational stages are required as those used in the conventional approach. By this one-pass modeling approach, a reactor core can be fully modeled in a small number of channels without sacrificing the needed detail and accuracy in and around the hot channels. The VIPRE-01 one-pass modeling approach has been approved by the NRC in application to PWR core DNB analyses.

VIPRE-01M has different model options that users can choose from for various purposes of core analyses. In this section, the standard model options, which are selected for Mitsubishi's thermal design applications, are described. Sensitivity studies have been conducted to verify the relevancy of VIPRE-01M for various design applications. The results of sensitivity studies are described in Appendix A.

### 4.1 Nodalization

#### (1) Radial Nodalization

For a PWR core design assuming radial power distribution and inlet flow distribution symmetric to the core center, a one-eighth core modeling is typically adopted for the subchannel analysis with the hot assembly located at the center of the core.

Using the one-eighth core modeling approach, a representative VIPRE-01M subchannel analysis model for the US-APWR reactor core (a total of 257 17 x 17 fuel assemblies), is shown in Figure 4-1. Hot assembly is located at the center of the core. 10 subchannels are modeled to account for the hot typical cell channel and the hot thimble cell channel as well as the surrounding cells. In core subchannel analyses, only the hot typical cell and the hot thimble cell channels and their surrounding individual subchannels will provide the needed information to the core thermal-hydraulic design. No needed detailed information will be lost over the modeling simplification process that the remaining core flow areas are modeled. The remaining cells in the hot assembly are grouped into 5 surrounding channels. The fuel assemblies in the rest of the one-eighth core can be lumped into 6 large channels. A total of 21 radial flow channels are established.

For the DNB analysis, each rod facing the detailed subchannels is modeled individually, because both of the heat input to the subchannel and the local heat flux should be counted correctly. In the lumped channel, fuel rods are treated as one lumped rod, which has average power of the actual rods in the channel.

EPRI has shown that the detailed radial noding is needed only for the hot channels and the neighboring flow area surrounding them [Ref.5]. Mitsubishi's sensitivity studies reached the same conclusion.

## (2) Axial Nodalization

EPRI stated in its VIPRE-01 report that VIPRE-01 predictions can be affected by the number of axial nodes selected. Not enough axial nodes may end up losing the required details for the flow field [Ref.5].

Sensitivity studies on the number of axial nodes were performed by Mitsubishi. The results indicated that the number of axial meshes does not have significant impact on DNBR analysis if it becomes greater than [ ]. However, increase of elevational discrepancy between cell center and grid location may decrease accuracy.

As mentioned above, the sensitivity on the axial nodalization itself is rather small, however, the larger axial mesh size reduce the Courant number and consequently may end up causing numerical instability when the profile fit type void model is used. Therefore, the axial mesh size smaller than [ ] are recommended for the typical thermal-hydraulic core analysis. It will be further discussed in Section 4.8.

## 4.2 Turbulent Mixing

In VIPRE-01M code, turbulent mixings of energy and momentum are associated with equal mass exchange between adjacent flow channels due to turbulence. It is described by the following equation;

$$E' = w' \Delta h \quad (4.1)$$

$$M' = FTM \cdot w' \Delta u \quad (4.2)$$

where,

- $E'$  : energy transfer rate per unit axial length due to turbulent mixing (Btu/ft-s)
- $M'$  : momentum transfer rate per unit axial length due to turbulent mixing ((lbm-ft/s)/ft-s)
- $w'$  : mass exchange rate per unit axial length (lbm/ft-s)
- $\Delta h$  : enthalpy difference between the adjacent channels (Btu/lbm)
- $\Delta u$  : axial velocity difference between adjacent channels (ft/s)
- $FTM$  : correction factor for difference between turbulent momentum mixing and turbulent energy mixing

The mass exchange rate across rod-to-rod gap,  $w'$ , can be expressed by the following correlation;

$$w' = \left[ \right] \quad (4.3)$$

where,

$ABETA$  : mixing parameter  
 $s$  : flow area between the channels across which turbulent mass exchange occurs (ft<sup>2</sup>/ft)  
 $G$  : axial mass velocity averaged over the channels on both sides of the gap (lbm/ft<sup>2</sup>s)

Mixing parameter,  $ABETA$  is equivalent to the Thermal Diffusion Coefficient (TDC) in the THINC code.  $ABETA$  is defined as a constant, obtained from thermal mixing tests simulating the actual fuel assembly geometries. Since TDC is defined as a mixing coefficient for the turbulent energy transfer rate between two unit subchannels,  $ABETA$ , when applied to lumped channels, should be modified as the following;

$$ABETA = \left[ \right] \quad (4.4)$$

where,

$N_{ch}$  : number of unit subchannel rows between the centers of two lumped channels

While  $ABETA$  is a significant parameter in predicting hot channel conditions, its effect on design DNB analyses is minimized due to the following assumptions:

- Conservative bounding power distribution is used for the hot assembly in design analysis.
- For conservatism reason, turbulent mixing across the fuel assembly boundary is neglected.

[ ]

Sensitivity study results are shown in Appendix A.

### 4.3 Hydraulic Resistance

Axial friction factor for single phase flow,  $f$ , is given by Blasius type equation, which is a function of Reynolds number.

$$f = a_f Re^{b_f} + c_f \quad (4.5)$$

The friction factor is evaluated as the maximum value of turbulent and laminar flow. The coefficients,  $a_f$ ,  $b_f$  and  $c_f$  are as follows.

$$\begin{array}{lll} \text{for turbulent flow} & a_f = \left[ \right] & b_f = \left[ \right] & c_f = \left[ \right] \\ \text{for laminar flow} & a_f = 64.0, & b_f = -1.0, & c_f = 0.0 \end{array} \quad (4.6)$$

This is a well accepted correlation [ ] A sensitivity study shows that the effect of axial friction factor is small for the DNB design analysis.

Heated wall effect on viscosity is not considered, since its effect is very small.

Form loss coefficients for grid spacers and other fuel components are prescribed constants based on flow test data.

Crossflow loss coefficient is given by following equation;

$$K_G = \left( a_G \text{Re}_{XF}^{b_G} + c_G \right) \frac{D_{SC}}{p} \quad (4.7)$$

where  $\text{Re}_{XF}$  is the Reynolds number for crossflow defined with representative dimension of rod diameter,  $D_{SC}$  is a distance between the centers of subchannels and  $p$  is a rod pitch. The constants of  $a_G$ ,  $b_G$  and  $c_G$  are derived [ ] for lateral resistance of square-array rod bundles;

$$a_G = \left[ \begin{array}{c} \\ \\ \end{array} \right] \quad b_G = \left[ \begin{array}{c} \\ \\ \end{array} \right] \quad c_G = \left[ \begin{array}{c} \\ \\ \end{array} \right] \quad (4.8)$$

where  $d_{rod}$  is a rod diameter. The sensitivity study in Appendix A shows that the effect of cross flow resistance is negligible small.

#### 4.4 Two-Phase Flow Model

[ ] is adopted for two-phase flow pressure drop calculations. Under most operating conditions in the PWR analyses, this assumption has been proved adequate.

[ ] is used to evaluate flow quality, which includes local boiling and thermal non-equilibrium effects. The relationship between flow quality and void fraction is provided by [ ] The model generates conservative void fraction predictions similar to those obtained by conventional design codes such as THINC. The overall model conservatism will be discussed in Appendix A and Section 7.

Subcooled void fraction might be affected by crud on the fuel rod surface. While VIPRE-01M code does not have the ability to consider crud for the boiling calculation, [ ]

#### 4.5 Engineering Factors

The enthalpy rise engineering factor  $F_{\Delta H}^E$  represents the hot rod power uncertainty caused by fuel manufacturing tolerance. It includes uncertainties of pellet weight and  $U_{235}$  enrichment.

$F_{\Delta H}^E$  is determined based on the sampling data involved. In the RTDP analysis, it is one of the parameters that are considered in deriving design limit DNBR. When it is considered in the VIPRE-01M analysis, the overall  $F_{\Delta H} (= F_{\Delta H}^N \times F_{\Delta H}^E)$  is reflected in VIPRE-01M input as the radial rod power distribution.

Heat flux engineering factor  $F_O^E$  represents the hot spot surface heat flux uncertainty caused by fuel manufacturing tolerance. [

#### 4.6 Core Inlet Flow Distribution

Existing flow tests showed that there has been some mal-distribution in core inlet flow. The inlet mass velocity of hot assembly could be approximately 5 to 10 % lower than the core inlet mass velocity average. However, inlet flow mal-distribution could be quickly flattened out in the entrance portion of the core, its mal-distribution effect on DNBR is negligible small. The sensitivity study shown in Appendix A concluded that core inlet flow mal-distribution will have no appreciable impact on the core Min. DNBR determination.

#### 4.7 Boundary Conditions

As in all subchannel analysis code applications, the boundary conditions required by the VIPRE-01M analyses are as follows:

- Core power
- Core system pressure
- Core inlet temperature
- Core inlet flow

These parameters are varying with time in transient safety analyses. VIPRE-01M can read the MARVEL-generated transient condition automatically through the established interface file. In addition to the above parameters, VIPRE-01M can read core exit enthalpy (temperature) and core exit pressure distribution. Core exit enthalpy is not used in the safety analysis and core exit pressure distribution is assumed to be uniform.

#### 4.8 Calculation Control Parameters

EPRI pointed out that, in order to ensure the numerical stability of the code, the Courant number should be kept as greater than 1, when the profile fit type void model is used. The time step size for the VIPRE-01M code is thus selected to be;

$$\Delta t > \frac{\Delta x}{u} \quad (4.9)$$

where  $\Delta t$ ,  $\Delta x$ , and  $u$  are time-step size, axial noding size, and axial velocity, respectively.



Since the use of greater time step size may lose the required details for the analysis, sufficiently small time step size and consequently small axial mesh size should be selected to accommodate the Courant number restriction. A sensitivity study on the time step size is conducted as presented in Appendix A. Based on the results, it is considered that [ ] for the time step size is appropriate for typical PWR core calculations. A combination of time step size of [ ] and axial mesh size less than [ ] keeps the Courant number greater than 1 under the condition of [ ] This set of numbers covers the typical PWR thermal-hydraulic analysis conditions.

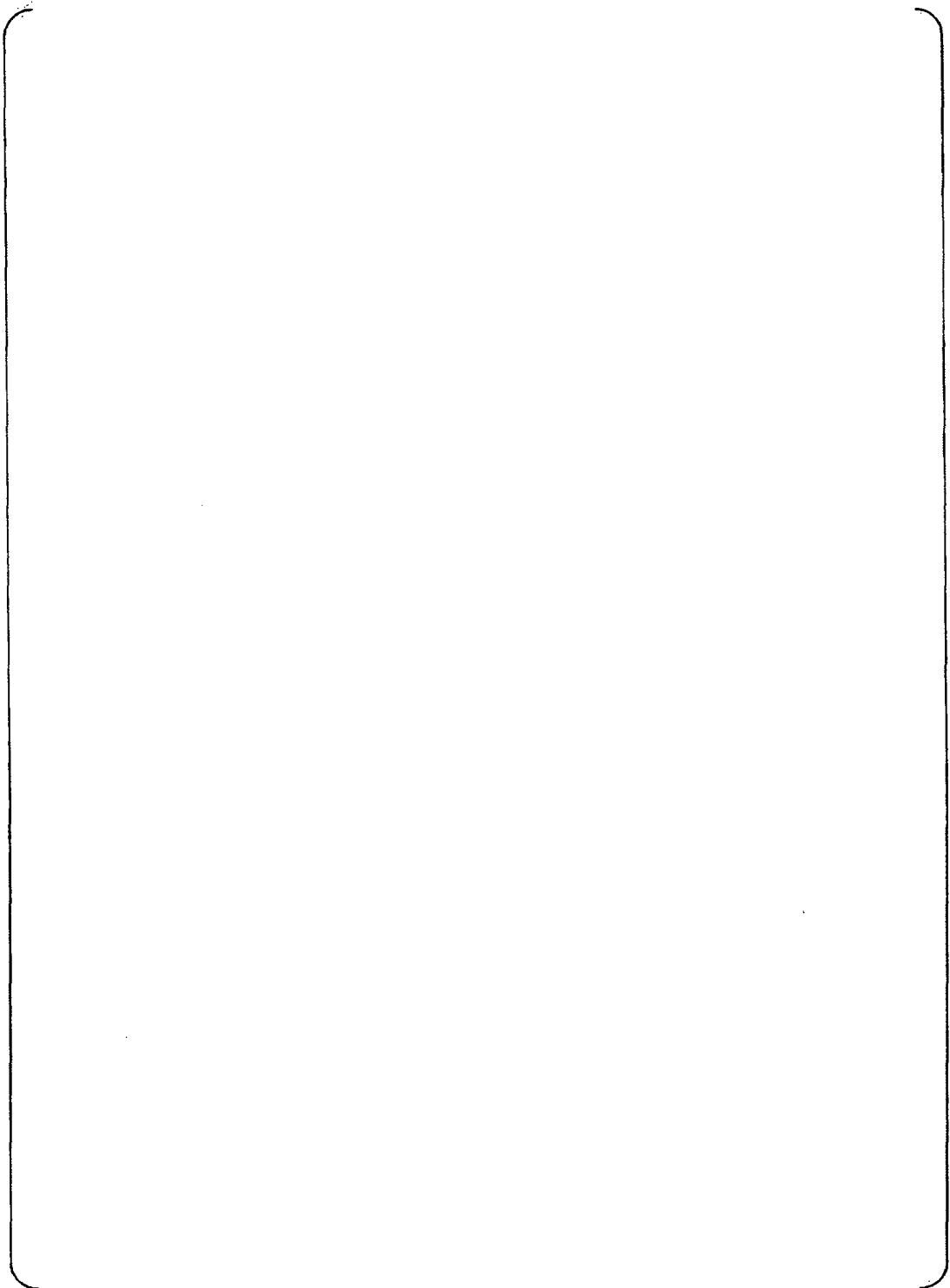


**Figure 4-1 Typical Modeling for VIPRE-01M 1/8 Core Analysis  
(17x17-257FA Core, 4-Loop Plant)**

---

## 5.0 DNB CORRELATIONS

### 5.1 DNB Correlations for Design Analysis

WRB-1 and WRB-2 DNB correlations are incorporated into VIPRE-01M for design calculation purposes. W-3 DNB correlation without spacer factor will be used when the calculated conditions are outside the applicability range of WRB-1 and WRB-2.

WRB-1 is based on the Westinghouse's R-grid and L-grid rod bundle DNB test data, and its verification was made in conjunction with THINC code. This correlation was approved by the NRC in 1984 [Ref.6].

WRB-2 is based on the Westinghouse's DNB test data simulating 17x17 type fuels including OFA and VANTAGE5, and its verification was made in conjunction with THINC code. This correlation was approved by the NRC in 1985 [Ref.7].

W-3 is a generic type of DNB correlation. W-3 without spacer factor is normally used for safety analyses of low pressure events, which are beyond the approved applicability ranges of WRB-1 and WRB-2.

### 5.2 Qualification of DNB Correlations with VIPRE-01M

Studies of WRB-1 and WRB-2 compatibility with VIPRE-01M are presented in Appendix B. The correlations were validated with the existing data bases. Statistical analysis results are summarized in Table 5-1 and Table 5-2. Both correlations give reasonable predictions on DNB heat flux when comparing the VIPRE-01M results with the THINC results [Ref. 6 & 7] for Westinghouse-type fuel assemblies and grid spacers.

Conservative limit DNBR of 1.17 can be achieved on a 95% probability at 95% confidence level basis.

### 5.3 Applicability of DNB Correlations for Mitsubishi Fuels

For the fuel assembly design, Mitsubishi intends to use one of the two recommended grid spacer designs: Z2 or Z3. Figure 5-1 shows the configuration of Mitsubishi grid spacers, Z2 and Z3. DNB tests for Z2 and Z3 were conducted at the Heat Transfer Research Facility of Columbia University. The DNB test analyses for Z2 and Z3 based on WRB-1 and WRB-2 were conducted in Appendix C. It is demonstrated that both WRB-1 and WRB-2 give excellent, while conservative, DNBR predictions for the Z2 and Z3. Statistical results of DNB test analyses are summarized in Table 5-3 through Table 5-6 for various combined sets of correlation and DNB test data. Limit DNBRs by each DNB correlations are determined on the 95% probability at 95% confidence level basis. As a result, it was confirmed that WRB-1 and WRB-2 can be conservatively applied to predict DNB heat flux for fuel assemblies with either Z2 or Z3 grid using limit DNBR 1.17.

**Table 5-1 Statistical Results of DNB Test Analyses using WRB-1 Correlation**

Test case	Data points	Mean of M/P	Standard deviation of M/P
-----------	-------------	-------------	---------------------------

$$\text{Limit } DNBR_{(95 \times 95)} = \left[ \quad \right]$$

**Table 5-2 Statistical Results of DNB Test Analyses using WRB-2 Correlation**

Test case	Data points	Mean of M/P	Standard deviation of M/P
-----------	-------------	-------------	---------------------------

$$\text{Limit } DNBR_{(95 \times 95)} = \left[ \quad \right]$$

**Table 5-3 Statistical Results of Z2 DNB Test Analyses using WRB-1 Correlation**

Test case	Cell type	Data points	Mean of M/P	Standard deviation of M/P
-----------	-----------	-------------	-------------	---------------------------

$$\text{Limit } DNBR_{(95 \times 95)} = \{ \quad \}$$

**Table 5-4 Statistical Results of Z3 DNB Test Analyses using WRB-1 Correlation**

Test case	Cell type	Data points	Mean of M/P	Standard deviation of M/P
-----------	-----------	-------------	-------------	---------------------------

$$\text{Limit } DNBR_{(95 \times 95)} = \{ \quad \}$$

**Table 5-5 Statistical Results of Z2 DNB Test Analyses using WRB-2 Correlation**

Test case	Cell type	Data points	Mean of M/P	Standard deviation of M/P
-----------	-----------	-------------	-------------	---------------------------

$$\text{Limit } DNBR_{(95 \times 95)} = \{ \quad \}$$

**Table 5-6 Statistical Results of Z3 DNB Test Analyses using WRB-2 Correlation**

Test case	Cell type	Data points	Mean of M/P	Standard deviation of M/P
-----------	-----------	-------------	-------------	---------------------------

$$\text{Limit } DNBR_{(95 \times 95)} = \{ \quad \}$$

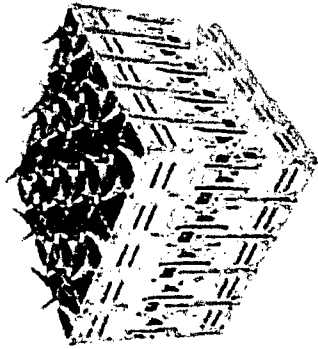
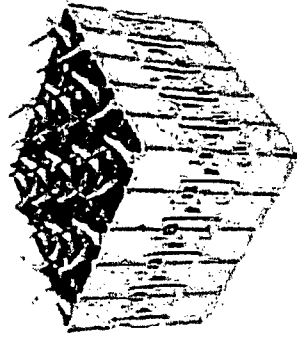
<div>Grid type</div> <div>5 x 5 test grid</div>	<div>Z2</div> <div></div>	<div>Z3</div> <div></div>
<div>Structure of grid strap</div>	<div></div>	<div></div>

Figure 5-1 Mitsubishi Grid Spacers, Z2 and Z3

## 6.0 TRANSIENT FUEL ROD MODELING

### 6.1 Nodalization

In transient analyses, VIPRE-01M fuel rod conduction model is used for predicting the thermal behavior of the fuel rod interior, such as the radial fuel temperature distribution and surface heat flux variation. Fuel pellet, fuel cladding and the gap between them are simulated separately. Fuel pellet is divided into [ ] in the radial direction, which is consistent with the treatment in the fuel design. Initial pellet heat up, in addition to the thermal diffusion coefficient of the fuel, is a predominant factor for fuel's thermal behavior. Therefore, the initial condition is carefully selected and modeled to match the results of the fuel rod design code, FINE.

### 6.2 Thermal Properties

In VIPRE-01M, the adopted thermal properties for the fuel are the same as those used in Mitsubishi's fuel design code, FINE, and/or other safety analysis codes. The properties added by Mitsubishi are shown in Appendix D.

The thermal properties used by Mitsubishi are not much different from those in original VIPRE-01 code, except that the degradation effect of fuel thermal conductivity along with burnup is accounted for.

### 6.3 Power Distribution

Depression of heat generation at the interior of a fuel pellet reduces centerline temperature of pellet. Radial power distribution within pellet is incorporated into the FINE code as a function of burnup and composition of pellet. VIPRE-01M uses power distribution from the FINE code as an input.

### 6.4 Gap Conductance

Fuel pellet temperature is highly dependent on the pellet-to-cladding gap conductance. The gap conductance is affected by the gas composition in the gap, gas pressure and temperature, and pellet densification/swelling and cladding creep-down as the result of burnup. However, since VIPRE-01M does not accommodate those effects, gap conductance needs to be specified [ ]

For transient analyses, the gap conductance is [ ] to give conservative results of the analyses.

## 6.5 Heat Transfer Coefficient

For typical transient analyses of non-LOCA events, pre-DNB modes of rod surface heat transfer is assumed. In such analyses, well-known empirical heat transfer correlations included in the VIPRE-01 model are used.

$$\left[ \right]$$

In some condition-IV (Non-LOCA) analyses for which the PCT analysis at post-DNB condition is required, VIPRE-01M is used just as an alternative to the traditional FACTRAN analysis. In the case, [

originally included in VIPRE-01 code, and Mitsubishi modified it [ ] The correlation is

] The same practices are conducted in the FACTRAN analysis.

## 6.6 Zr-Water Reaction

Baker-Just correlation [Ref.22] is used in PCT analysis to account for the thickness of oxide layer and heat generation at the cladding surface;

$$W^2 = K_1 \exp\left(-\frac{K_2}{R'T}\right) t$$

where,

- $W$  :Amount of Zr reacted (kg/m<sup>2</sup>)
- $K_1$  =33.3x10<sup>2</sup> ((kg/m<sup>2</sup>)<sup>2</sup>/s)
- $K_2$  =45,500 (cal/mol)
- $R'$  :Gas constant =1.987 (cal/mol-K)
- $T$  :Temperature (K)
- $t$  :Time (sec)

This correlation was incorporated into the PCT analysis by Mitsubishi. [

]



## 7.0 QUALIFICATION FOR DESIGN APPLICATION

### 7.1 Steady State Analysis

Several results of the VIPRE-01M analyses have been compared with the THINC-IV results for the purpose of verifying the acceptability of VIPRE-01M for DNB design analysis. The analyses were done for a 17x17(14ft), 257 fuel-assembly core. Several plant conditions were selected to cover the typical DNB analysis domain. The conditions are shown in Table 7-1.

All of the VIPRE-01M models were set up following the descriptions in Section 4.

#### 7.1.1 Thermal-Hydraulic Characteristics

Hot channel mass velocity and equilibrium quality predictions are compared between VIPRE-01M and THINC-IV in Figures 7-1 through 7-16. {

} Relatively small differences in mass velocity distribution are observed between the codes. The differences in mass velocity distribution in the upper core region are mainly caused by the subcooled void models used in each code. {

The flow distribution effect on fluid enthalpy is relatively small. Therefore, the equilibrium qualities are fairly close between the codes.

#### 7.1.2 DNBR

Min. DNBRs in each analysis case are shown in Table 7-1. The differences of Min. DNBR are within{ } VIPRE-01M results are derived with standard{ } and they are more conservative than those of THINC-IV{ } Therefore, it is considered that the modeling of VIPRE-01M is appropriate for DNB design analysis of PWR cores.

### 7.2 Transient Analysis

Fuel rod model capabilities for the safety analysis are verified by comparing fuel rod performance code FINE and transient fuel rod analysis code FACTRAN. Locked rotor DNB and PCT analysis for the 14x14 (12ft)-121 fuel assemblies core were performed.

#### 7.2.1 Initial Rod Temperature

Calculated results of fuel temperature by VIPRE-01M have been compared with the FINE code results to verify the capability of VIPRE-01M for initial fuel temperature calculation for transient analyses.

Thermal properties incorporated by Mitsubishi were used. The degradation of fuel thermal conductivity along with increased burnup was considered. In the analysis performed for 14x14 fuel, comparisons were done for both BOL and EOL conditions. [

] Fuel centerline, average, and surface temperatures as a function of linear heat rate are compared between both codes in Figure 7-17 and Figure 7-18. The radial temperature distributions are shown in Figure 7-19. Excellent agreements are observed.

The discussion above indicates that generating an initial condition for safety analyses, which is consistent with the FINE result, can be achieved [

### 7.2.2 Heat Flux and DNBR

Comparisons with FACTRAN and THINC codes were conducted for verifying applicability of VIPRE-01M to certain transient analysis functions.

As a typical transient DNB analysis, a Complete Loss of Flow accident analysis was performed for a two-loop plant. The transients of power and primary loop flow rate were shown in Figure 7-20. The reference analysis was a combination of transient heat flux prediction by FACTRAN and DNBR analysis by THINC-III. VIPRE-01M simulates both simultaneously. Also the state point DNBR analysis at limiting condition was compared between VIPRE-01M and THINC-III.

Transient fuel temperature behavior highly depends on the initial fuel temperature condition. Therefore, [

] Transient behavior of fuel surface heat flux and Min. DNBR by WRB-1 correlation is compared with FACTRAN/THINC-III results in Figure 7-21. Fairly good agreements are observed. Table 7-2 shows the results of transient and steady state DNBR analysis results. State point analysis shows a slightly more conservative result, because it neglects the delay of coolant condition change. However, the difference is small. Therefore, it has been concluded that transient calculation of fuel temperature and Min. DNBR by VIPRE-01M is acceptable.

### 7.2.3 Peak Cladding Temperature

The NRC has approved the applicability of the VIPRE-01 code on heat transfer calculation up to the point of DNB occurrence. Heat transfer and fuel behavior after DNB occurrence, such as that simulated in LOCA analysis, is not considered in the code. However, even in Non-LOCA analysis, it is required to evaluate PCT after DNB for several events. Therefore, the applicability of VIPRE-01M code as the alternative of traditional FACTRAN analysis was verified under appropriate conservative assumptions.

A Locked Rotor transient analysis was performed for two-loop plant. The transients of power and primary loop flow rate were shown in Figure 7-22. Fuel properties used are of Mitsubishi models. Cladding material is assumed as ZIRLO™ in both analyses.

It is conservatively assumed that DNB occurs [ ] At that time, local heat transfer mode at hot spot changes from nucleate boiling to film boiling immediately. Heat transfer coefficient in film boiling mode is given by Bishop-Sandberg-Tong correlation [ ] Bulk coolant density used by the correlation is conservatively kept constant as the initial core averaged value for the consistency with FACTRAN analysis. [ ]

[ ] When DNB occurs, [ ] assuming the collapse of cladding tube. Oxidization and heat generation by Zr-Water reaction are taken into account on cladding surface with Baker-Just equation.

Cladding temperature and Zr-Water reaction transients are shown in Figure 7-23 comparing with FACTRAN analysis. VIPRE-01M and FACTRAN analyses showed a great similarity in results.

The results indicate that VIPRE-01M can substitute the PCT analysis function of FACTRAN code adequately.

**Table 7-1 Analyzed Cases and Results of Benchmarking with THINC-IV**

No.	Pressure (psia)	Power (fraction)	Tin (F)	Flow (fraction)	$F_{\Delta H}^N$ (-)	Min. DNBR (WRB-2)
1						
2						
3						
4						
5						
6						
7						
8						

\* % difference from THINC-IV result

**Table 7-2 DNBR Results of Transient and Steady State Analyses**

	Time (s)	Heat Flux (%)	Flow (%)	Min. DNBR (WRB-1)	
				Transient	Steady State
VIPRE-01M					
FACTRAN/THINC-III					

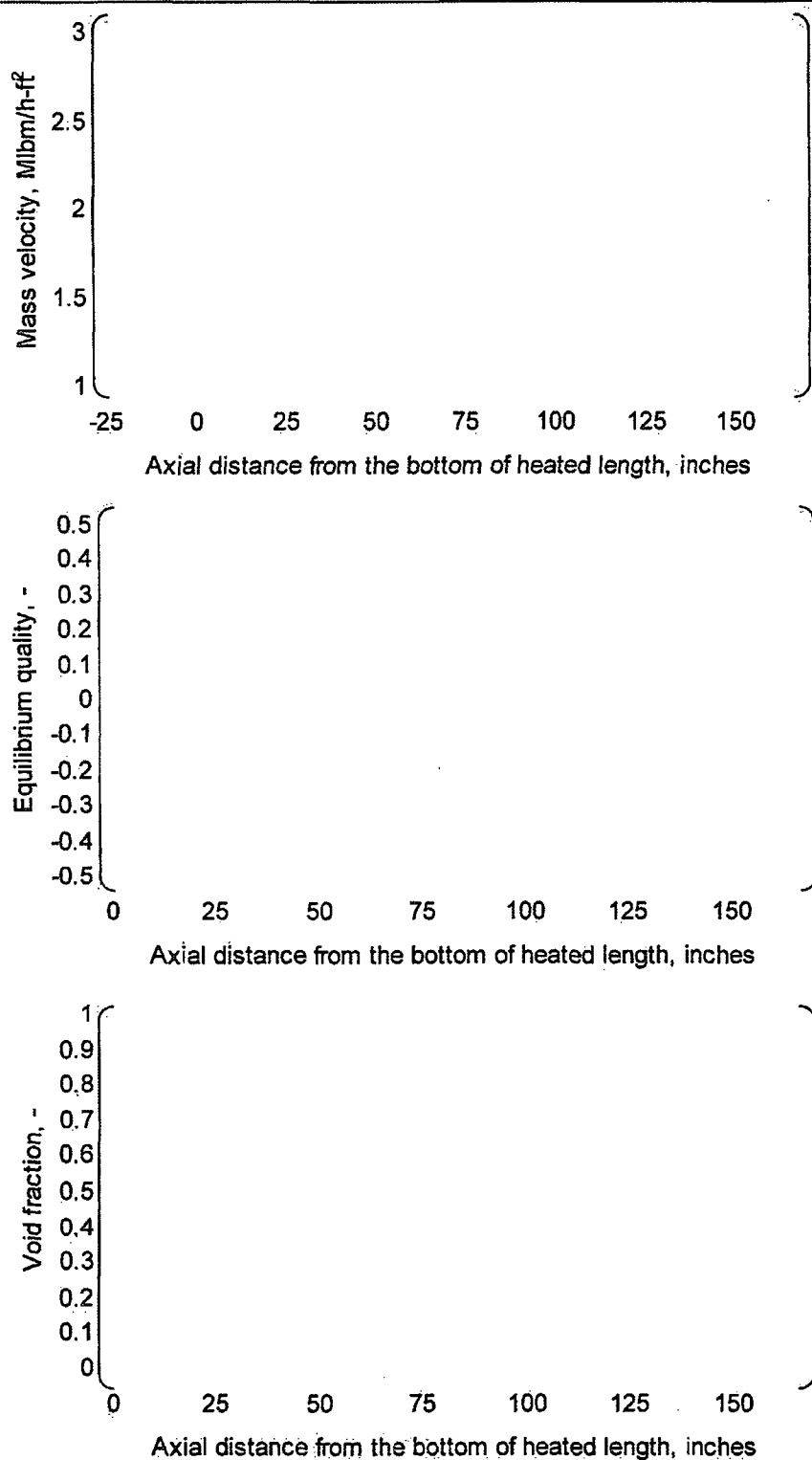


**Figure 7-1 Comparison between VIPRE-01M and THINC-IV  
(Case-1 Typical Cell)**

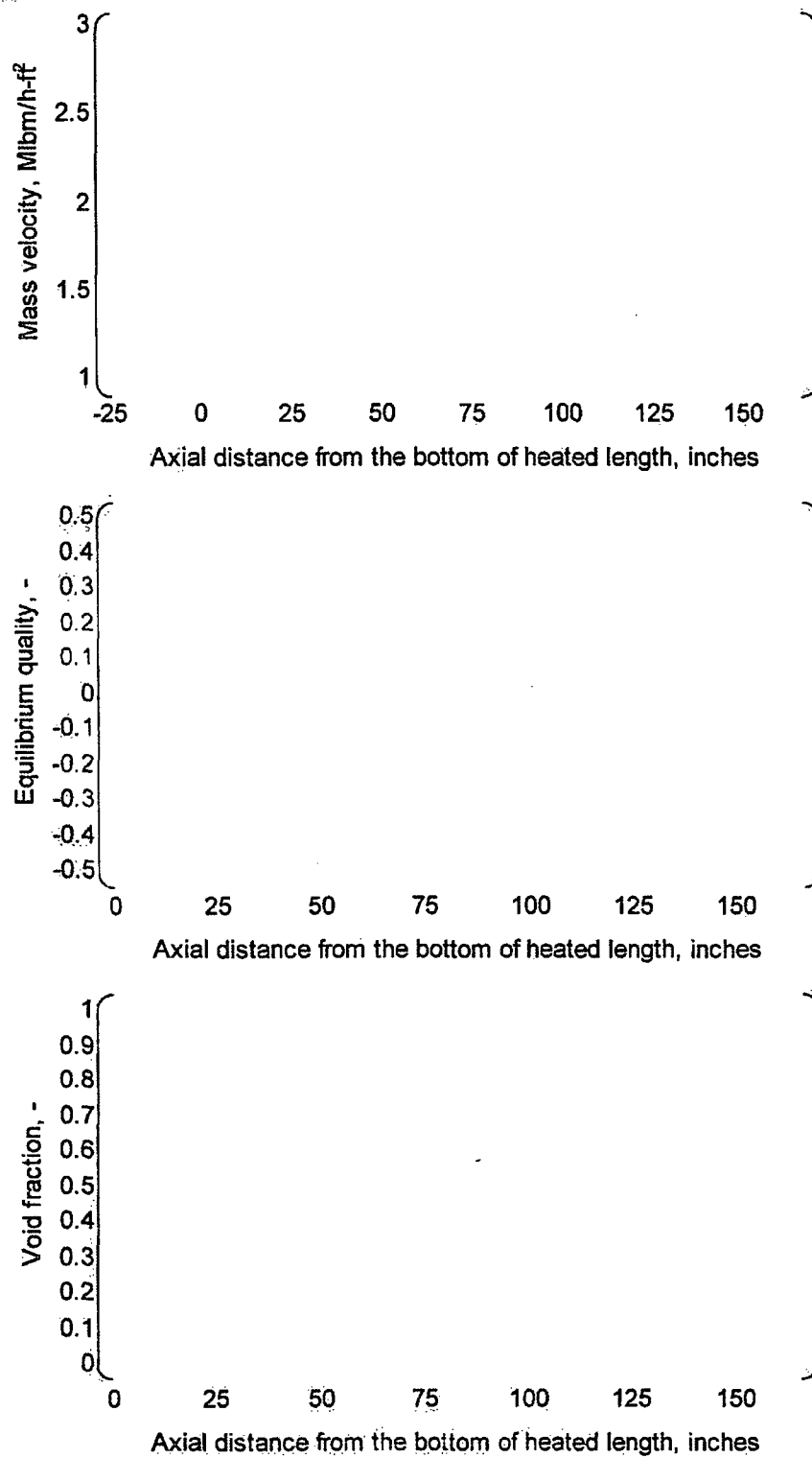


**Figure 7-2 Comparison between VIPRE-01M and THINC-IV  
(Case-1 Thimble Cell)**

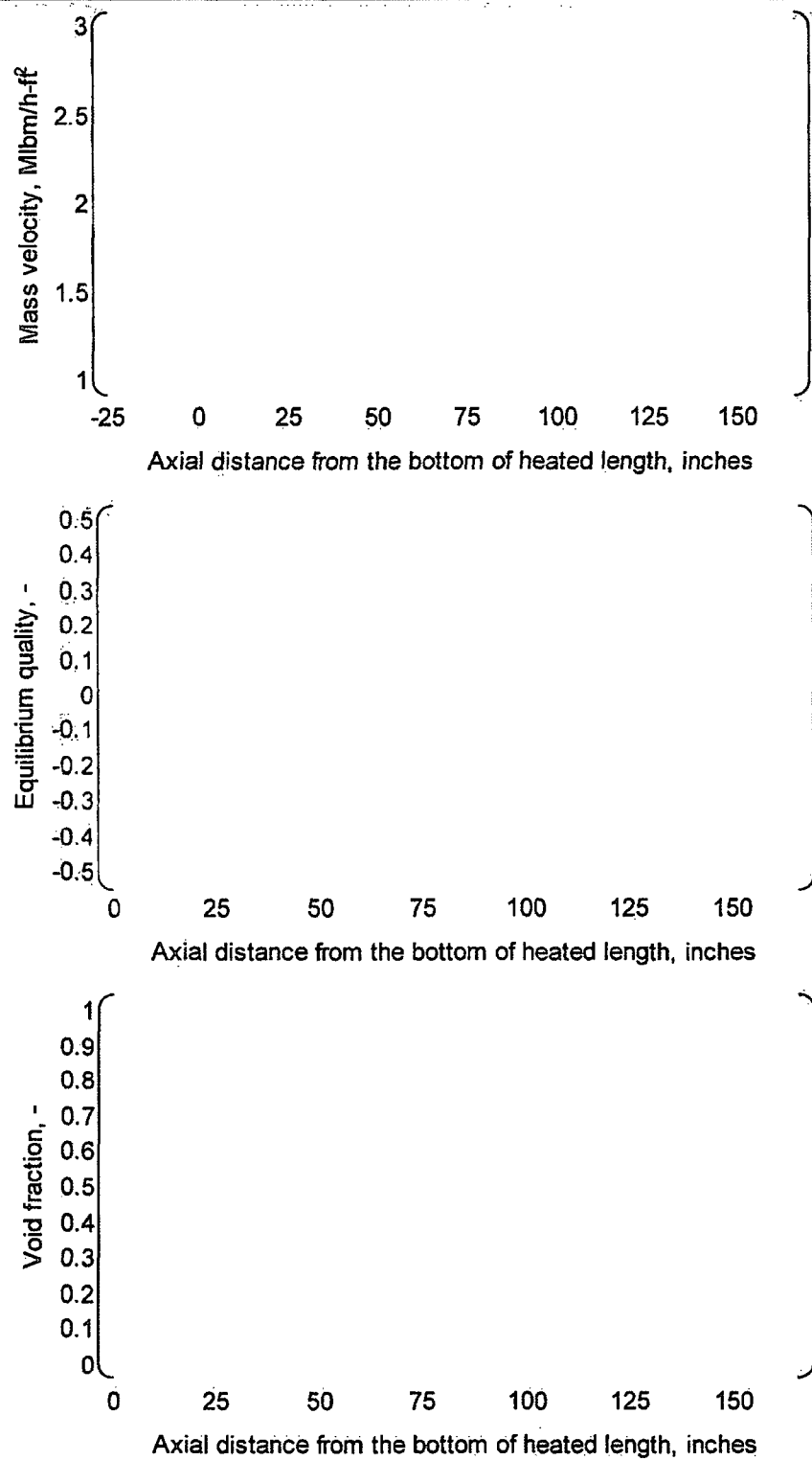


**Figure 7-3 Comparison between VIPRE-01M and THINC-IV  
(Case-2 Typical Cell)**

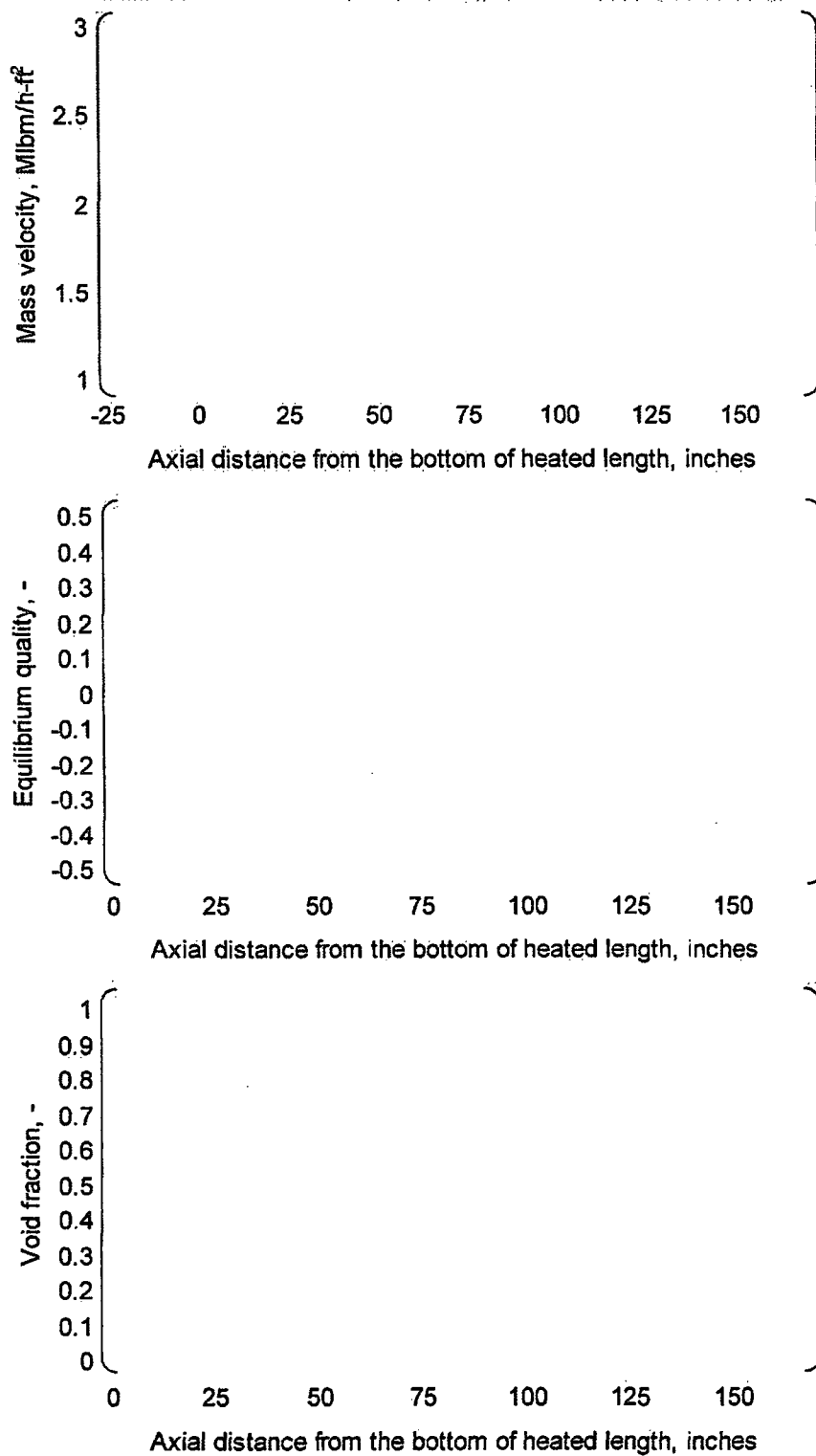


**Figure 7-4 Comparison between VIPRE-01M and THINC-IV  
(Case-2 Thimble Cell)**



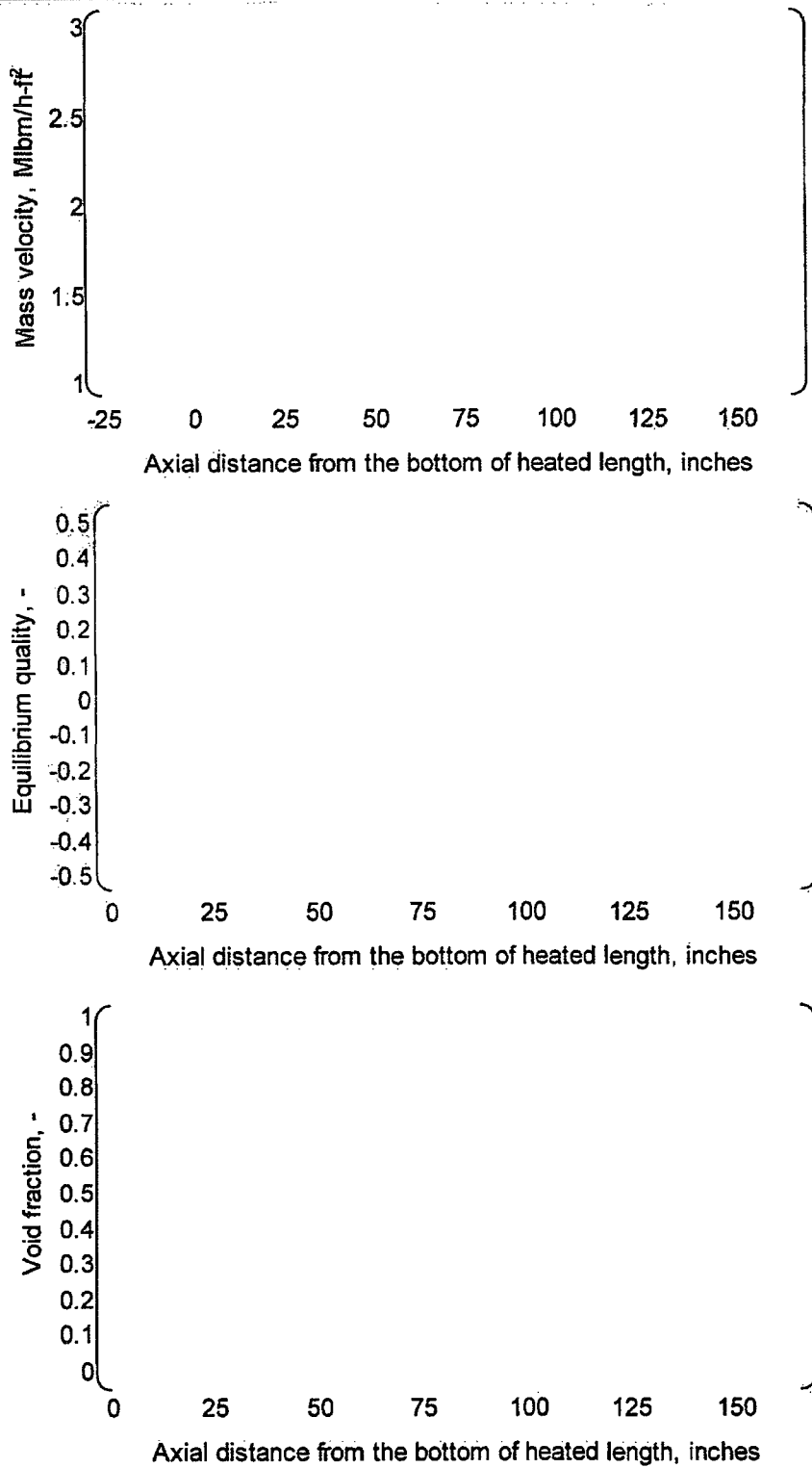


**Figure 7-5 Comparison between VIPRE-01M and THINC-IV  
(Case-3 Typical Cell)**

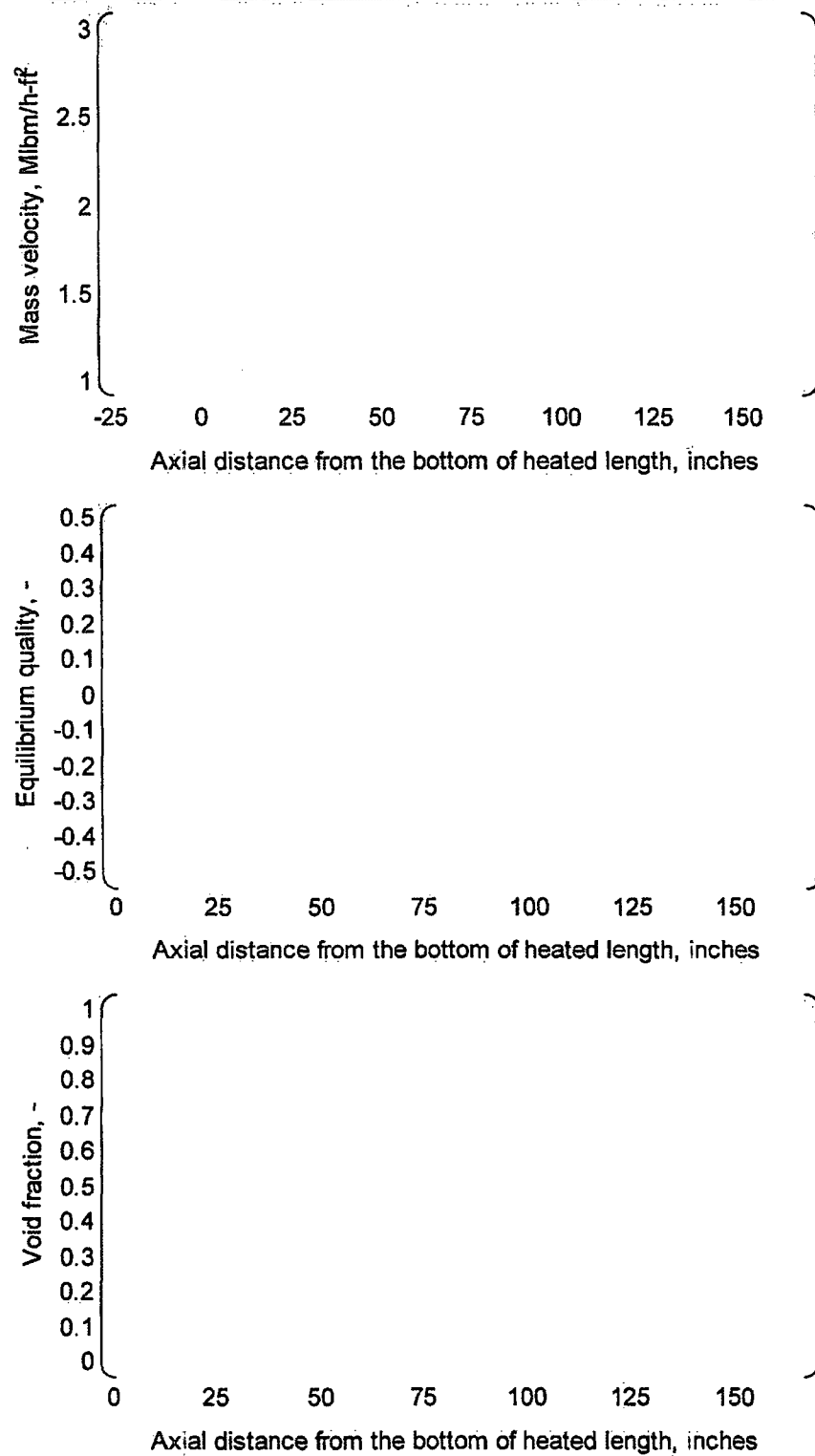


**Figure 7-6 Comparison between VIPRE-01M and THINC-IV  
(Case-3 Thimble Cell)**

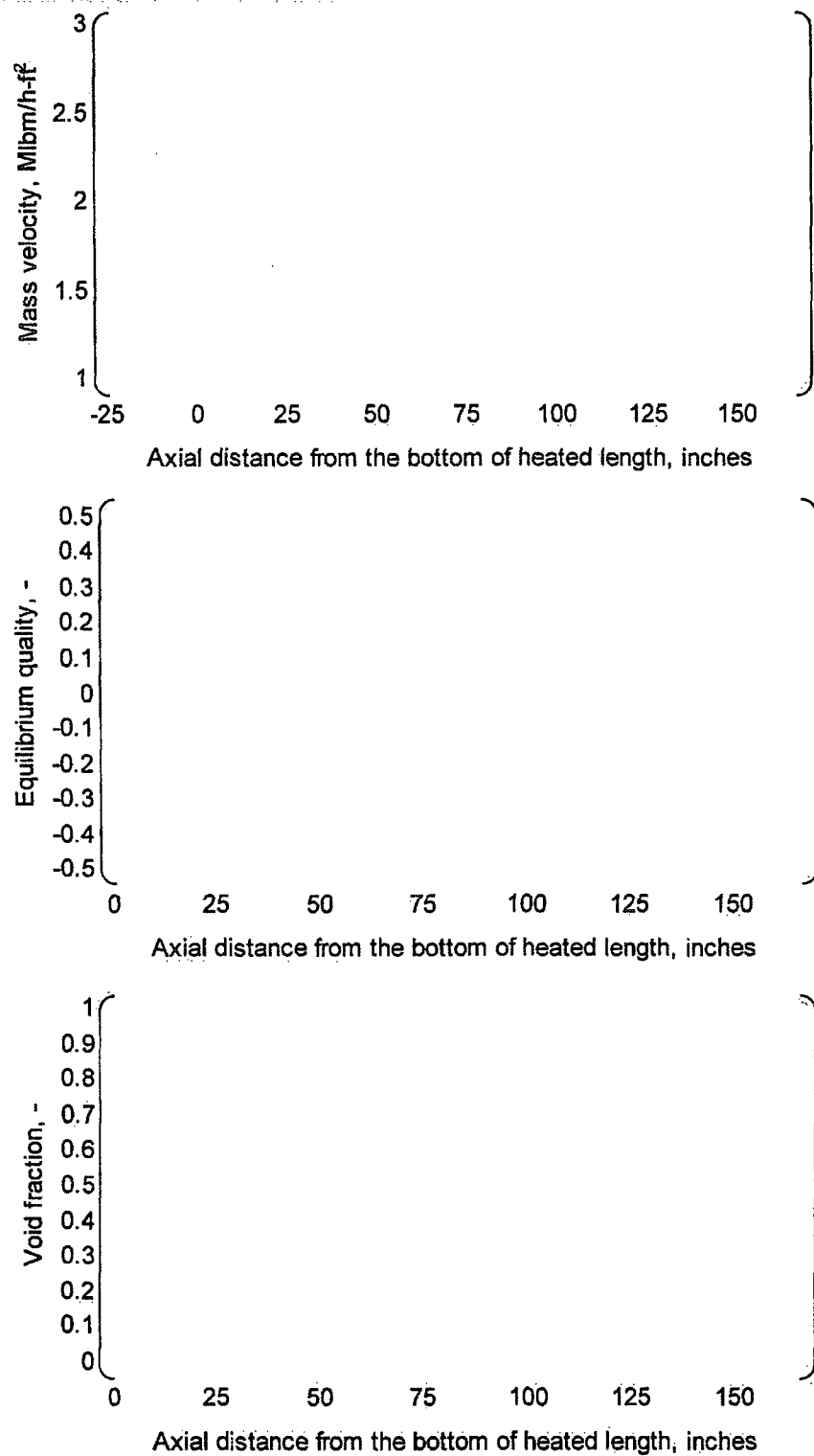


**Figure 7-7 Comparison between VIPRE-01M and THINC-IV  
(Case-4 Typical Cell)**

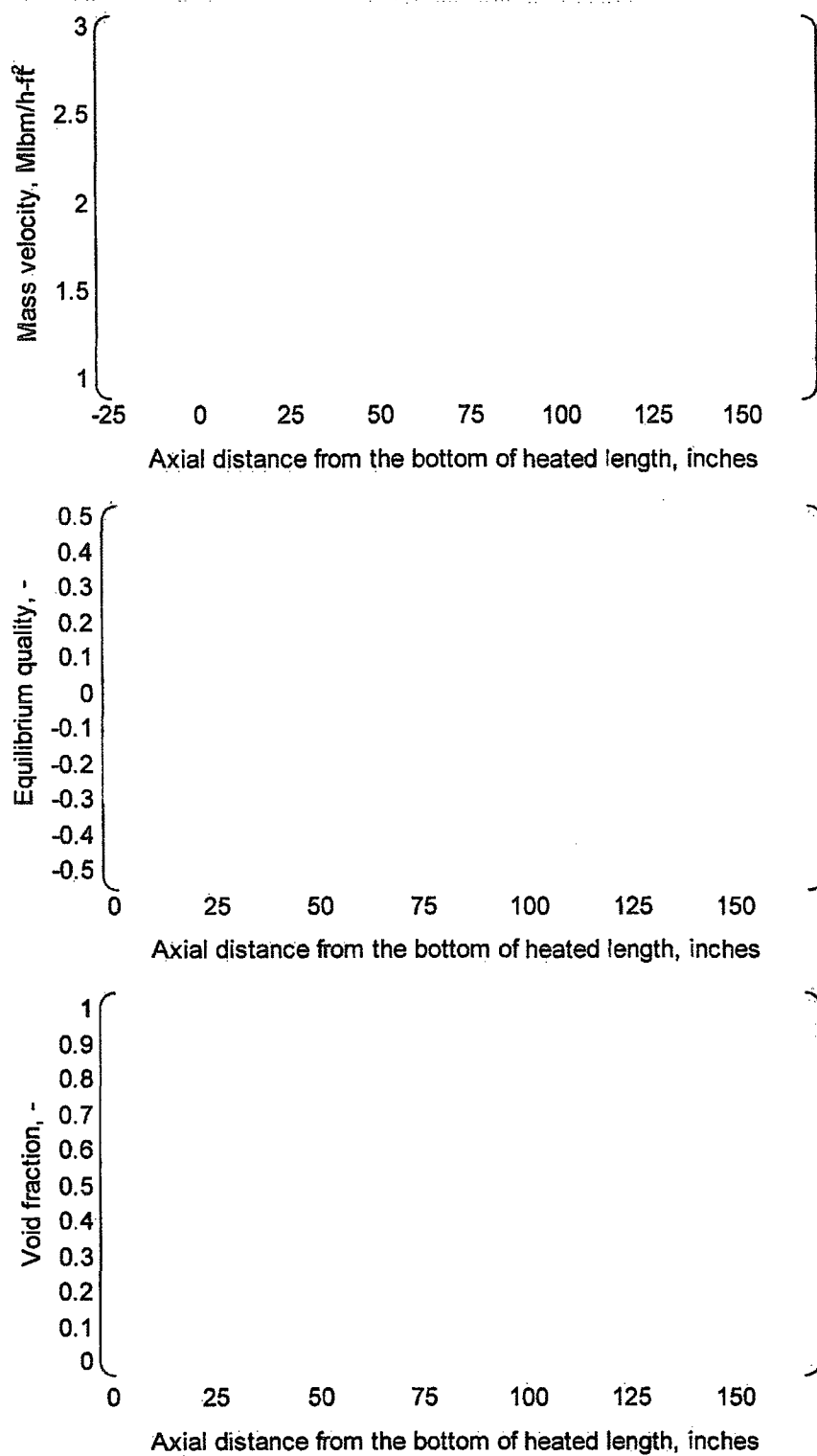


**Figure 7-8 Comparison between VIPRE-01M and THINC-IV  
(Case-4 Thimble Cell)**

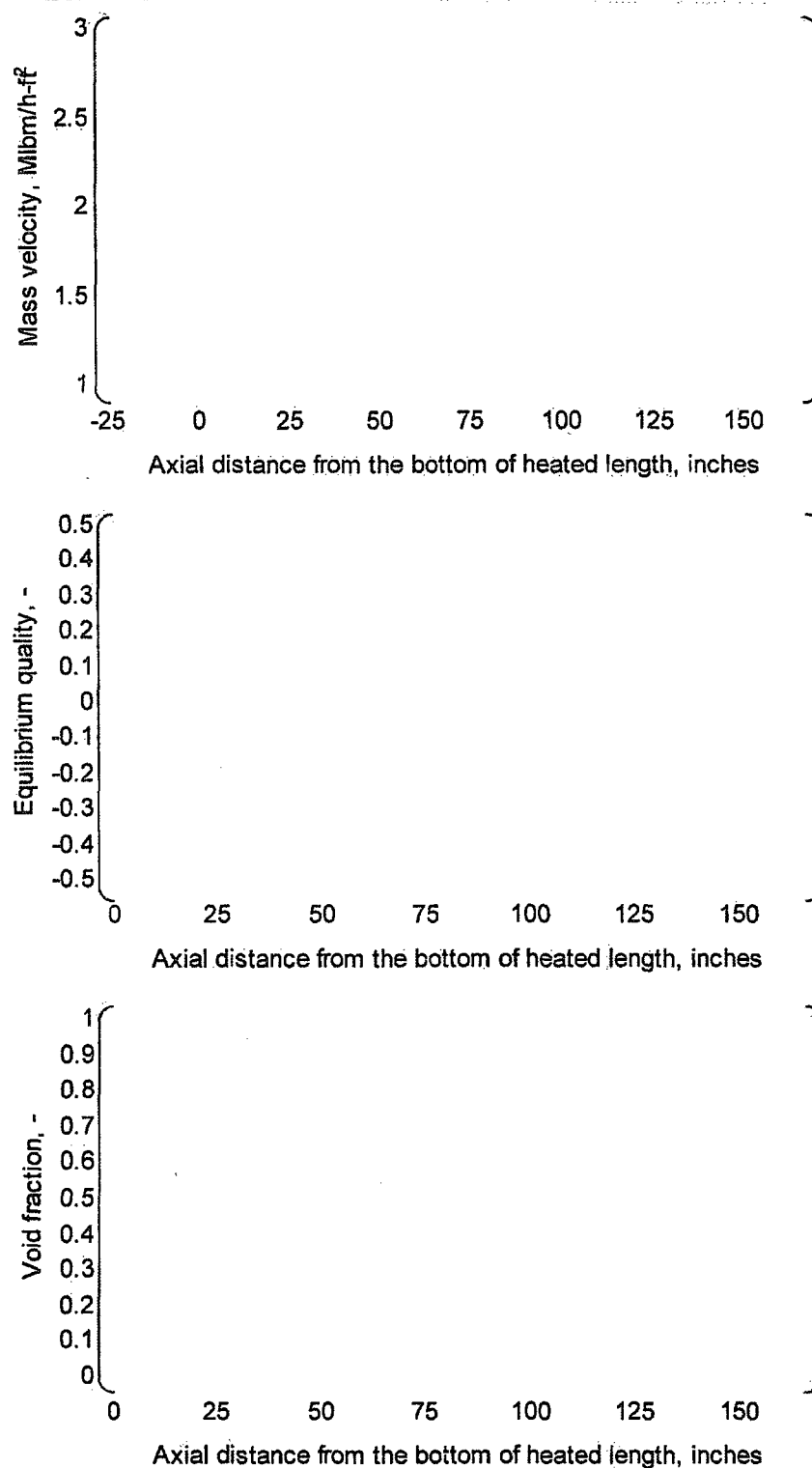


**Figure 7-9 Comparison between VIPRE-01M and THINC-IV  
(Case-5 Typical Cell)**

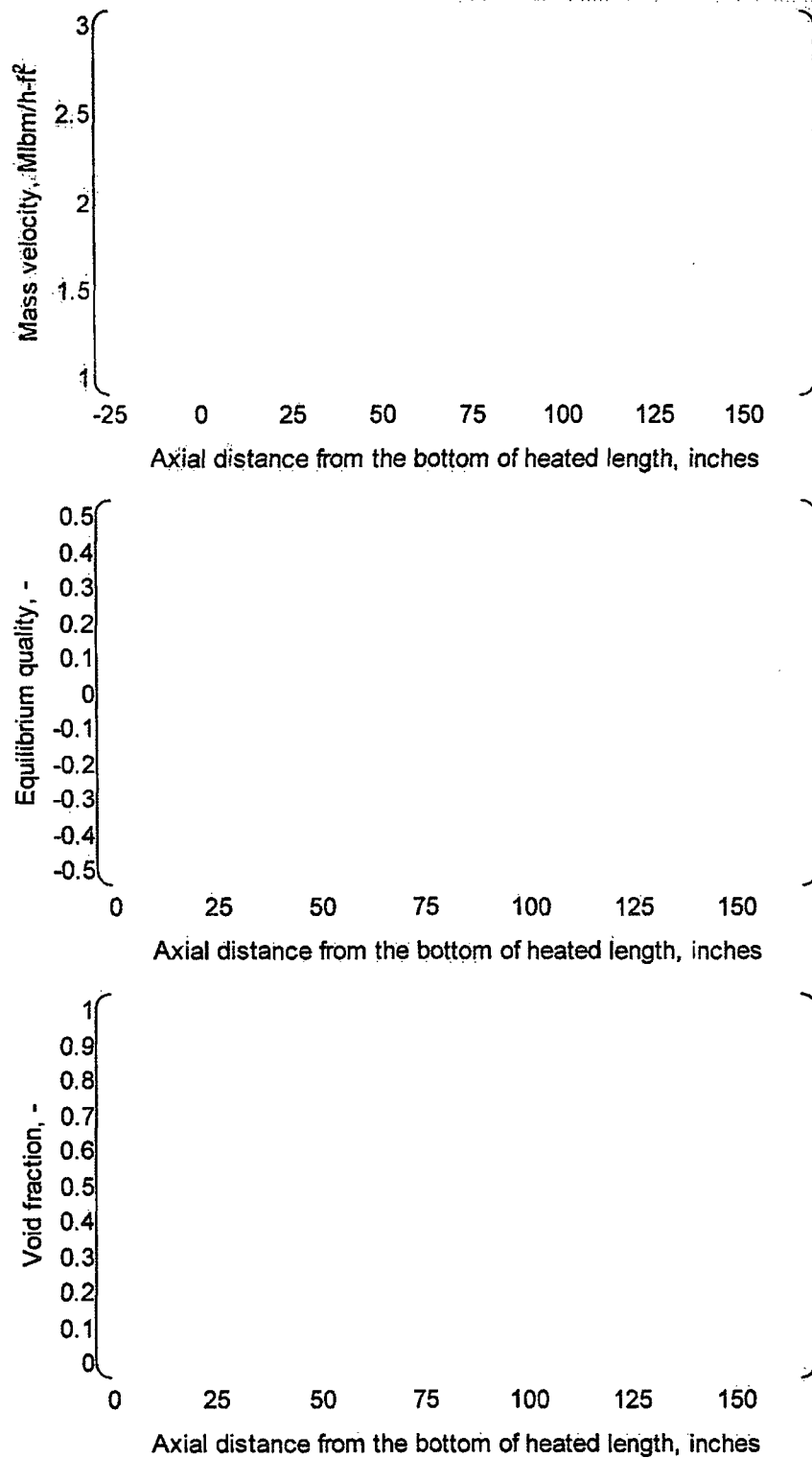


**Figure 7-10 Comparison between VIPRE-01M and THINC-IV  
(Case-5 Thimble Cell)**

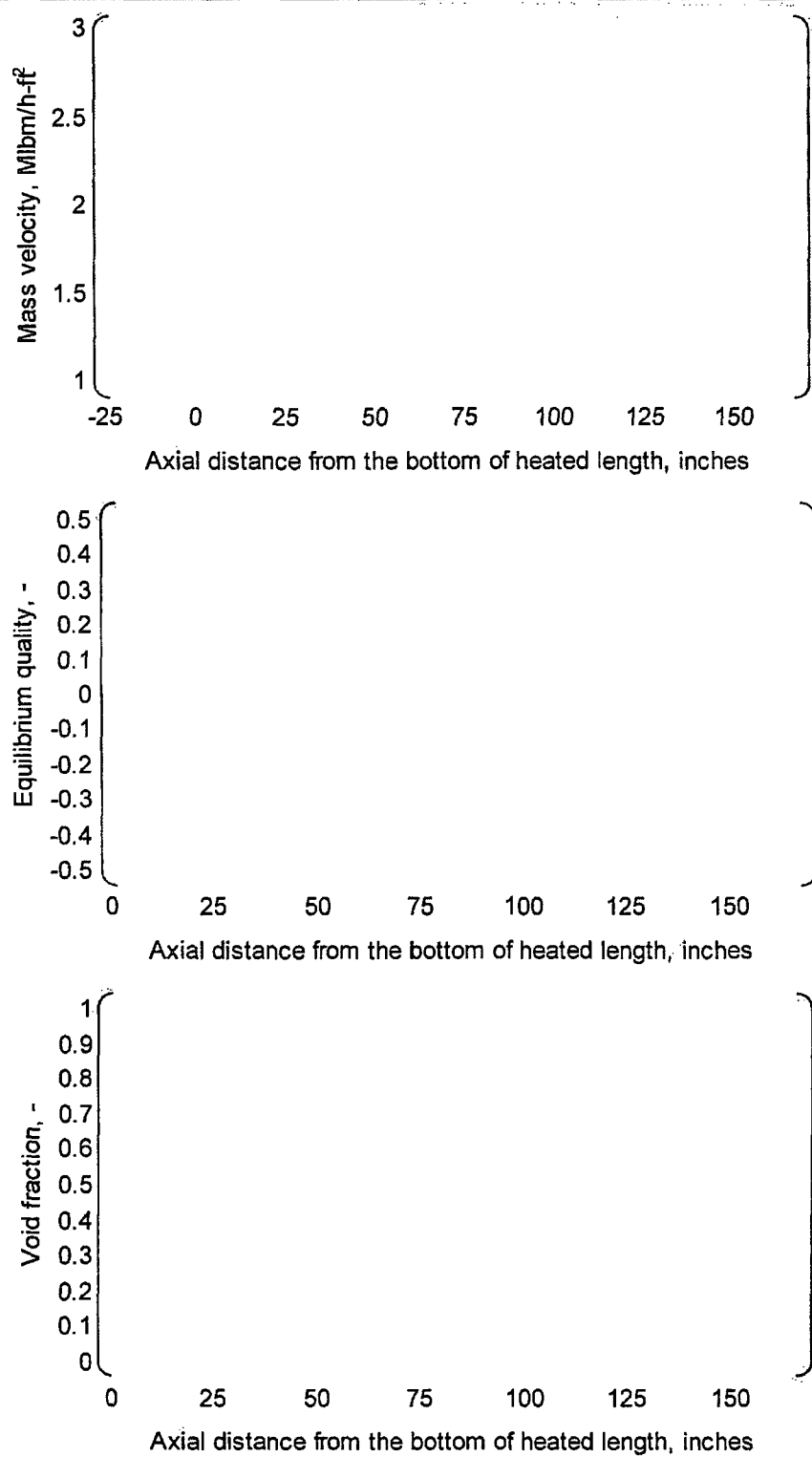


**Figure 7-11 Comparison between VIPRE-01M and THINC-IV  
(Case-6 Typical Cell)**

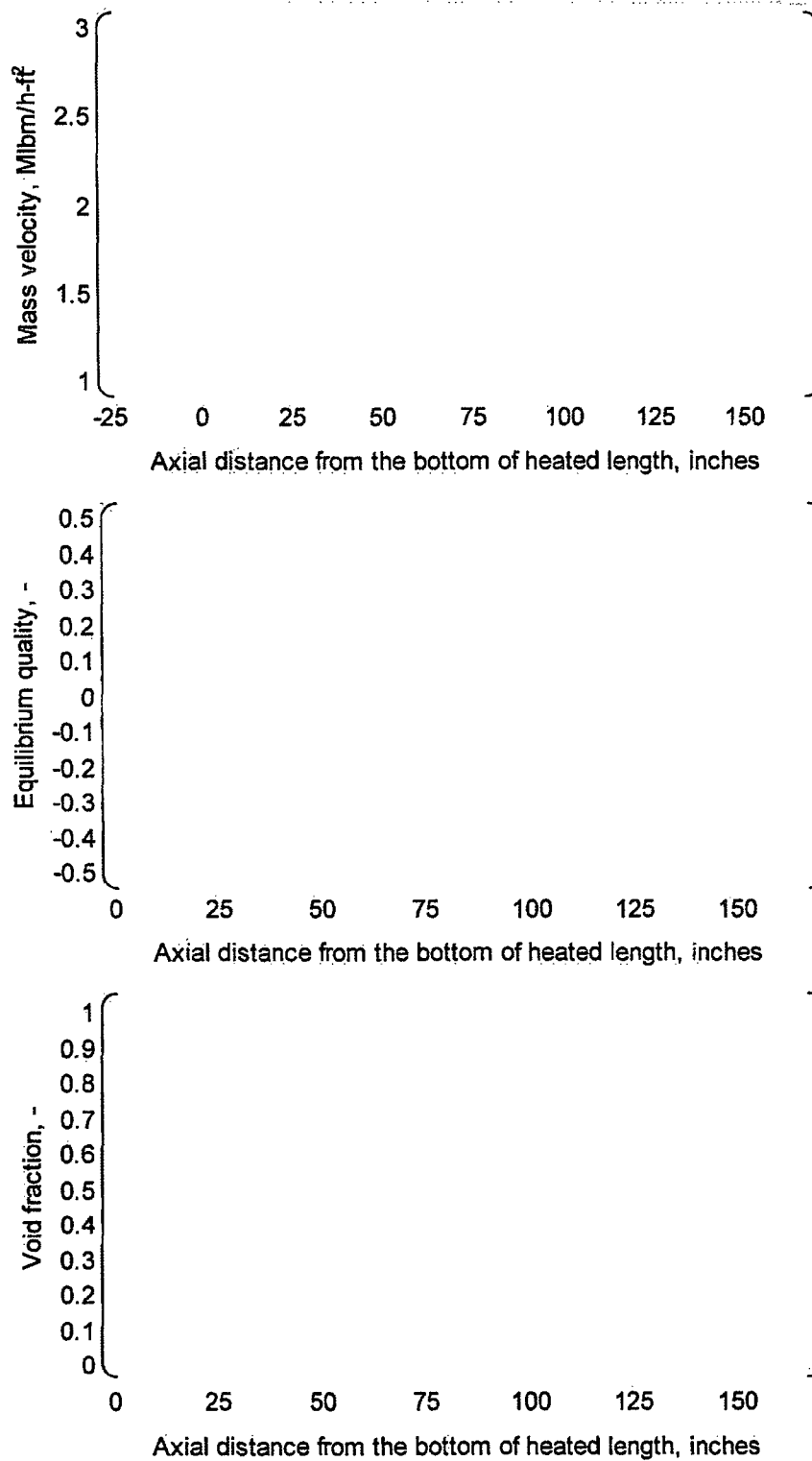


**Figure 7-12 Comparison between VIPRE-01M and THINC-IV  
(Case-6 Thimble Cell)**



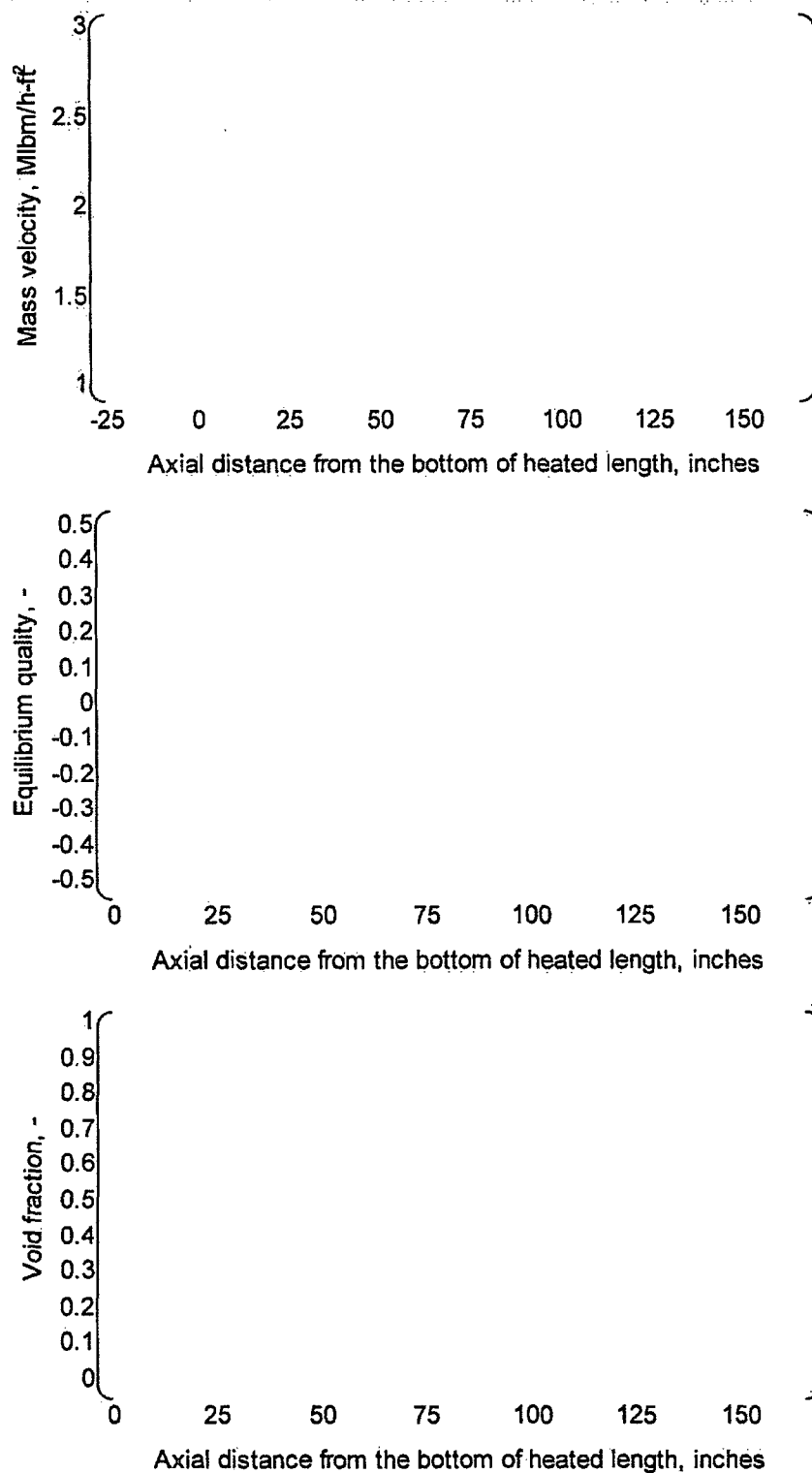


**Figure 7-13 Comparison between VIPRE-01M and THINC-IV  
(Case-7 Typical Cell)**

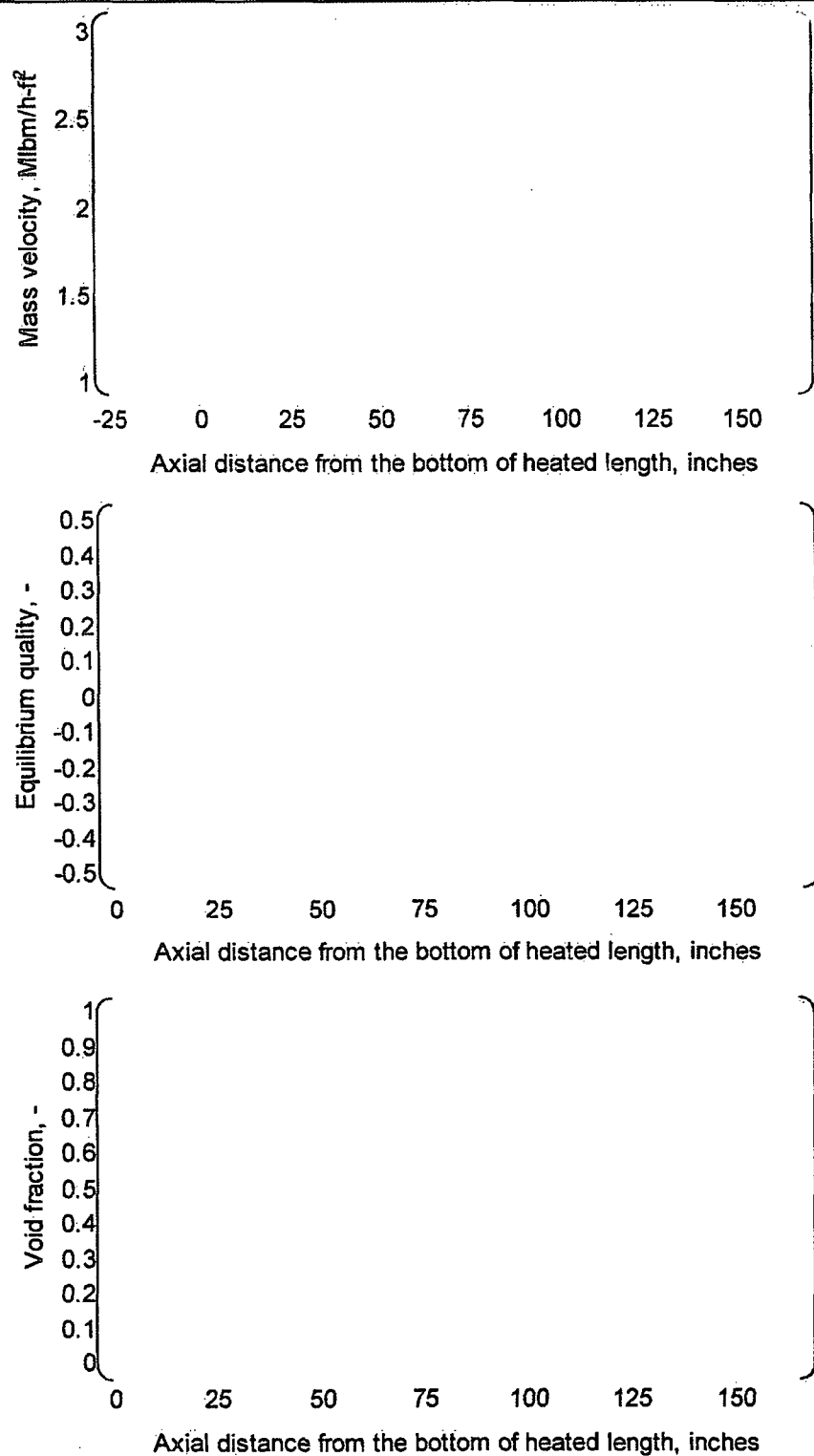


**Figure 7-14 Comparison between VIPRE-01M and THINC-IV  
(Case-7 Thimble Cell)**

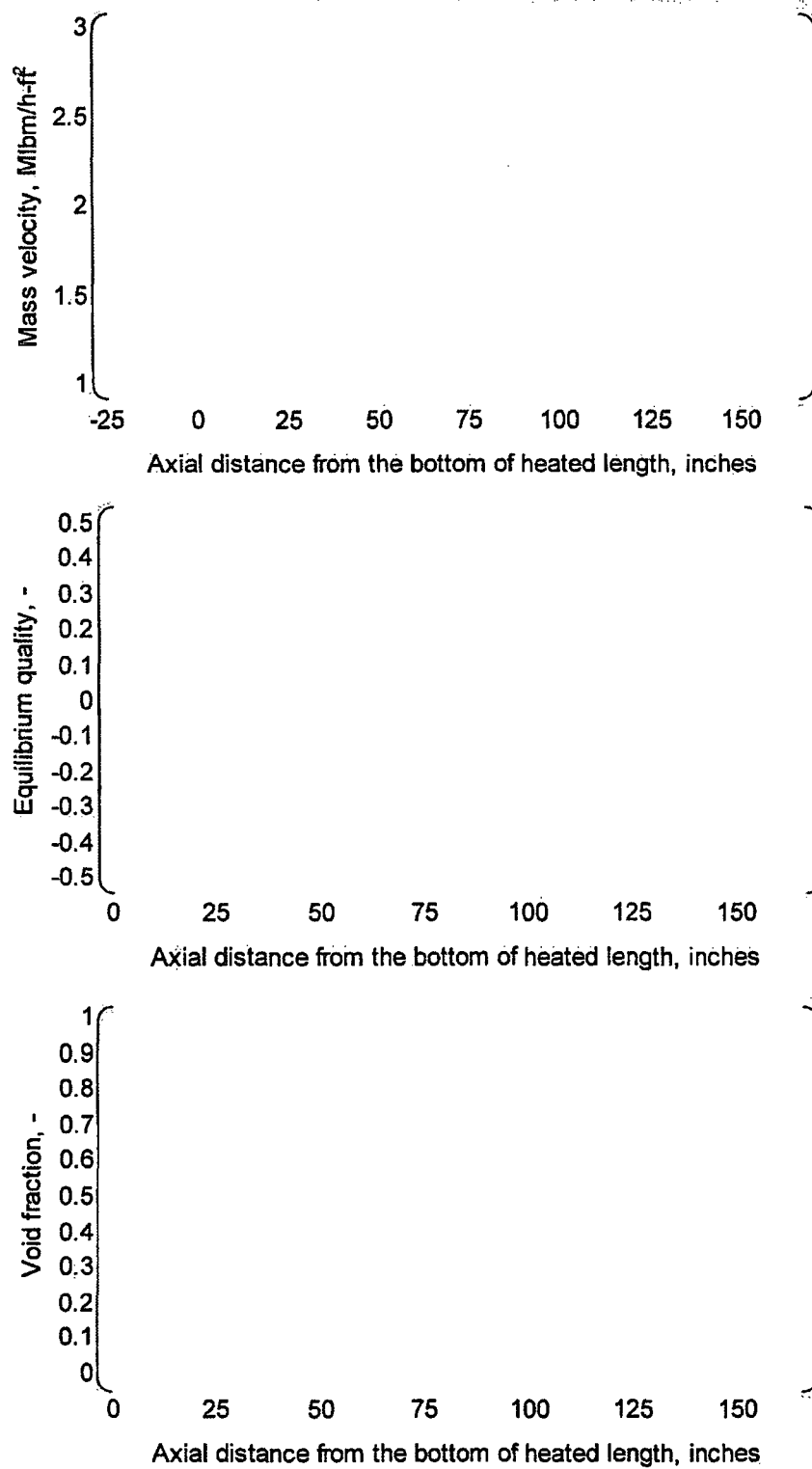


**Figure 7-15 Comparison between VIPRE-01M and THINC-IV  
(Case-8 Typical Cell)**

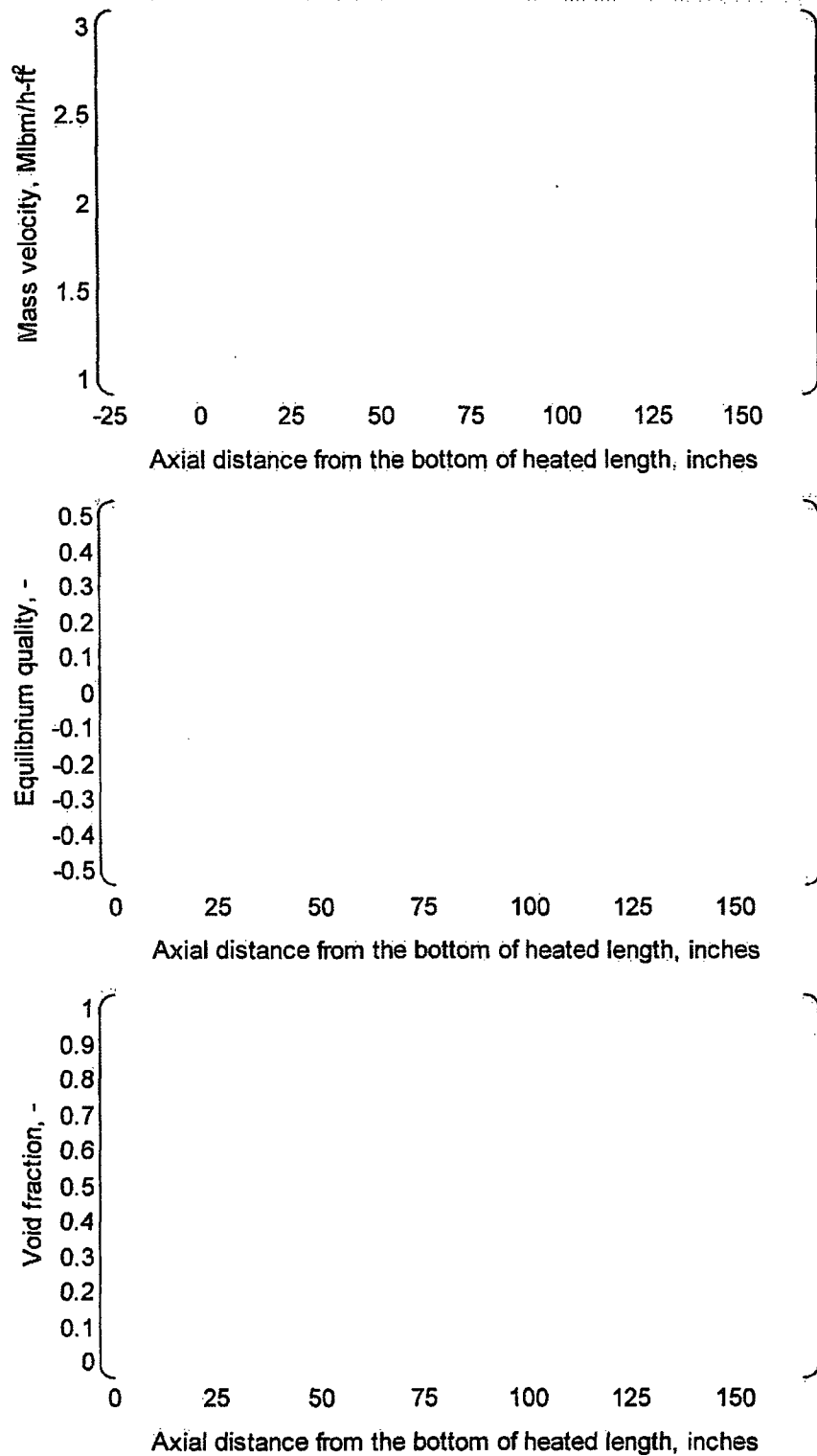


**Figure 7-16 Comparison between VIPRE-01M and THINC-IV  
(Case-8 Thimble Cell)**

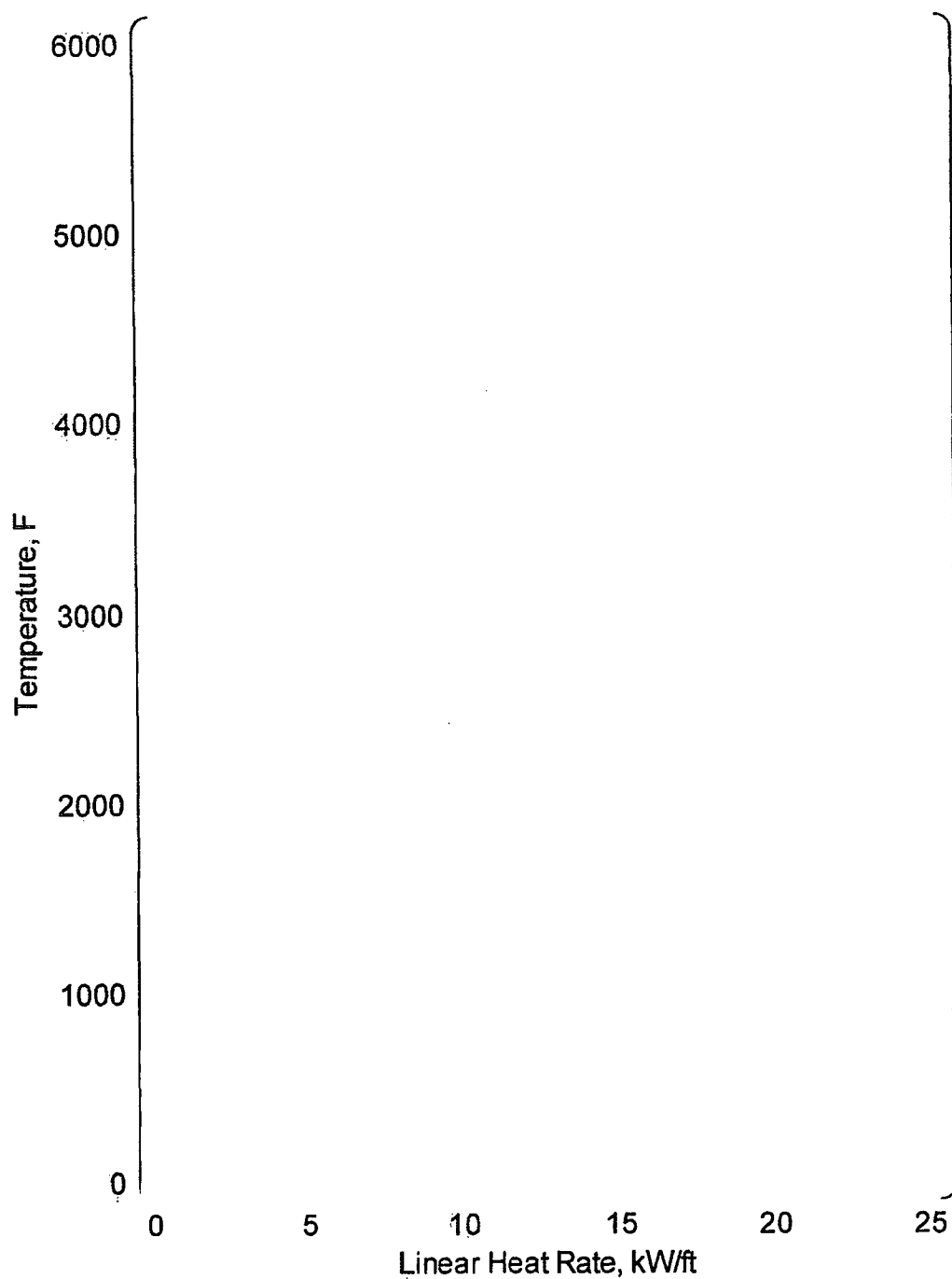


**Figure7-17 Comparison of Fuel Temperature between VIPRE-01M and FINE  
(14x14 Fuel - BOL)**

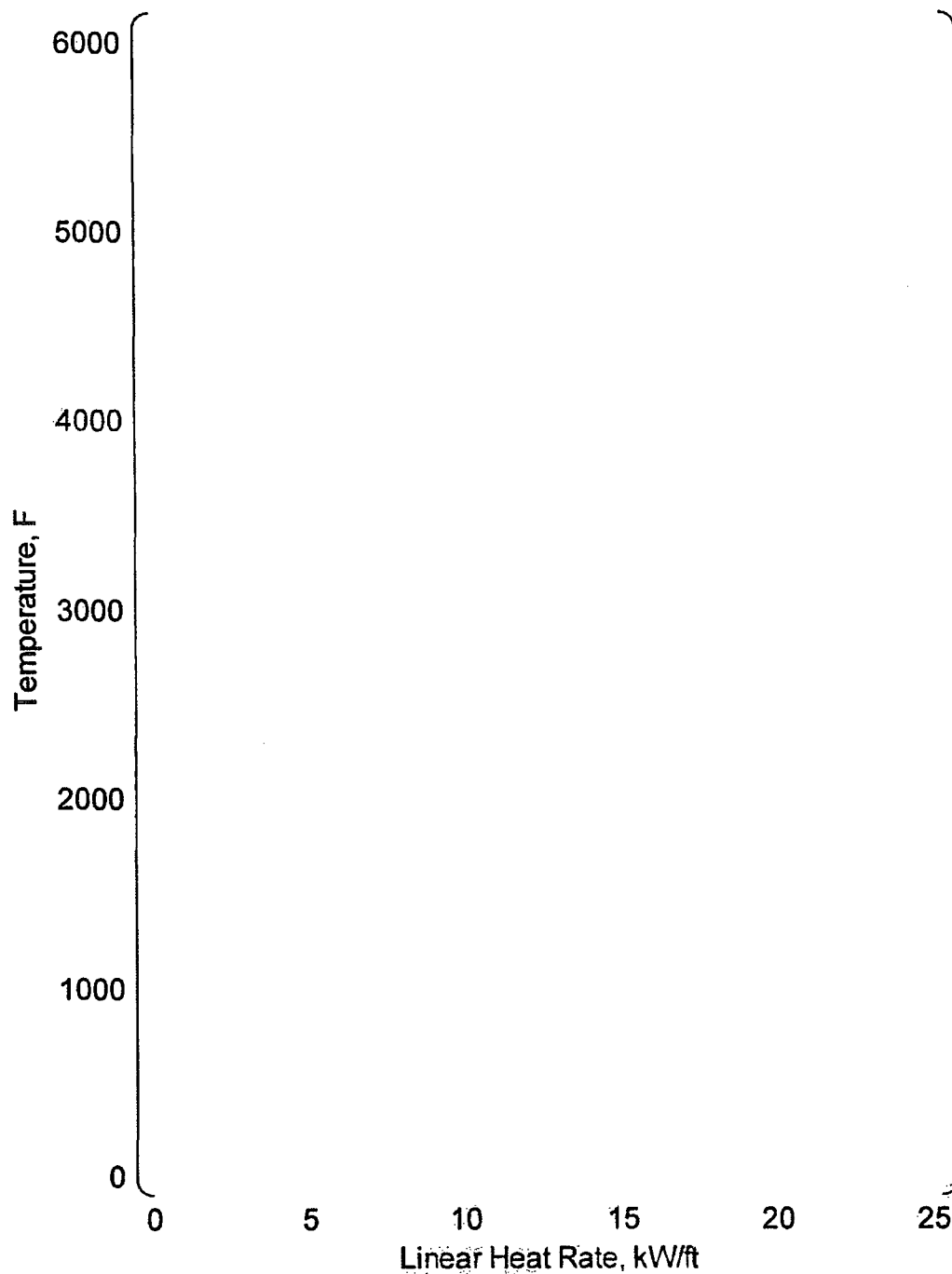


**Figure 7-18 Comparison of Fuel Temperature between VIPRE-01M and FINE  
(14x14 Fuel - EOL (71GWd/t))**

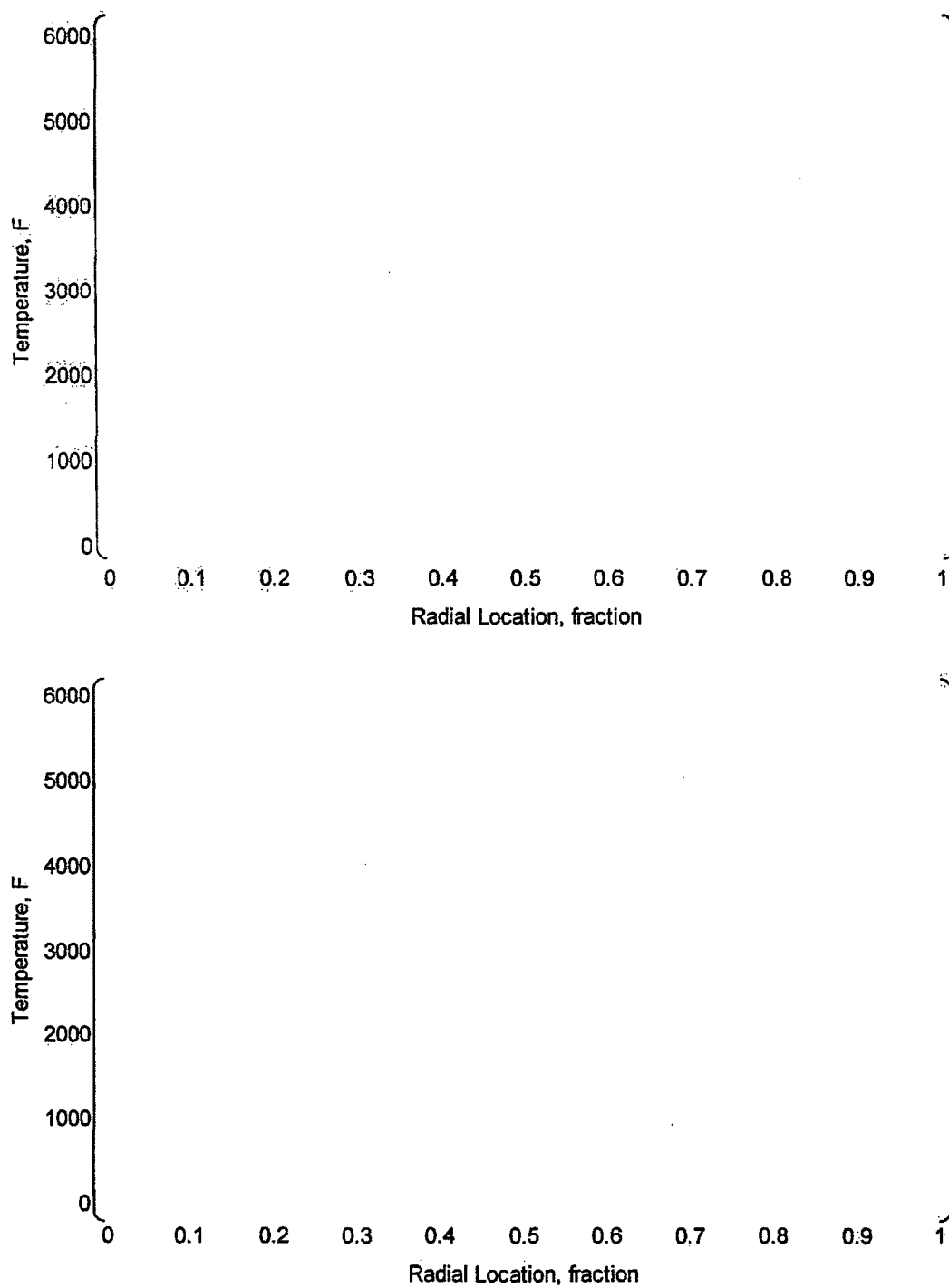


**Figure 7-19 Comparison of Fuel Temperature Distribution  
between VIPRE-01M and FINE**

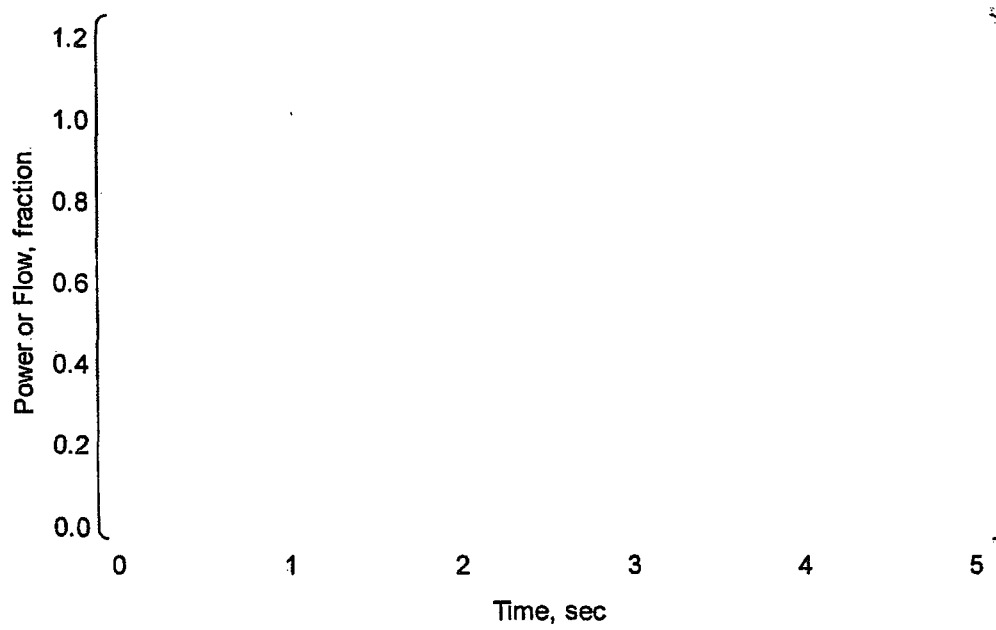


**Figure 7-20 System Transient Conditions for Loss of Flow Analysis**



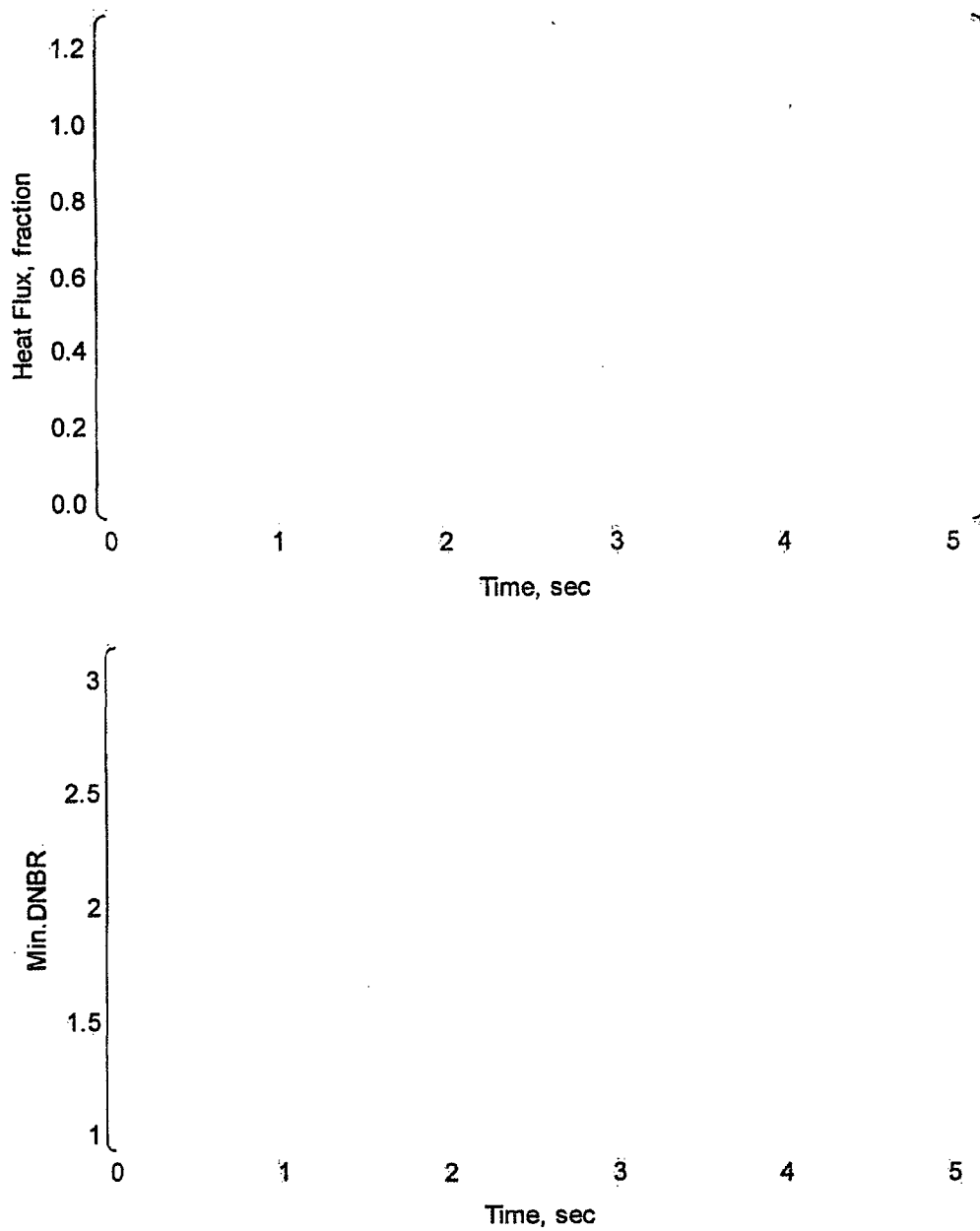


**Figure 7-21 Comparison of the DNBR Analysis Results  
between VIPRE-01M and FACTRAN/THINC-III**

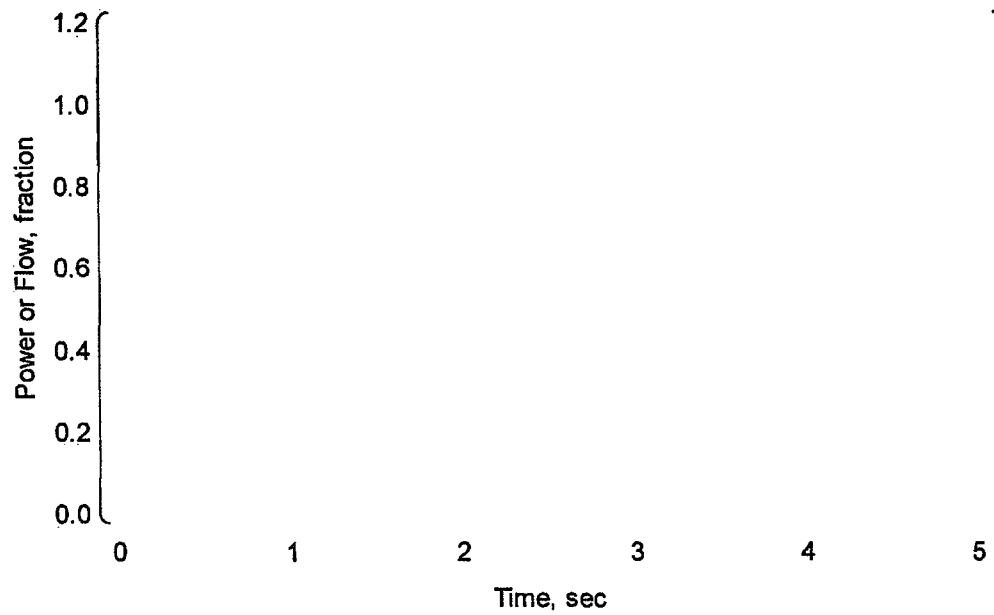


**Figure 7-22 System Transient Conditions for Locked Rotor Analysis**

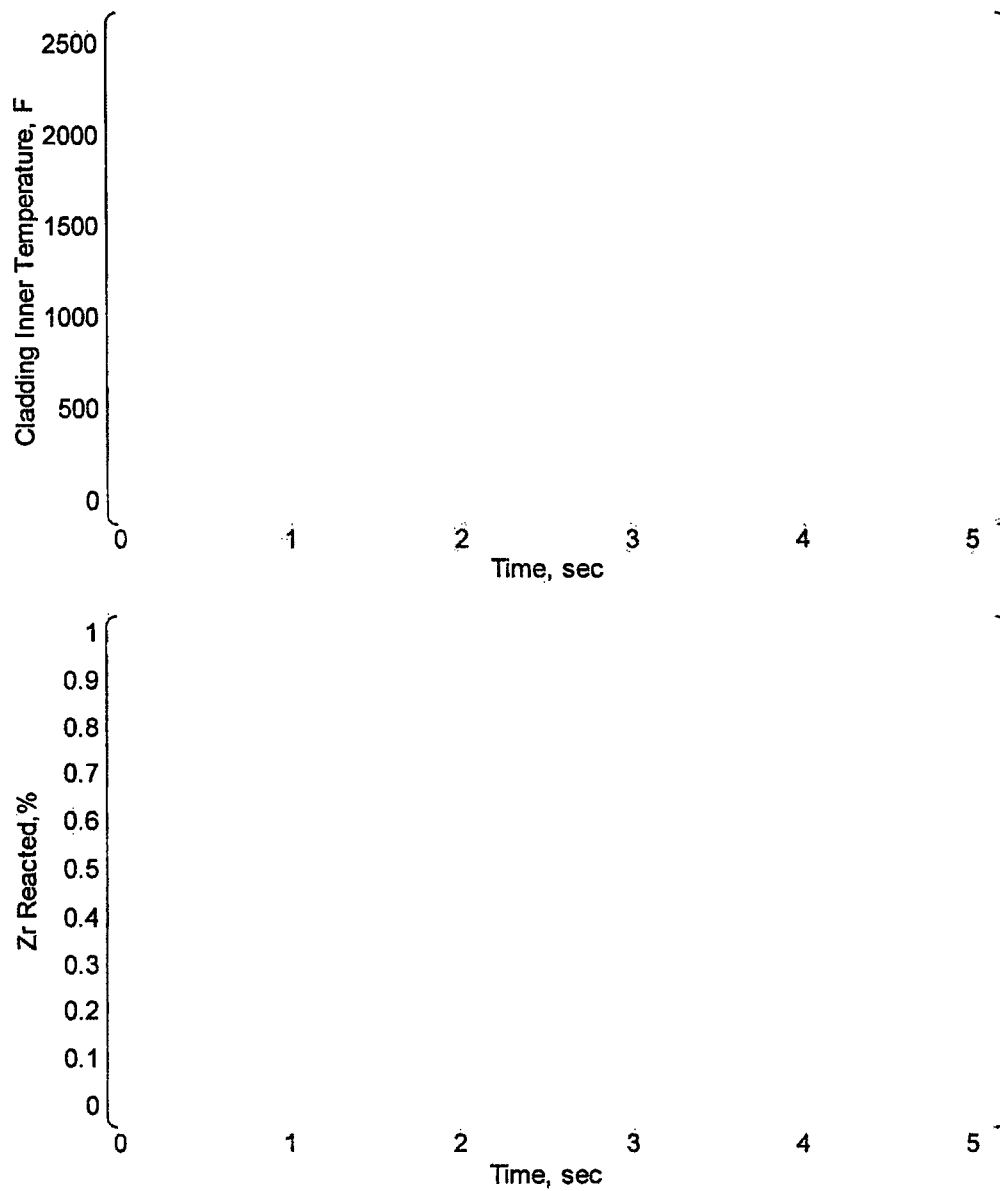


**Figure 7-23 Comparison of Peak Cladding Temperature Analysis  
between VIPRE-01M and FACTRAN**

## 8.0 CONCLUSION

Mitsubishi's Thermal Design Methodology consists of the following three areas:

- (1) Revised Thermal Design Procedure [Ref.12]
- (2) VIPRE-01M (VIPRE-01 [Ref.1 - 5]) subchannel analysis code
- (3) WRB-1 and WRB-2 DNB correlations [Ref.6, 7]

The Revised Thermal Design Procedure is identical to Westinghouse's methodology which has been approved by the NRC.

VIPRE-01M is just an extension of the NRC-approved VIPRE-01 code for enhanced design applications. The NRC-approved main body of the code, namely, governing equation system, solver and constitutive models, are not changed. Therefore, the NRC's review for VIPRE-01 is still valid for VIPRE-01M. The application method for design analysis and verification of design models added by Mitsubishi are described in this report and shown to comply with the VIPRE-01 SER.

The VIPRE-01M models selected for the thermal design analysis of PWR core are all well-accepted and/or conservative. These models predict the core thermal-hydraulic behaviors adequately and are shown to generate conservative DNBRs in comparisons with the NRC-approved THINC code models and the models which are recommended by EPRI.

The main design application tools added by Mitsubishi are the specific DNB correlations, WRB-1 and WRB-2, and fuel thermal properties that are consistent with the fuel performance code, FINE. The added fuel thermal properties take into account the impact of degradation of pellet on thermal conductivity along with burnup. The thermal properties were demonstrated to be correctly introduced and were verified by comparison with FINE and FACTRAN codes for steady state and transient conditions respectively. In addition, the replacement of FACTRAN in PCT analysis by VIPRE-01M for certain non-LOCA transient analyses were justified and validated.

WRB-1 and WRB-2 correlations are the most widely used vendor correlations in the US. Mitsubishi intends to use these two correlations for DNBR determinations for its PWR fuels. Since all DNB correlations have to be subchannel-code-compatible, a comprehensive study was conducted to verify that WRB-1 and WRB-2 are compatible to VIPRE-01M.

The verification of both correlations with their associated DNB test database, based on the VIPRE-01M code, showed that the correlation limit of DNBR on the 95% probability at 95% confidence level basis are less than 1.17, which is the value originally shown by Westinghouse in conjunction with THINC code and approved by the NRC.

WRB-1 and WRB-2 correlations can also be conservatively applied to Mitsubishi's latest fuel designs. The DNB test analyses for Mitsubishi Z2 and Z3 grid spacer designs showed that the correlation limit 1.17 is conservatively applicable to the fuels.

The Mitsubishi-proposed thermal design methodology is essentially identical to those adopted for most existing PWR designs in the US. The code and correlations are verified and

---

demonstrated to be applicable to the core thermal-hydraulic design analyses and all Non-LOCA Safety Analyses relevant to DNB.

---

**9.0 REFERENCES**

1. C. W. Stewart, et al., "VIPRE-01: A Thermal-Hydraulic Code for Reactor Cores, Volume 1 (Revision 4): Mathematical Modeling", NP-2511-CCM-A, Electric Power Research Institute (EPRI), February 2001
2. C. W. Stewart, et al., "VIPRE-01: A Thermal-Hydraulic Code for Reactor Cores, Volume 2 (Revision 4): User's Manual", NP-2511-CCM-A, Electric Power Research Institute (EPRI), February 2001
3. C. W. Stewart, et al., "VIPRE-01: A Thermal-Hydraulic Code for Reactor Cores, Volume 3 (Revision 4): Programmer's Manual", NP-2511-CCM-A, Electric Power Research Institute (EPRI), February 2001
4. C. W. Stewart, et al., "VIPRE-01: A Thermal-Hydraulic Code for Reactor Cores, Volume 4 (Revision 4): Applications", NP-2511-CCM-A, Electric Power Research Institute (EPRI), February 2001
5. C. W. Stewart and J. M. Cuta, et al., "VIPRE-01: A Thermal-Hydraulic Code for Reactor Cores, Volume 5 (Revision 4): Guidelines", NP-2511-CCM-A, Electric Power Research Institute (EPRI), February 2001
6. F. E. Motley, et al., "New Westinghouse Correlation WRB-1 for Predicting Critical Heat Flux in Rod Bundles with Mixing Vane Grids", WCAP-8762-P-A, Westinghouse Electric Corporation, 1984
7. Edited by S. L. Davidson, "Reference Core Report VANTAGE 5 Fuel Assembly", WCAP-10444-P-A, Westinghouse Electric Corporation, 1985
8. H. Chelmer, et al., "THINC-IV - An Improved Program for Thermal-Hydraulic Analysis of Rod Bundle Cores", WCAP-7956-A, Westinghouse Electric Corporation, February 1989
9. T. Shimomura, et al., "Fuel System Design Criteria and Methodology", MUAP-07008-P, Mitsubishi Heavy Industries, 2007
10. H. G. Hargrove, "FACTRAN - A FORTRAN-IV Code for Thermal Transients in a UO<sub>2</sub> Fuel Rod", WCAP-7908-A, Westinghouse Electric Corporation, December 1989
11. A. J. Friedland, S. Ray, "Revised Thermal Design Procedure", WCAP-11397-P-A, Westinghouse Electric Corporation, April 1989
12. D. S. Rowe, "COBRA-IIIC: A Digital Computer Program for Steady-State and Transient Thermal-Hydraulic Analysis of Rod Bundle Nuclear Fuel Elements", BNWL-1695, Pacific Northwest Laboratory, March 1973
13. C. L. Wheeler, et al., "COBRA IV-I: An Interim Version of COBRA for Thermal-Hydraulic Analysis of Rod Bundle Nuclear Fuel Elements and Cores", BNWL-1962, Pacific Northwest Laboratory, March 1976
14. T. L. George, "COBRA-WC: A Version of COBRA for Single Phase Multi-assembly Thermal-Hydraulic Transient Analysis", PNL-3259, Pacific Northwest Laboratory, July 1980
15. R. Bowering and P. Moreno, "COBRA-IIIC/MIT Computer Code Manual", prepared by Massachusetts Institute of Technology (MIT) for EPRI, March 1976
16. L. S. Tong, "Boiling Crisis and Critical Heat Flux", TID-25887, Atomic Energy Commission, 1972
17. J. Ogawa, et al., "Non-LOCA Methodology", MUAP-07010-P, Mitsubishi Heavy Industries, 2007
18. "Quality Assurance Program (QAP) for Design Certification of the US-APWR", PQD-HD-18046-Rev.1, Mitsubishi Heavy Industries, Ltd., 2006
19. L. S. Tong and J. Weisman, "Thermal Analysis of Pressurized Water Reactors", Second Edition, TID-25887, American Nuclear Society, 1979
20. I. E. Idelchik, "Handbook of Hydraulic Resistance", 3rd Edition, CRC Press, 1994

- 
- 21 A. A. Bishop, et al., "Forced Convection Heat Transfer at High Pressure After the Critical Heat Flux", ASME-65-HT-31, 1965
  22. L. Baker Jr., and L. C. Just, "Studies of Metal-Water Reactions at High Temperatures", ANL-6548, Argonne National Laboratories, May, 1962

## APPENDIX A

### SENSITIVITY STUDIES

#### A.1 NODALIZATION

##### Radial Nodalization

EPRI has shown that the detailed radial noding, with which the core flow area is divided into unit subchannels, is needed only for the area in the vicinity of the hot channel [Ref.A-1]. The sensitivity studies conducted by Mitsubishi endorse this conclusion. The sensitivity study cases are listed in Table A.1-1 and the radial nodal configurations for the sensitivity studies are shown in Figure A.1-1 for comparison purpose. The 21-channel model (reference case), which is recommended as the standard design model, is shown in Figure 4-1 of this report. The results shown in Figure A.1-2 and A.1-3, and in Table A.1-1 indicate that different radial nodalization models do not have any appreciable impact on the DNBR analysis, as long as the flow cells surrounding the hot rod are modeled into detailed subchannels.

The reference case, the 21 flow channel model, was selected as a standard model for the DNB analysis.

**Table A.1-1 Sensitivity Study on Radial Nodalization**

Case	No. of channels	Min. DNBR (WRB-2)		
		Nominal condition	Over power condition(*)	High $F_{\Delta H}^N$ condition (**)

(\*)  $\left( \frac{\text{Power}}{\text{Area}} \right)$  of rated power

(\*\*)  $F_{\Delta H}^N = \left( \frac{\Delta T}{\Delta T_{\text{sat}}} \right)$



**Axial Nodalization**

EPRI has stated that VIPRE-01 predictions are sensitive to axial noding so that enough nodes must be provided to resolve the details in the flow field [Ref.A-1]. Sensitivity studies were performed to determine the number of axial nodes needed. Analyzed cases are shown in Figure A.1-4. Results are shown in Table A.1-2 and Figure A.1-5 through Figure A.1-7. [

These results reveal that about 20 nodes in the axial direction are adequate for thermal-hydraulic analysis of flow redistribution in the core. ]

**Table A.1-2 Sensitivity Study on Axial Nodalization**

Case	No. of axial nodes in the heated length	Min. DNBR (WRB-2)		
		Nominal condition	Over power condition(*)	High $F_{\Delta H}^N$ condition (**)

(\*)  $F_{\Delta H}^N$  of rated power  
 (\*\*)  $F_{\Delta H}^N = \{ \quad \}$

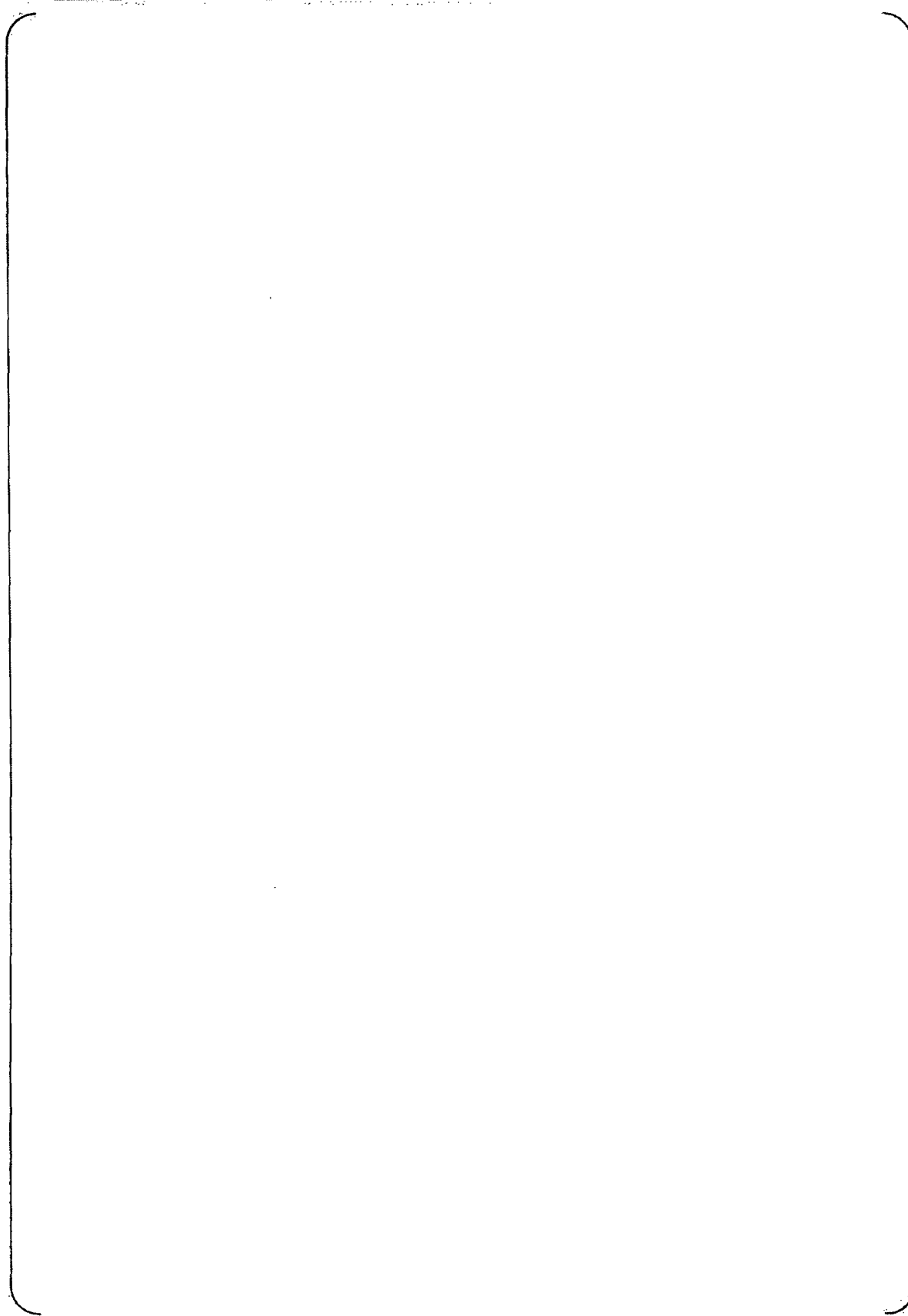


**Figure A.1-1 Sensitivity Study Cases for Radial Nodalization**

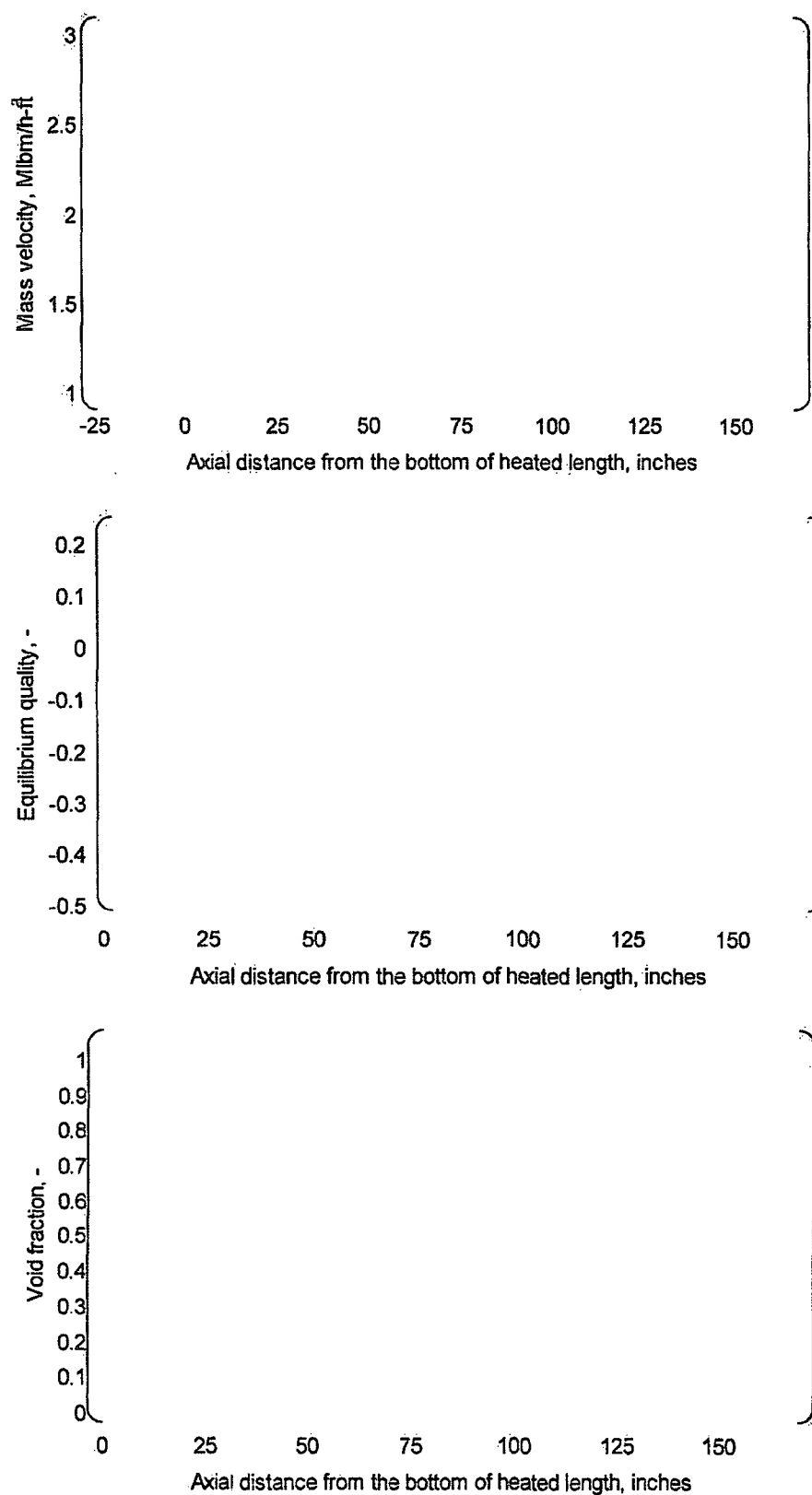


**Figure A.1-2 Sensitivity Study on Radial Nodalization  
(Over Power Condition, Typical Cell)**

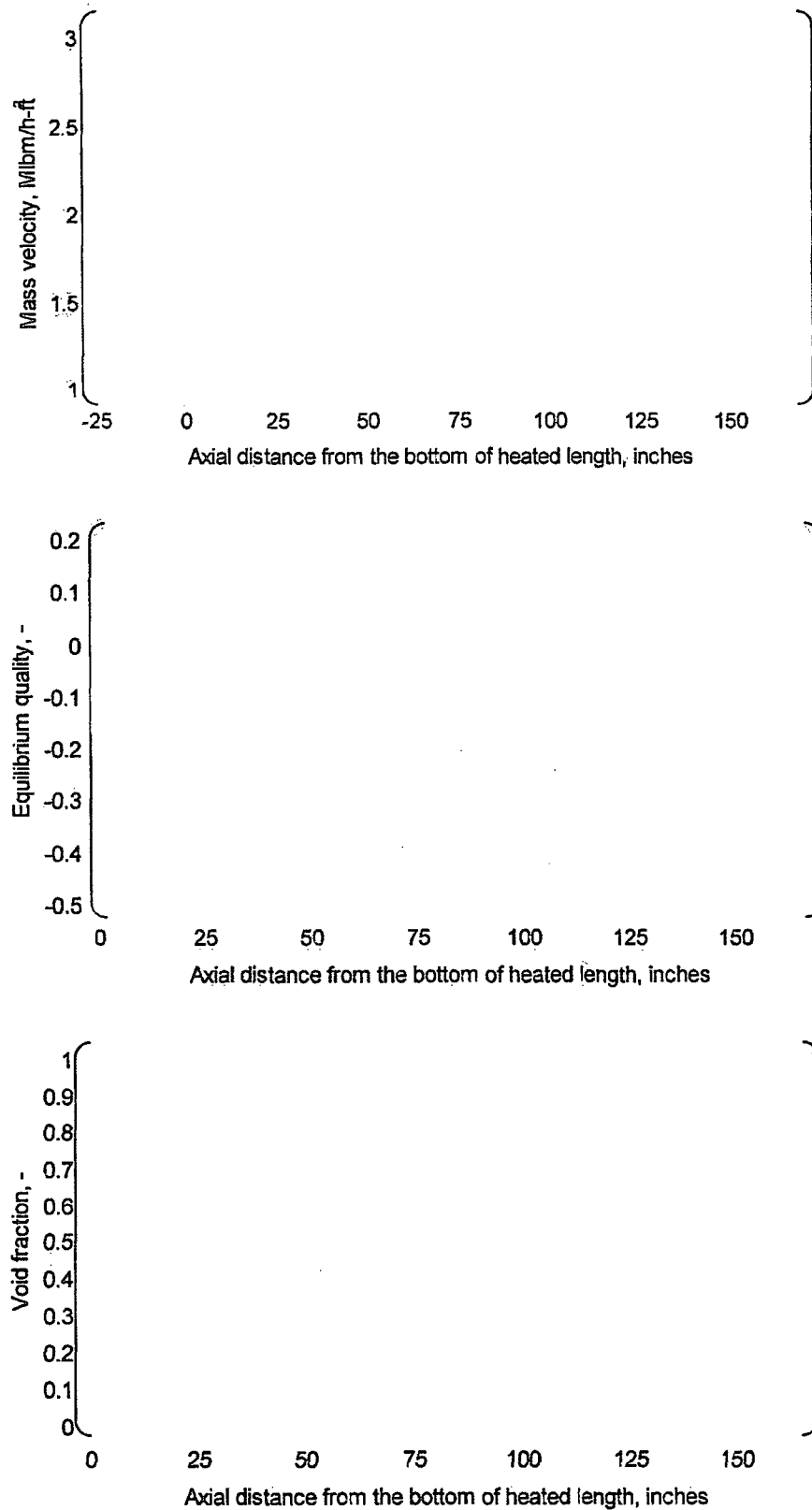


**Figure A.1-3 Sensitivity Study on Radial Nodalization  
(Over Power Condition, Thimble Cell)**

**Figure A.1-4 Sensitivity Study Cases for Axial Nodalization**

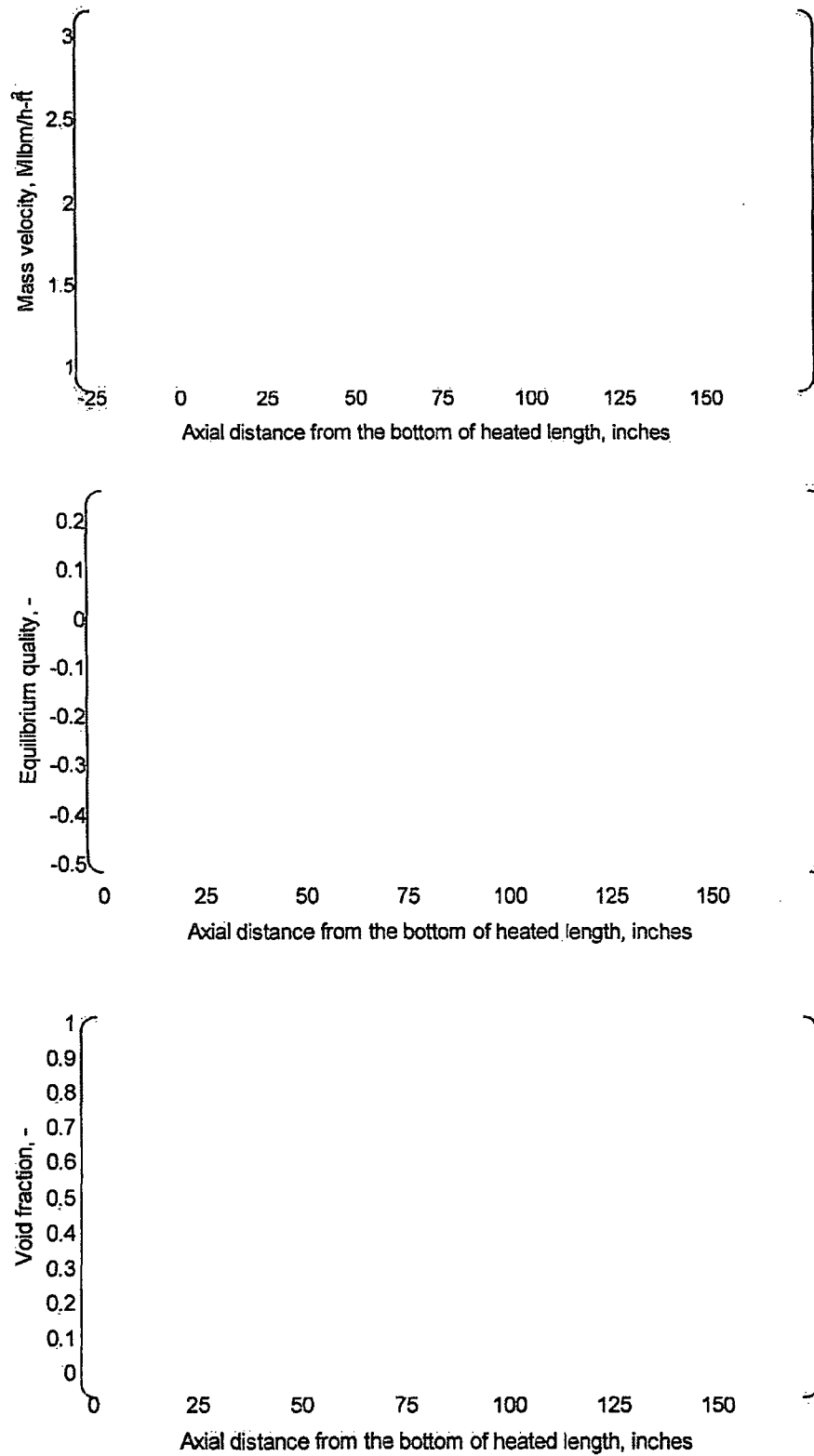


**Figure A.1-5 Sensitivity Study on Axial Nodalization  
(Over Power Condition, Typical Cell)**

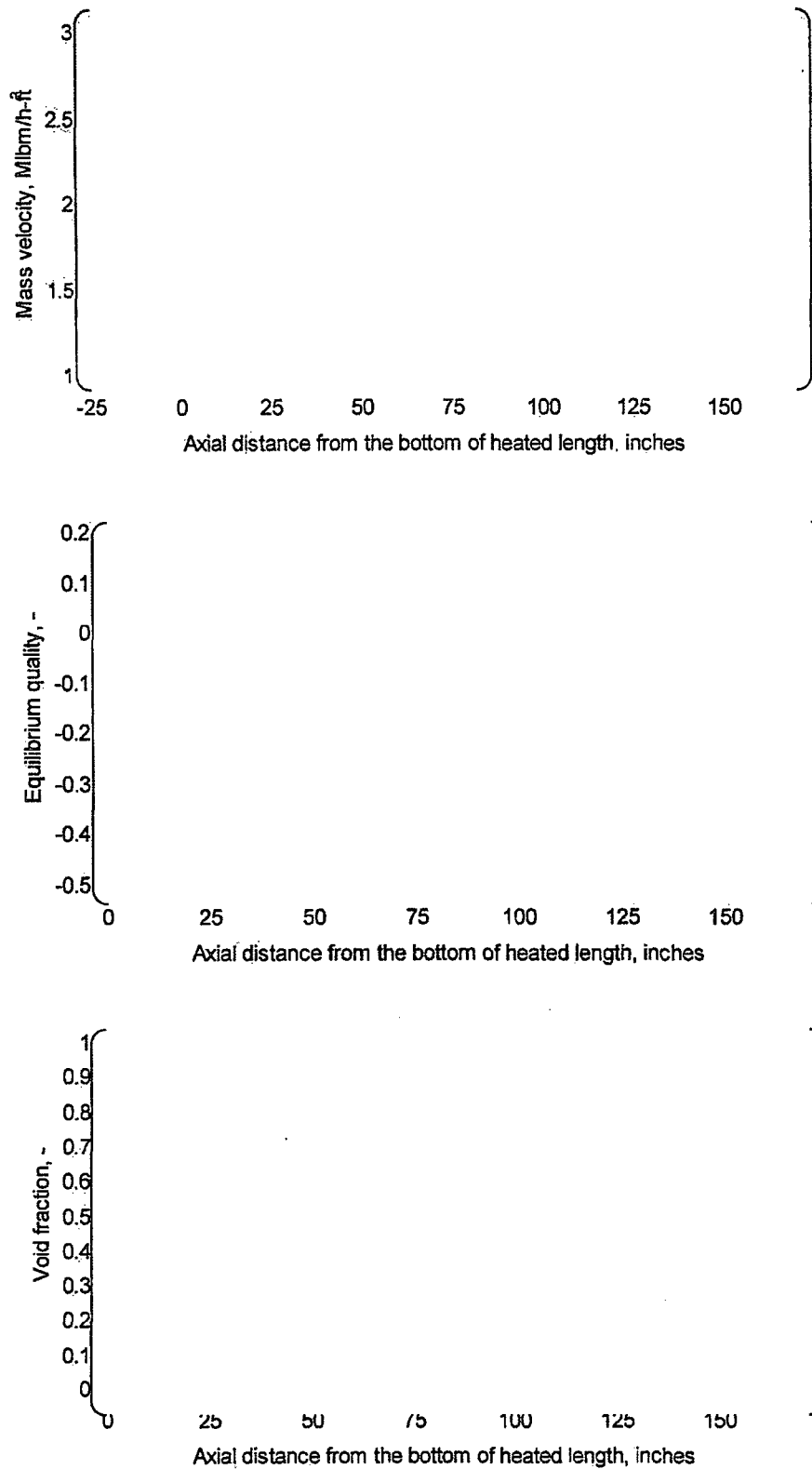


**Figure A.1-6 Sensitivity Study on Axial Nodalization  
(Over Power Condition, Thimble Cell)**

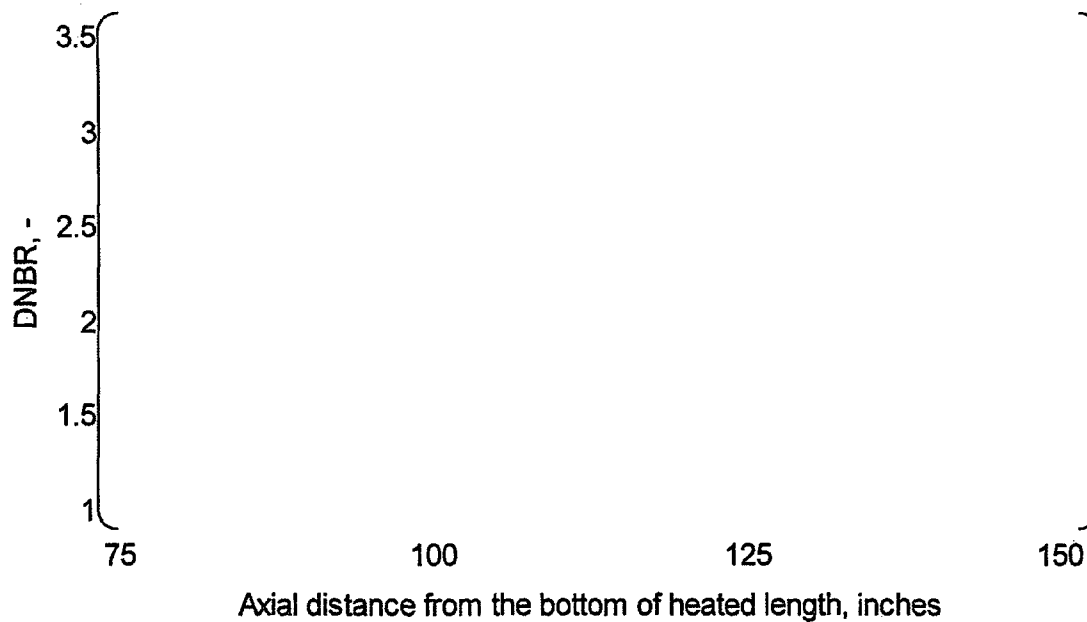
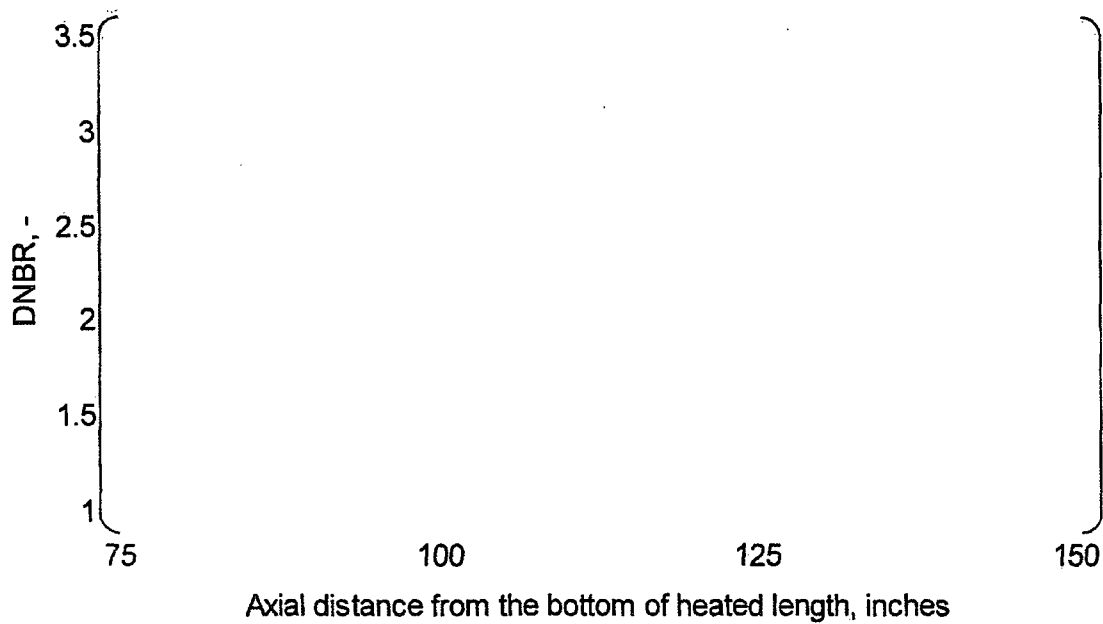


**Figure A.1-7 Sensitivity Study on Axial Nodalization  
(DNBR)**



## A.2 TURBULENT MIXING

Turbulent mixing is expressed by Equation (4.3) of this report. The mixing parameter ABETA is defined as a constant. Although the mixing parameter is an important parameter for adequately predicting hot channel conditions, its effect on DNB design analysis is relatively small. It is because, for typical core modeling, VIPRE-01M analysis is conducted under the condition [ ] under which the cross-channel mixing effect becomes minimized.

The sensitivity studies for ABETA were performed for the cases listed in Table A.2-1. The hot channel thermal-hydraulic conditions were not significantly affected by different ABETA values as shown in Figure A.2-1 and Figure A.2-2. DNBR results in Table A.2-1 show relatively small effects in DNBR when different ABETA were adopted.

Table A.2-1 Sensitivity Study on Turbulent Mixing Parameter ABETA

Case	ABETA	Min. DNBR (WRB-2)		
		Nominal condition	Over power condition(*)	High $F_{\Delta H}^N$ condition (**)

(\*) [ ] of rated power  
 (\*\*)  $F_{\Delta H}^N = [ ]$

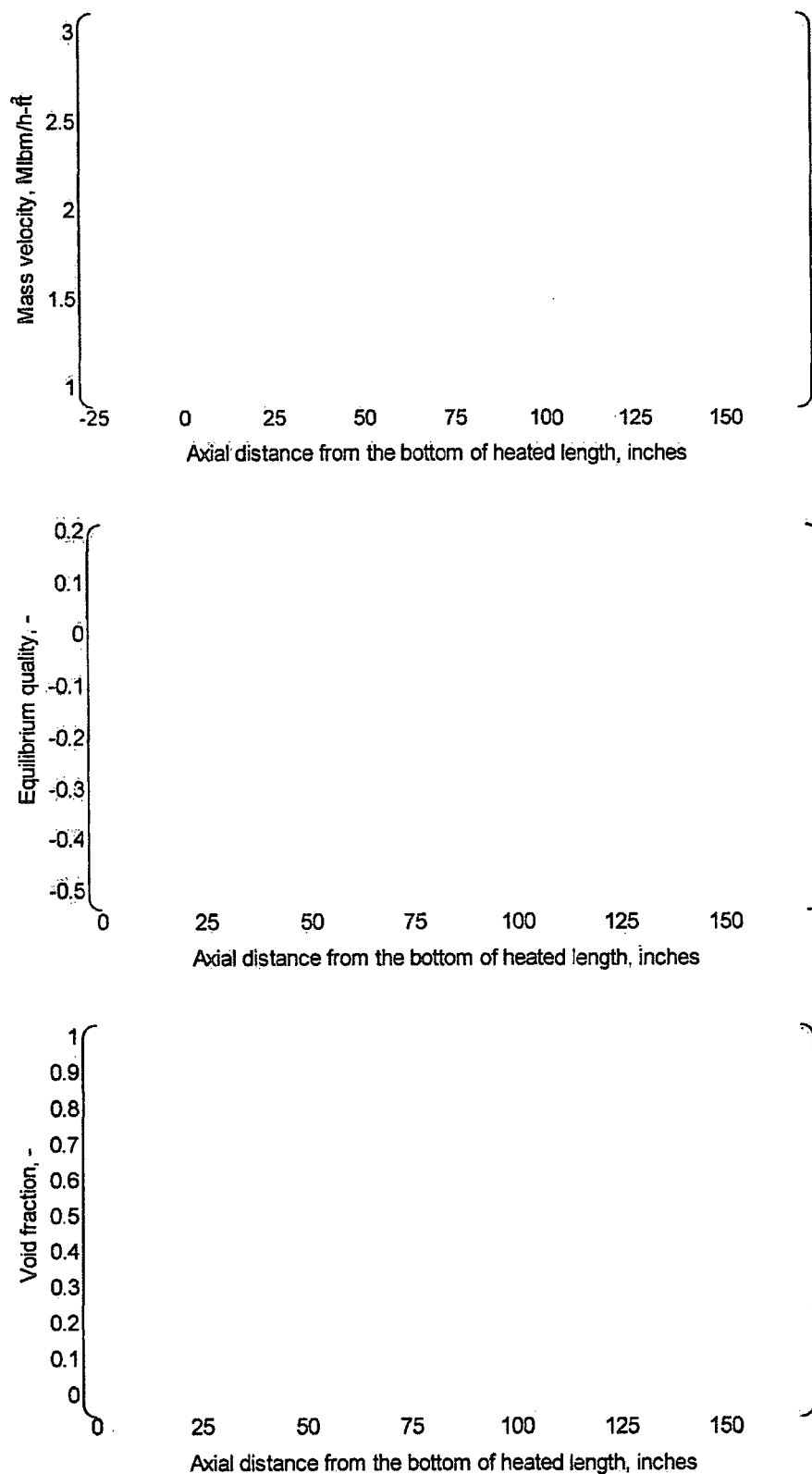


**Figure A.2-1 Sensitivity Study on Turbulent Mixing Parameter  $ABETA$   
(Over Power Condition, Typical Cell)**

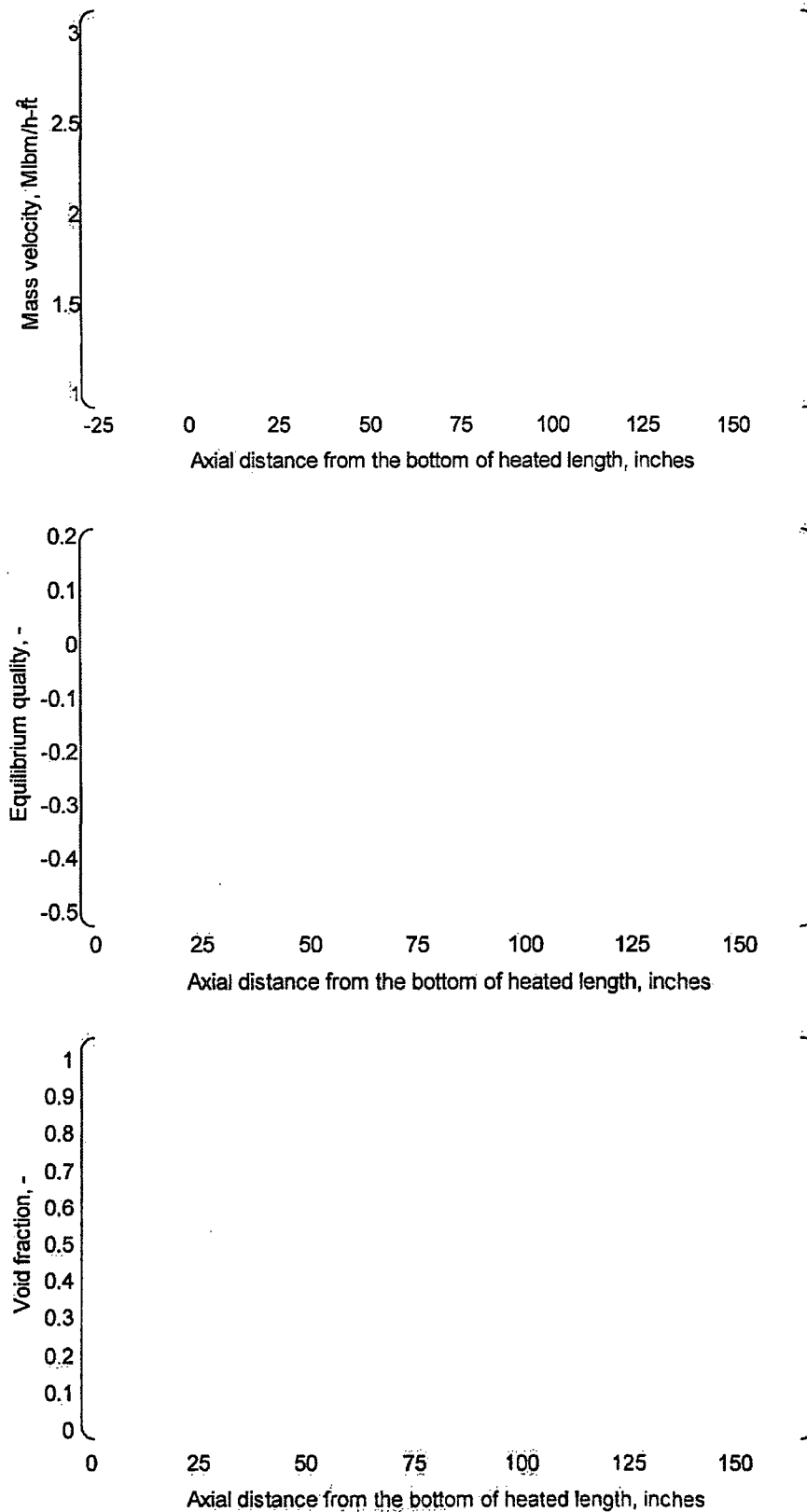


**Figure A.2-2 Sensitivity Study on Turbulent Mixing Parameter ABETA  
(Over Power Condition, Thimble Cell)**

### A.3 HYDRAULIC RESISTANCE

#### Axial Hydraulic Resistance

In the VIPRE-01M analysis, a Blasius type empirical correlation is used for the axial friction factor, which is a function of the Reynolds number. This formulation is shown in Equation (4.5) of this report.

The sensitivity studies have been performed for the three sets of coefficients  $a_f$ ,  $b_f$  and  $c_f$  which are shown in Table A.3-1. The reference case is a commonly used correlation [

Case 1 is the Blasius correlation [

Case 2 is a coefficient set selected to approximate

Moody's diagram [

The sensitivity studies indicate that the axial friction factor has a relatively small effect on the DNB analyses.

**Table A.3-1 Sensitivity Study on Axial Friction Factor**

Case	Coefficients			Min. DNBR (WRB-2)		
	$a_f$	$b_f$	$c_f$	Nominal condition	Over power condition(*)	High $F_{\Delta H}^N$ condition (**)
<div style="text-align: right;">           (*) <math>\left[ \frac{f}{f_{ref}} \right]</math> of rated power            (**) <math>F_{\Delta H}^N = \left[ \frac{F_{\Delta H}^N}{F_{\Delta H}^{N,ref}} \right]</math> </div>						

#### Radial Hydraulic Resistance

Radial loss coefficient at the rod-to-rod gap, which is defined by Equation (4.7) of this report, is manipulated for the sensitivity study purposes. Radial loss coefficient of the reference case is based on [ ] The sensitivity studies are performed using double the original  $a_g$  value and half of the original  $a_g$  value as shown in Table A.3-2. The results show that the effect of radial loss coefficient on DNB analyses is negligible.

**Table A.3-2 Sensitivity Study on Radial Loss Coefficient**

Case	Coefficients			Min. DNBR (WRB-2)		
	$a_g$	$b_g$	$c_g$	Nominal condition	Over power condition(*)	High $F_{\Delta H}^N$ condition (**)
<div style="text-align: right;">           (*) <math>\left[ \frac{f}{f_{ref}} \right]</math> of rated power            (**) <math>F_{\Delta H}^N = \left[ \frac{F_{\Delta H}^N}{F_{\Delta H}^{N,ref}} \right]</math> </div>						

#### A.4 TWO-PHASE FLOW MODEL

The two-phase flow model in VIPRE-01M mainly consists of the following models.

- Subcooled Boiling Model
- Bulk Void / Quality Relation
- Two-Phase Friction Multiplier

The two-phase flow model may strongly affect the flow redistribution in the core. Therefore, careful attention should be paid and the model should be selected conservatively.

Regarding void / quality relation, [ ]

In the typical PWR conditions, [ ]

Therefore, [ ]

[ ] are chosen as a reference case. [ ] EPRI's survey showed that EPRI's two-phase model gives fairly good prediction for the wide range of coolant conditions. [ ]

The sensitivity studies for the wide range of conditions shown in [ ] are conducted and the results are presented in [ ] of this report. The results show that the reference model gives relatively larger void fraction and more conservative DNBR predictions at the conditions in which the boiling is dominant.

## A.5 CORE INLET FLOW DISTRIBUTION

Core inlet flow distribution is one of the input boundary conditions for core thermal-hydraulic analyses. From the existing flow test, several flow distribution patterns are observed at the core inlet. However, it hardly affects the DNBR analysis, because the PWR core has an open lattice configuration. Inlet flow distribution is immediately flattened at the lower portion of the core.

The sensitivity studies for the core inlet flow distribution are shown in the Table A.5-1, and Figure A.5-1 and A.5-2. The results show that the effect of core inlet flow distribution is negligible small.

**Table A.5-1 Sensitivity Study on Core Inlet Flow Distribution**

Case	Hot Assembly Inlet Flow (% of core average)	Min. DNBR (WRB-2)		
		Nominal condition	Over power condition(*)	High $F_{\Delta H}^N$ condition (**)

(\*)  $\left[ \frac{\text{Power}}{\text{Rated Power}} \right]$  of rated power  
 (\*\*)  $F_{\Delta H}^N = \left[ \frac{\text{Power}}{\text{Rated Power}} \right]$

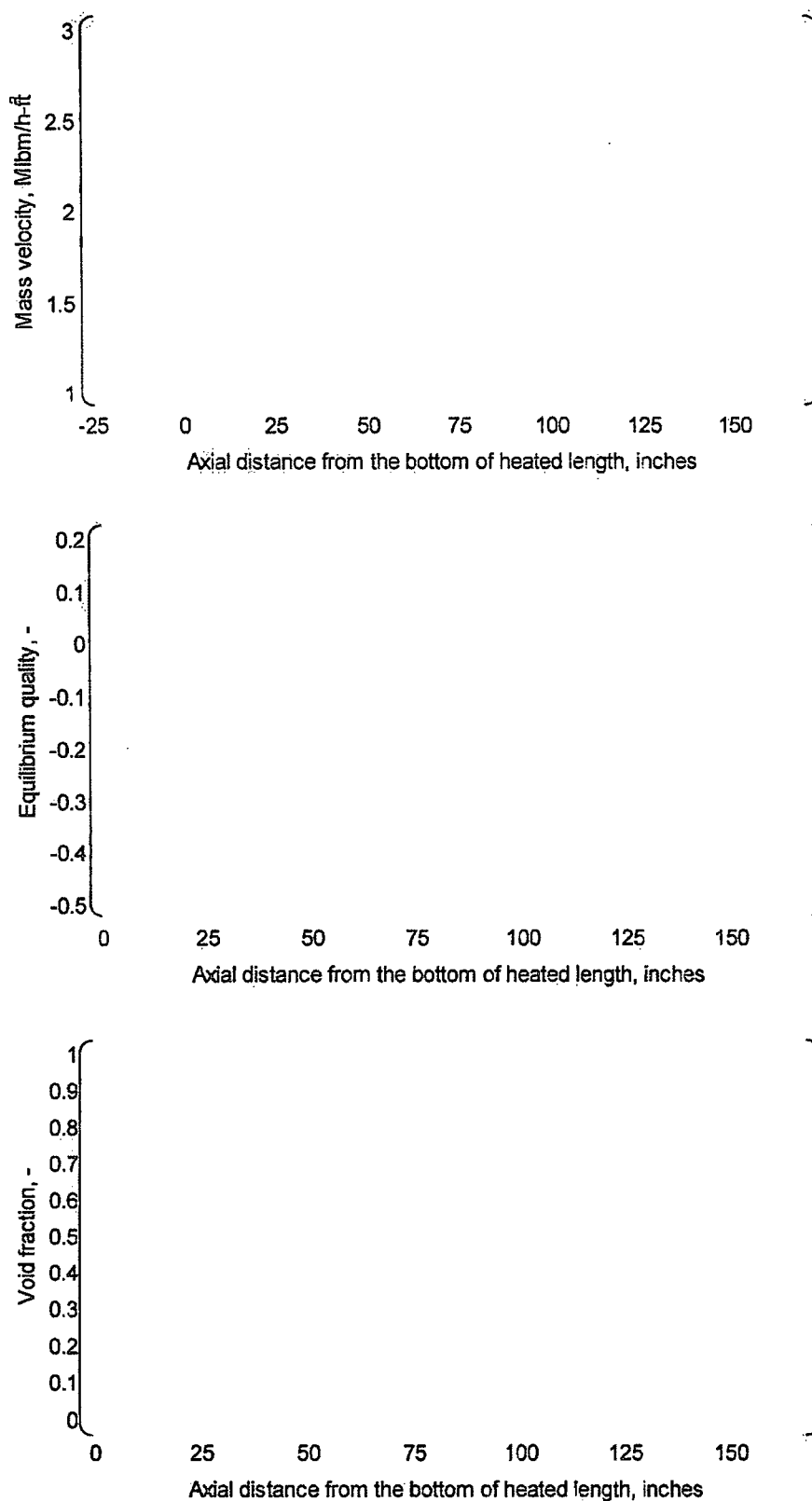


**Figure A.5-1 Sensitivity Study on Hot Assembly Inlet Flow  
(Over Power Condition, Typical cell)**

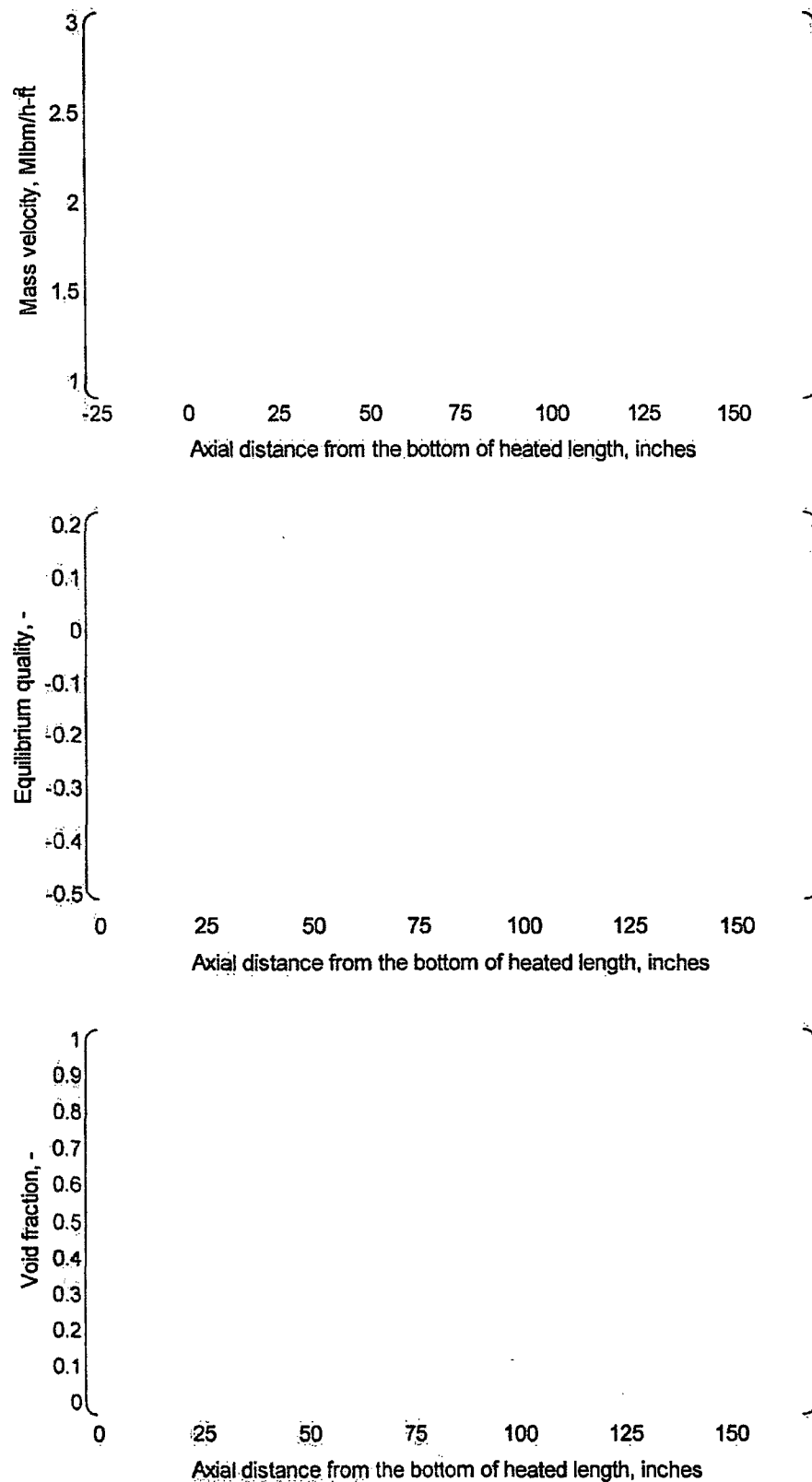


**Figure A.5-2 Sensitivity Study on Hot Assembly Inlet Flow  
(Over Power Condition, Thimble cell)**



## A.6 TIME STEP SIZE

In the VIPRE-01M transient analysis, time step size is specified as an input. User should select time step size for the transient condition appropriately. Generally, smaller time step size is considered in order to derive more accurate and more reliable results in transient analysis. However, when profile fit type void model is used, it is required for numerical stability reason that time step size is selected to keep the Courant number greater than 1. A sensitivity study on the time step size was conducted to obtain the reasonable time step size and axial mesh size for thermal-hydraulic core analyses.

A Loss of Flow analysis shown in Section 7.2.2 is selected as a reference case analysis. In conducting the sensitivity study on time step size{ } smaller axial mesh size corresponding to{ } is selected to keep the Courant number greater than 1

As shown in Table A.6-1, the results indicate that{ } time step size provides a sufficient accuracy in such transient analysis. For that time step size, the axial mesh size less than{ } can keep the Courant number greater than 1 under the condition{ } Those limitations are reasonable for typical thermal-hydraulic core analyses.

**Table A.6-1 Sensitivity Study on Time Step Size**

Case	Time step size (s)	Min. DNBR (WRB-1)

## A.7 REFERENCE

- A-1. C. W. Stewart and J. M. Cuta, et al., "VIPRE-01: A Thermal-Hydraulic Code for Reactor Cores, Volume 5 (Revision 4): Guidelines", NP-2511-CCM-A, Electric Power Research Institute (EPRI), February 2001

## APPENDIX B

# QUALIFICATION OF WRB-1/2 DNB CORRELATIONS WITH VIPRE-01M

### B.1 INTRODUCTION

Mitsubishi intends to apply both WRB-1 and WRB-2 DNB correlations [Ref.B-1, B-2] for its PWR core thermal-hydraulic designs. Local coolant conditions required by the DNB correlations are provided by its subchannel analysis code VIPRE-01M. This appendix documents the qualification of WRB-1 and WRB-2 with VIPRE-01M to ensure that Mitsubishi can use both DNB correlations with VIPRE-01M for PWR core design. In the qualification process, DNB data analyses using the original data sets of WRB-1 and WRB-2 were conducted.

### B.2 WRB-1/WRB-2 DNB CORRELATIONS

#### B.2.1 WRB-1 DNB Correlation

WRB-1 DNB correlation was developed based on the Westinghouse's R-grid and L-grid rod bundle DNB test data. The verification of WRB-1 was conducted in conjunction with THINC code and it was already approved by the NRC in 1984 [Ref.B-1].

The WRB-1 provides a predicted DNB heat flux  $q''_{WRB-1}$  by the following formulation;

$$\frac{q''_{WRB-1}}{10^6} = PF + A_1 + B_3 \frac{(G_{LOC})}{10^6} - B_4 \frac{(G_{LOC})}{10^6} X_{LOC} \quad (B.1)$$

where  $PF$  is a performance factor dependent on a rod diameter defined in Ref.B-1,  $G_{LOC}$  and  $X_{LOC}$  are local mass flux and local quality, respectively. The specific formulations of  $A_1$ ,  $B_3$  and  $B_4$  are Westinghouse proprietary information which can be found in Ref.B-1. The applicable range of WRB-1 is summarized as follows.

Pressure:	$1440 \leq P \leq 2490$	(psia)
Local mass flux:	$0.9 \leq G_{LOC}/10^6 \leq 3.7$	(lbm/h-ft <sup>2</sup> )
Local quality:	$-0.2 \leq X_{LOC} \leq 0.3$	(-)
Heated length:	$L_h \leq 14$	(feet)
Grid spacing:	$13 \leq g_{sp} \leq 32$	(inches)
Equivalent hydraulic diameter:	$0.37 \leq d_e \leq 0.60$	(inches)
Equivalent heated hydraulic diameter:	$0.46 \leq d_h \leq 0.58$	(inches)

#### B.2.2 WRB-2 DNB Correlation

WRB-2 DNB correlation was developed based on the Westinghouse's 17x17 fuel DNB test data including OFA and VANTAGE5. The verification of WRB-2 was conducted in conjunction with THINC code and it was already approved by the NRC in 1985 [Ref.B-2].

The WRB-2 provides a predicted DNB heat flux  $q''_{WRB-2}$  by the following formulation:

$$\frac{q''_{WRB-2}}{10^6} = A_1 + B_3 \frac{(G_{LOC})}{10^6} - B_4 \frac{(G_{LOC})}{10^6} X_{LOC} \quad (B.2)$$

The specific formulations of  $A_1$ ,  $B_3$  and  $B_4$  are Westinghouse proprietary information which can be found in Ref.B-2. The applicable range of WRB-2 is summarized as follows.

Pressure:	$1440 \leq P \leq 2490$	(psia)
Local mass flux:	$0.9 \leq G_{LOC}/10^6 \leq 3.7$	(lbm/h-ft <sup>2</sup> )
Local quality:	$-0.1 \leq X_{LOC} \leq 0.3$	(-)
Heated length:	$L_h \leq 14$	(feet)
Grid spacing:	$10 \leq g_{sp} \leq 26$	(inches)
Equivalent hydraulic diameter:	$0.37 \leq d_e \leq 0.51$	(inches)
Equivalent heated hydraulic diameter:	$0.46 \leq d_h \leq 0.59$	(inches)

### B.3. DNB DATA ANALYSES FOR WRB-1 AND WRB-2

#### B.3.1 Data Base for Analyses

WRB-1 was developed based on 24 DNB test cases including Westinghouse's R-grid and L-grid rod bundles [Ref.B-1]. All data were acquired at the Heat Transfer Research Facility of Columbia University and EPRI report [Ref.B-3] summarized all the database, such as test bundle geometries, flow conditions and measured DNB heat fluxes. Mitsubishi analyses were conducted based on the data base presented in the EPRI report. Among the 24 test cases, [ ] for R-grid rod bundle were applied for Mitsubishi qualification process as shown in Table B.3-1. In each test case, data points were basically chosen to be corresponding with those used in the development of THINC/WRB-1 [Ref.B-1]. However, some data were not used in Mitsubishi analyses as shown hereunder.

WRB-2 was developed based on 11 test cases including Westinghouse's R-grid, OFA and VANTAGE5 rod bundles [Ref.B-2]. Among the 11 cases, [ ] for R-grid rod bundles were applied to Mitsubishi qualification as shown in Table B.3-2. The data points in each test case were completely corresponding with those picked up in the WRB-1 data base.

**Table B.3-1 Data Base for WRB-1/VIPRE-01M Analyses**

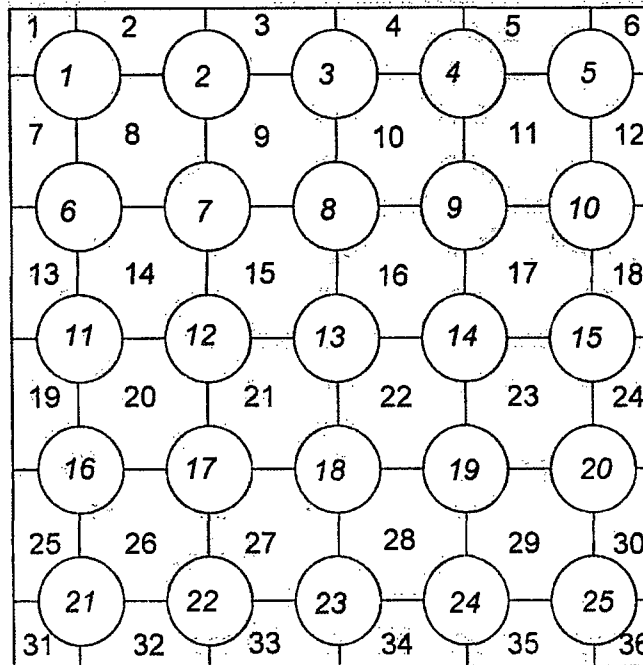
Test case	Geometry	Heater rod diameter (inches)	Thimble tube diameter (inches)	Heated length (feet)	Axial heat flux distribution	Grid spacing (inches)	Number of data points
-----------	----------	------------------------------	--------------------------------	----------------------	------------------------------	-----------------------	-----------------------

**Table B.3-2 Data Base for WRB-2/VIPRE-01M Analyses**

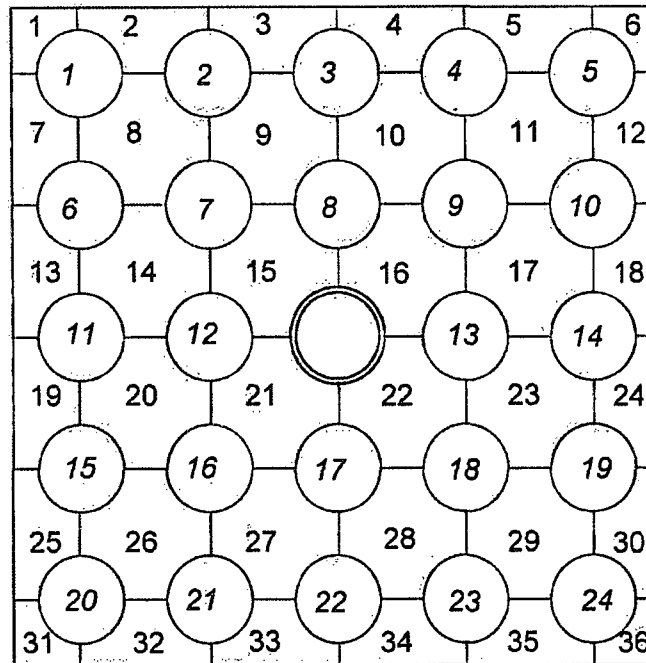
Test case	Geometry	Heater rod diameter (inches)	Thimble tube diameter (inches)	Heated length (feet)	Axial heat flux distribution	Grid spacing (inches)	Number of data points
-----------	----------	------------------------------	--------------------------------	----------------------	------------------------------	-----------------------	-----------------------

### **B.3.2 Modeling**

The VIPRE-01M modeling for the 5x5 and 4x4 test geometries are shown in Figure B.3-1 and B.3-2, respectively. All the heater rods and the subchannels in a full test bundle were simulated in a radial noding and individual radial power factors for heater rods were taken into account. In the axial direction, the heated length was divided into a sufficient number of nodes per the guideline proposed in Section 4.1 (2). The hydraulic resistance and the two-phase flow model adopted were those described in Sections 4.3 and 4.4, respectively.

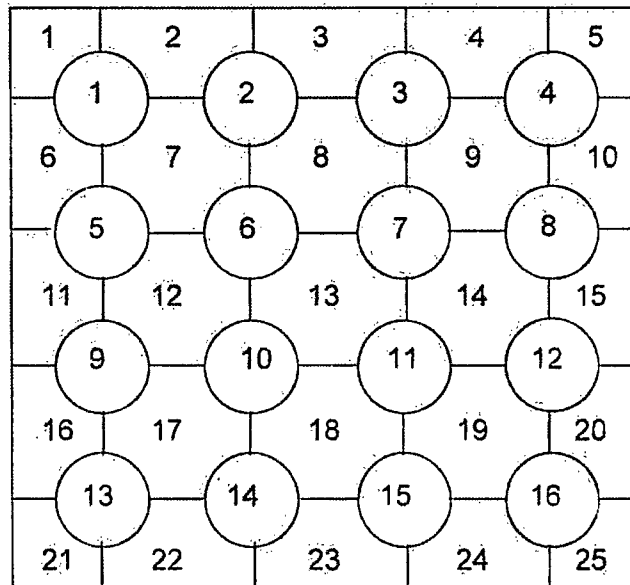


(a) Typical cell test section

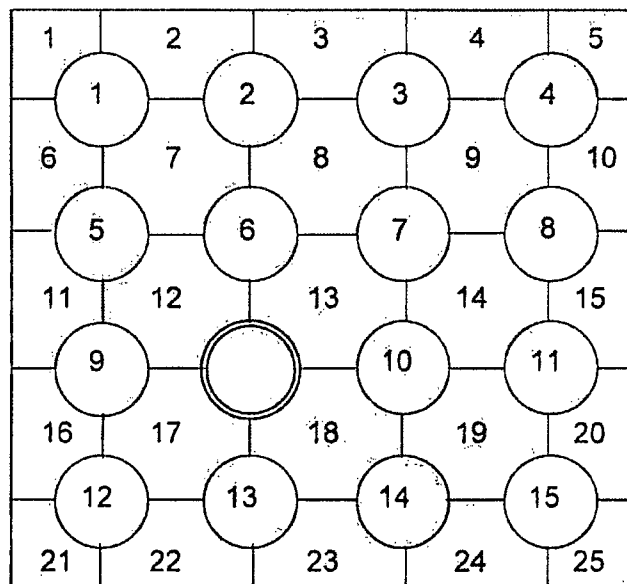


(b) Thimble cell test section

**Figure B.3-1 VIPRE-01M Modeling for 5x5 Test Geometries**



(a) Typical cell test section



(b) Thimble cell test section

**Figure B.3-2 VIPRE-01M Modeling for 4x4 Test Geometries**

### B.3.3 Results of Data Analyses

Table B.3-3 and B.3-4 show the summary of results for WRB-1 and WRB-2 DNB data base analyses, respectively. These tables show the number of data points ( $n$ ), the mean of M/P which is the ratio of measured to predicted DNB heat flux ( $m$ ) and the sample standard deviation of M/P ( $s$ ).

Based on the results in Tables B.3-3 and B.3-4, limit DNBR can be evaluated as follows;

$$\text{Limit DNBR}_{(95 \times 95)} = \frac{1}{m - k \cdot S} \quad (\text{B.3})$$

where  $k$  is a one-sided tolerance factor based on 95% confidence level and 95% portion of the population covered, and  $S$  is a modified sample standard deviation of M/P which takes into account the degree of freedom. The detail of statistical procedure to evaluate limit DNBR is shown in Tables B.3-5 and B.3-6. The number of  $k$  can be obtained from Ref.B-4. As a result, it was confirmed that limit DNBRs are less than 1.17 for both WRB-1 and WRB-2 data analyses.

Figure B.3-3 to B.3-10 show the data distribution of M/P and the dependency of M/P on local mass flux, system pressure and local quality conditions. Figures B.3-3 to B.3-6 illustrate the data plots for WRB-1 data analyses and the others for WRB-2 data analyses. These figures show that M/P data plots are uniformly distributed and there is no significant tendency against the fluid conditions.



**Table B.3-3 Data Analyses for WRB-1 Data Base**

Test case	Data points (n)	Mean of M/P (m)	Standard deviation of M/P (s)

**Table B.3-4 Data Analyses for WRB-2 Data Base**

Test case	Data points (n)	Mean of M/P (m)	Standard deviation of M/P (s)

**Table B.3-5 Statistical Procedure for Limit DNBR based on WRB-1 Data Base**

Number of data	n	
Degree of freedom	N	
Mean of M/P	m	
Standard deviation of M/P	s	
Modified Standard deviation of M/P	S	
Owen's k-factor	k	
Limit DNBR		

\*WRB-1 correlation includes( ) constants.

**Table B.3-6 Statistical Procedure for Limit DNBR based on WRB-2 Data Base**

Number of data	n	
Degree of freedom	N	
Mean of M/P	m	
Standard deviation of M/P	s	
Modified Standard deviation of M/P	S	
Owen's k-factor	k	
Limit DNBR		

\*WRB-2 correlation includes( ) constants.

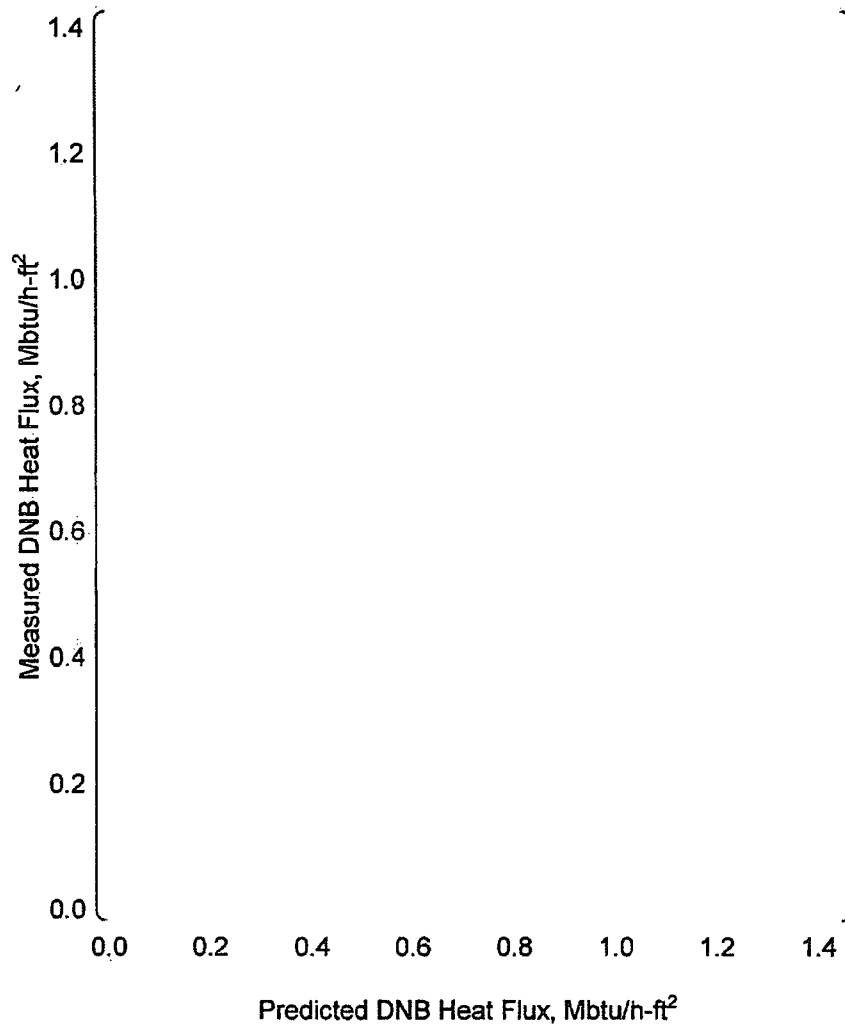


**Figure B.3-3 Measured vs. Predicted DNB Heat Flux based on WRB-1/IPRE-01M**

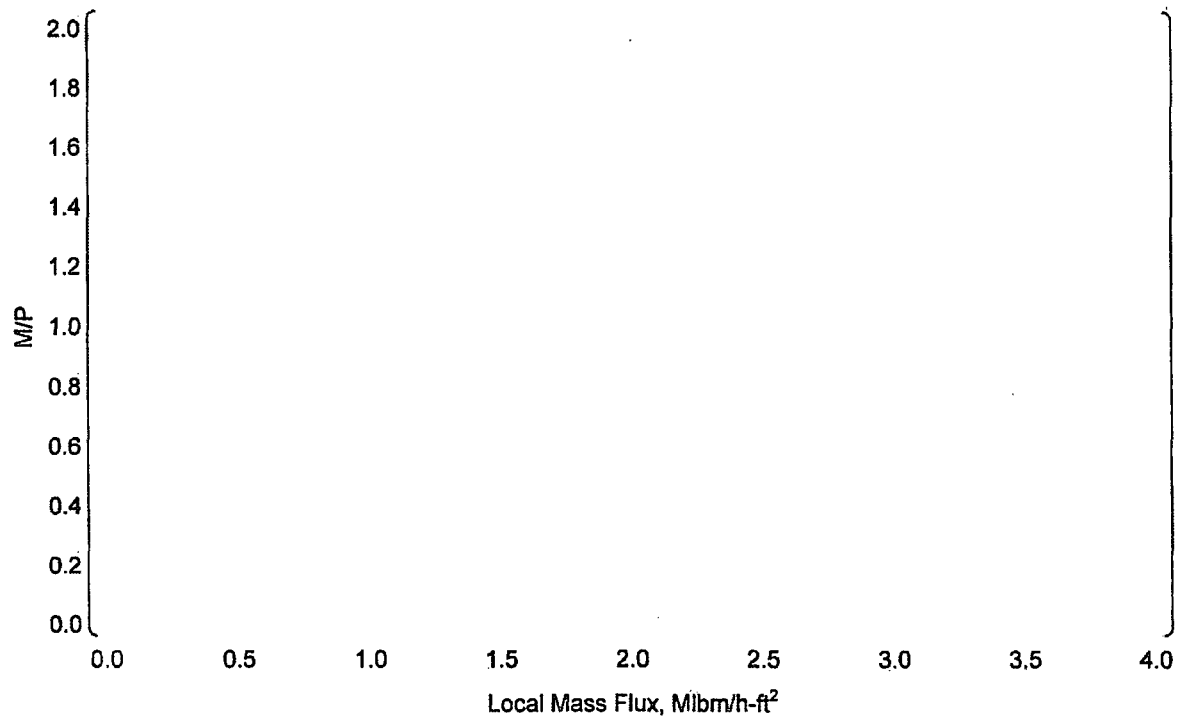
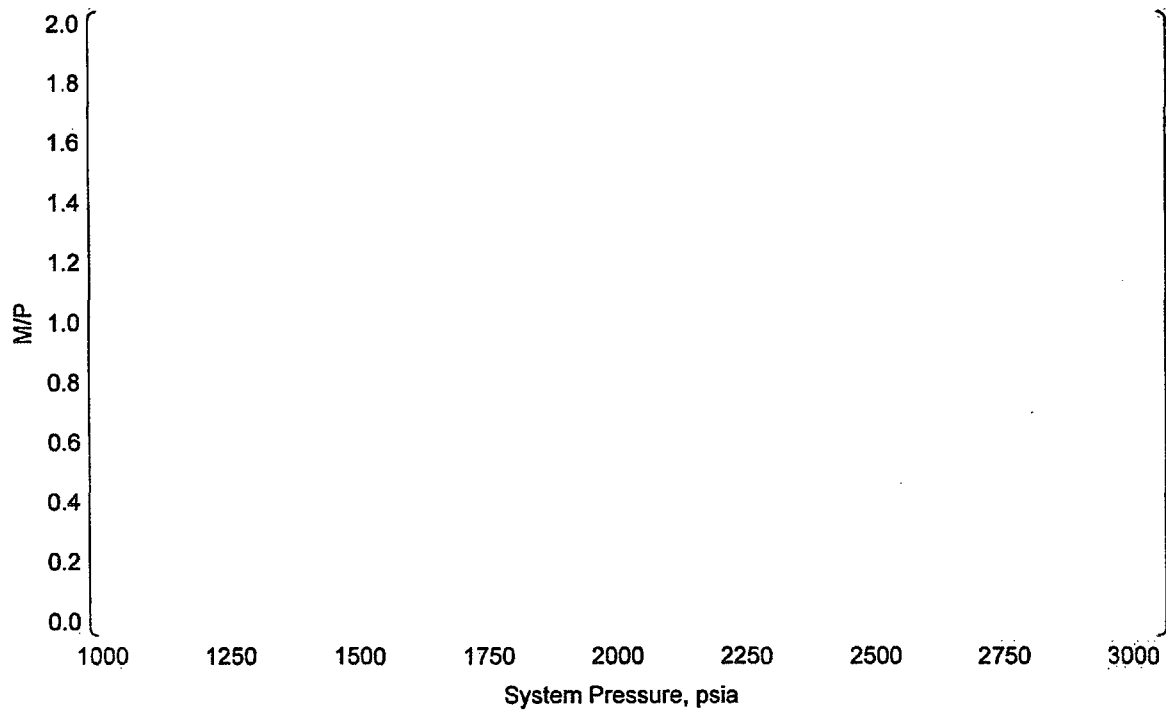
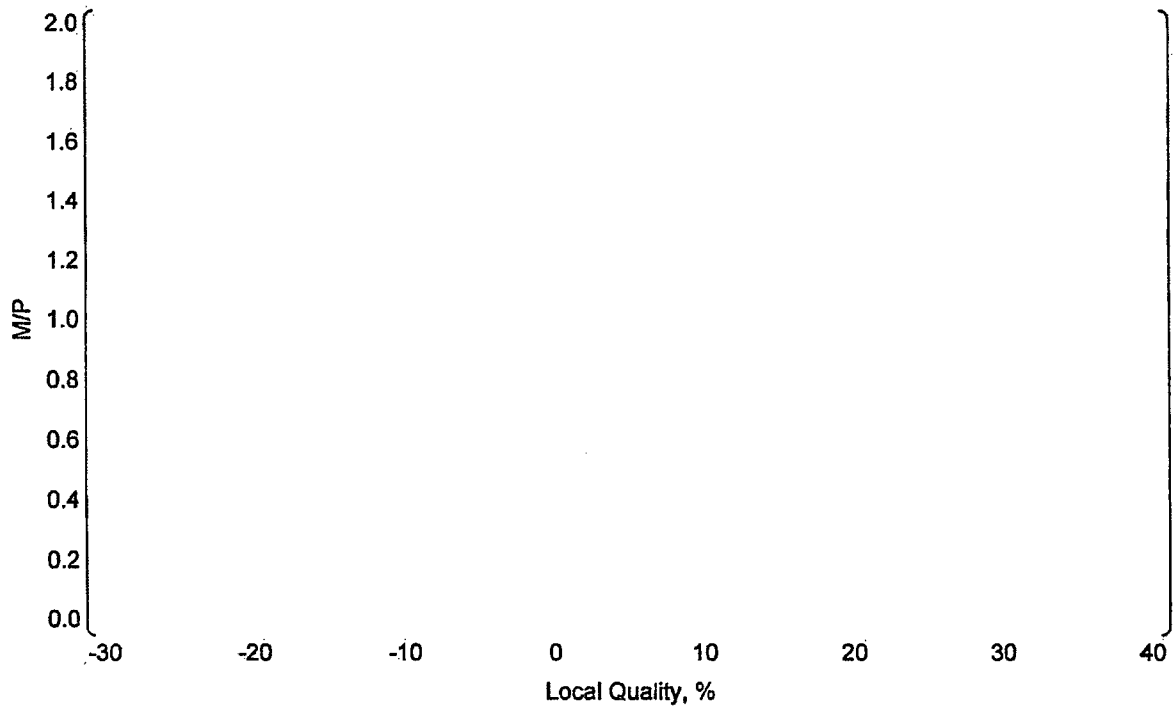


Figure B.3-4 M/P vs. Local Mass Flux based on WRB-1/VIPRE-01M



**Figure B.3-5 M/P vs. System Pressure based on WRB-1/VIPRE-01M**



**Figure B.3-6 M/P vs. Local Quality based on WRB-1/VIPRE-01M**

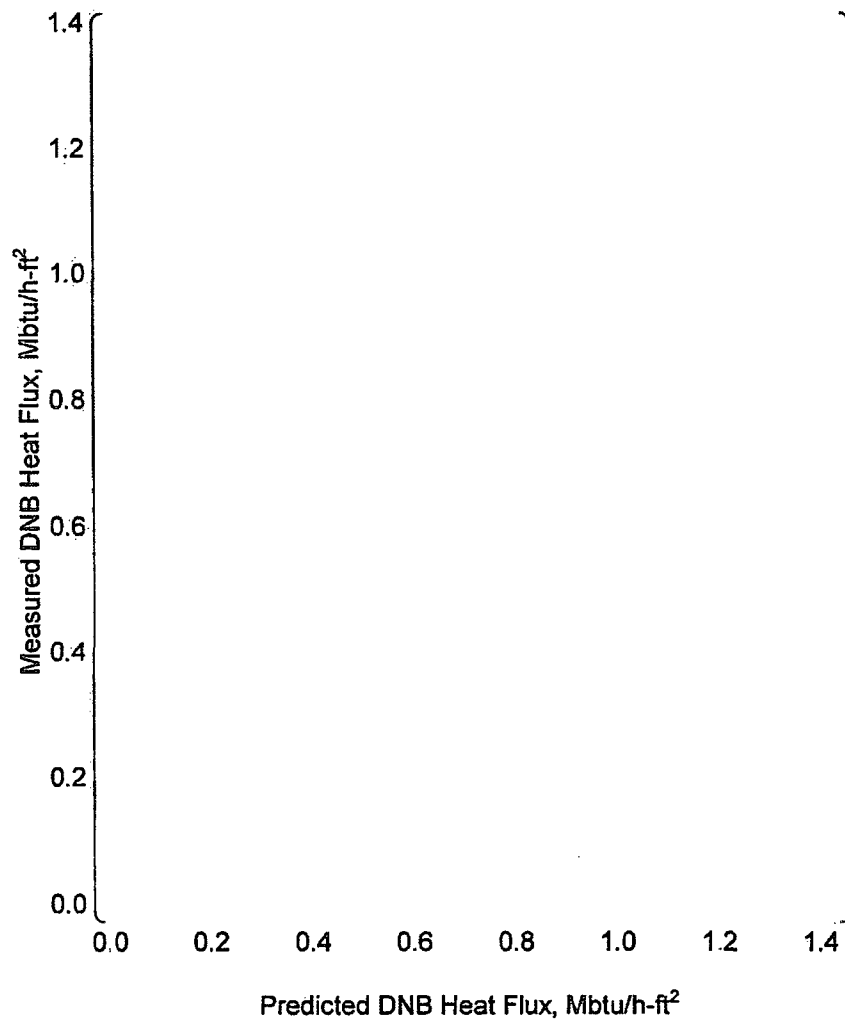


**Figure B.3-7 Measured vs. Predicted DNB Heat Flux based on WRB-2/VIPRE-01M**

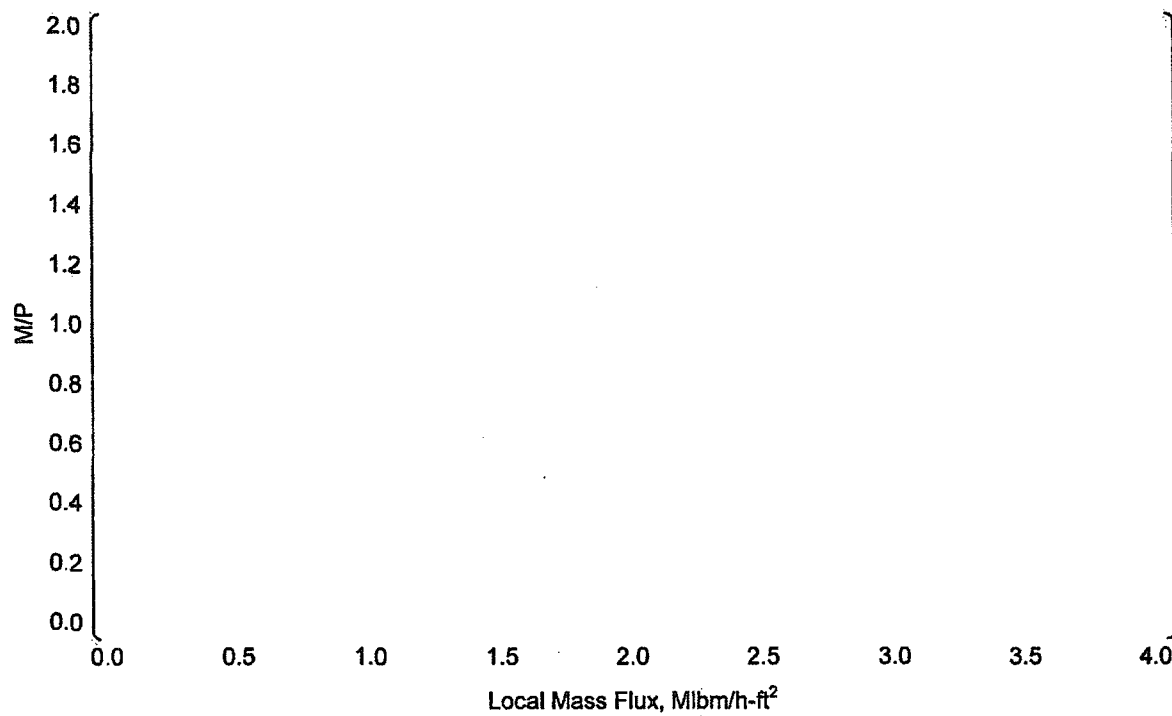
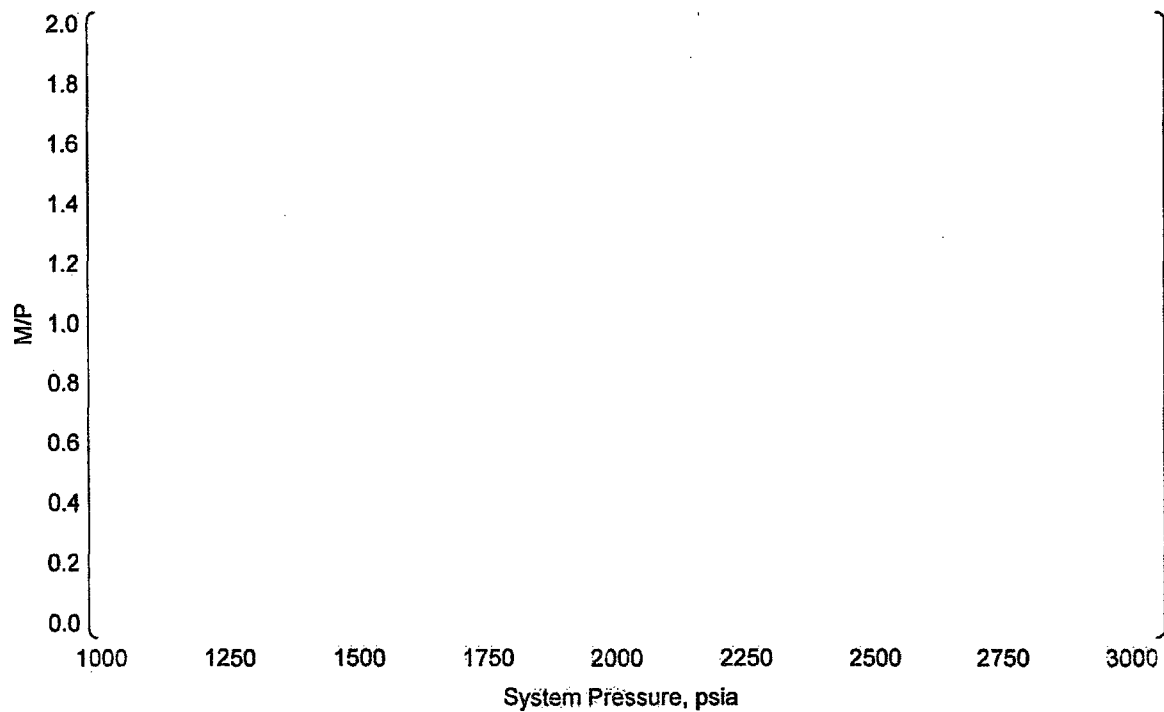
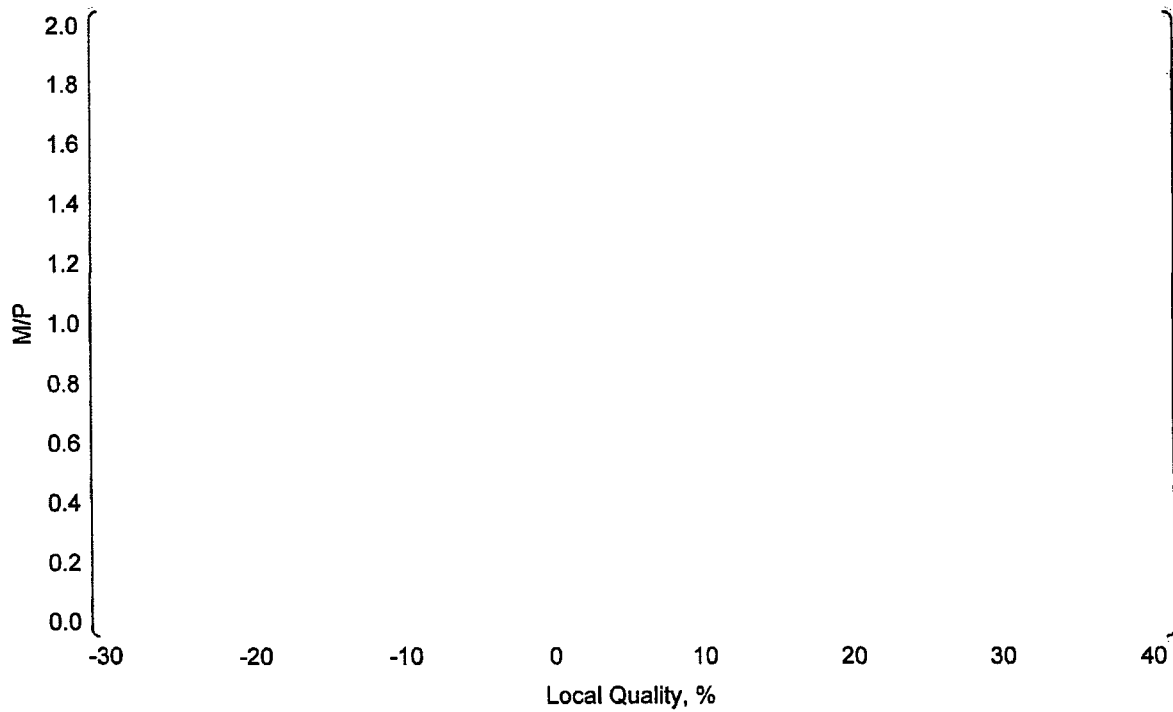


Figure B.3-8 M/P vs. Local Mass Flux based on WRB-2/VIPRE-01M





**Figure B.3-9 M/P vs. System Pressure based on WRB-2/VIPRE-01M**



**Figure B.3-10 M/P vs. Local Quality based on WRB-2/VIPRE-01M**

**B.4 CONCLUSION**

The verifications of WRB-1 and WRB-2 correlations with their own original data base were conducted based on VIPRE-01M. As a result, it was confirmed that (1) limit DNBRs on the 95% probability at 95% confidence level basis are less than 1.17 which were originally shown by Westinghouse in conjunction with THINC code, and (2) there is no significant tendency in M/P against fluid conditions. Therefore, it is concluded that WRB-1 and WRB-2 correlations are compatible with VIPRE-01M for PWR core design applications.

**B.5 REFERENCES**

- B-1. F. E. Motley, et al., "New Westinghouse Correlation WRB-1 for Predicting Critical Heat Flux in Rod Bundles with Mixing Vane Grids", WCAP-8762-P-A, 1984
- B-2. S. L. Davidson, "Reference Core Report Vantage 5 Fuel Assembly", WCAP-10444-P-A, 1985
- B-3. C. F. Fighetti & D.G. Reddy, "Parametric Study of CHF Data, Volume 3, Part 1: Critical Heat Flux Data Compilation", EPRI NP-2609, 1982
- B-4. R. E. Odeh & D. B. Owen, "Tables for Nominal Tolerance Limits, Sampling Plans, and Screening", 1980

## APPENDIX C

### APPLICABILITY OF WRB-1/2 CORRELATIONS FOR MITSUBISHI FUELS

#### C.1 INTRODUCTION

Mitsubishi conducted DNB tests for fuel assemblies with Zircaloy grid spacers named by Z2 and Z3 at the Heat Transfer Research Facility of Columbia University.

In this appendix, DNB data analyses for Z2 and Z3 were conducted to confirm the applicability of WRB-1 and WRB-2 DNB correlations for the two grid spacers. Local fluid conditions substituting in the DNB correlations were calculated based on VIPRE-01M code which was verified in Appendix B.

#### C.2 DNB TESTS FOR Z2 AND Z3 GRID SPACERS

Table C.2-1 summarizes the test geometries for four test cases containing typical cell and thimble cell tests for Z2 and Z3. The details of all test geometries are shown in Figure C.2-1 to C.2-4 for the radial geometry and in Figure C.2-5 to C.2-8 for the axial geometry.

The test section was composed of a 5x5 heater rod bundle and eight mixing vane grids oriented in the axial direction. In the two test cases Z2-2 and Z3-2, one unheated thimble tube was placed in the center to simulate a thimble cell.

The heated axial length of heater rods was 12 feet and each of the heater rods provided a non-uniform heat flux distribution in the axial direction, i.e., a chopped cosine shape of which peak-to-average ratio was ( ) Among the heater rods arranged 5x5 in the radial direction, the peripheral rods had about ( ) lower mean heat flux than the interior rods so as to prohibit the peripheral rods from the occurrence of DNB. To detect the onset of DNB, several thermocouples were axially located inside the heater rods and temperatures on the heater rod surface were measured during the test.

**Table C.2-1 DNB Test Section Geometry**

Test case	Geometry	Heater rod diameter (inches)	Thimble tube diameter (inches)	Heated length (feet)	Axial heat flux distribution	Grid spacing (inches)
-----------	----------	------------------------------	--------------------------------	----------------------	------------------------------	-----------------------



**Figure C.2-1 Radial Geometry and Power Distribution for Z2-1**

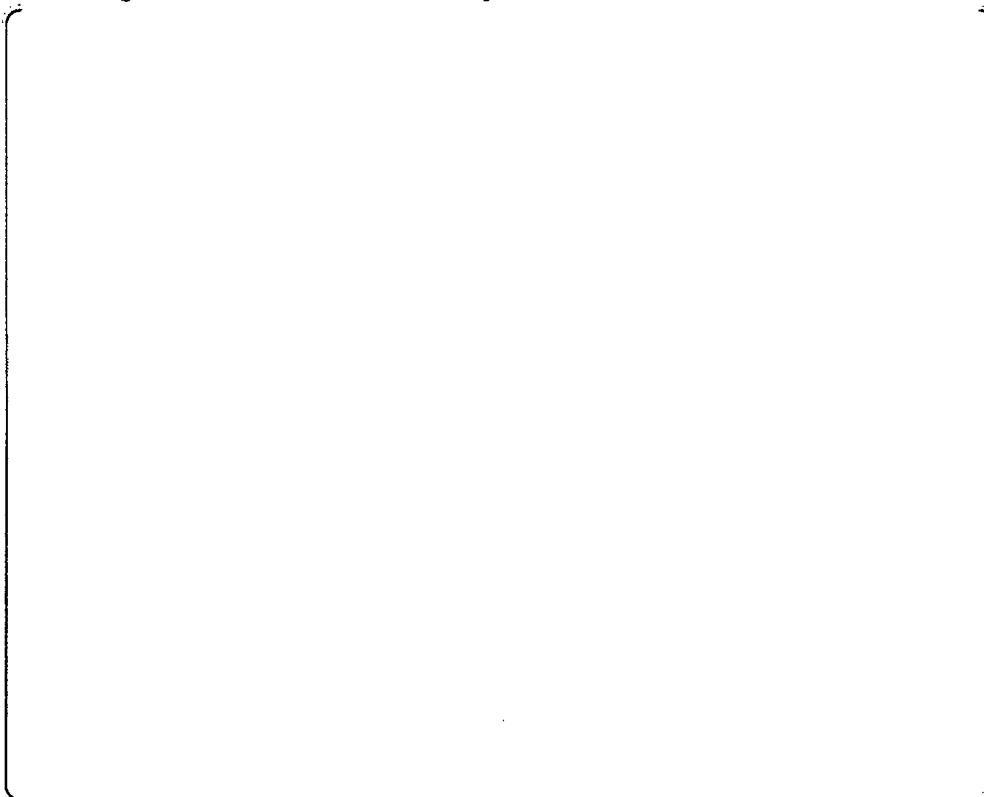


**Figure C.2-2 Radial Geometry and Power Distribution for Z2-2**



**Figure C.2-3 Radial Geometry and Power Distribution for Z3-1**



**Figure C.2-4 Radial Geometry and Power Distribution for Z3-2**

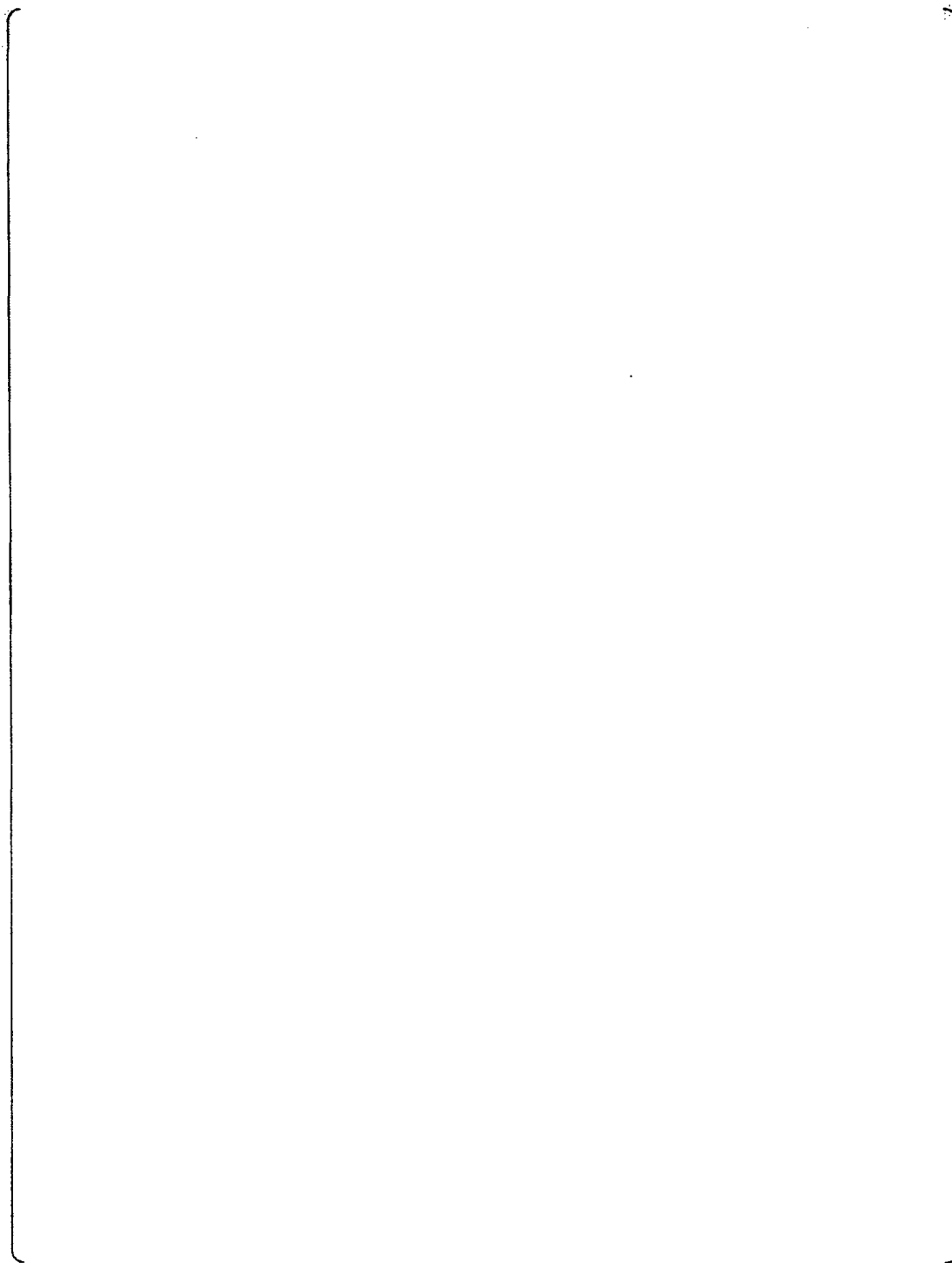


**Figure C.2-5 Axial Geometry for Z2-1**



**Figure C.2-6 Axial Geometry for Z2-2**



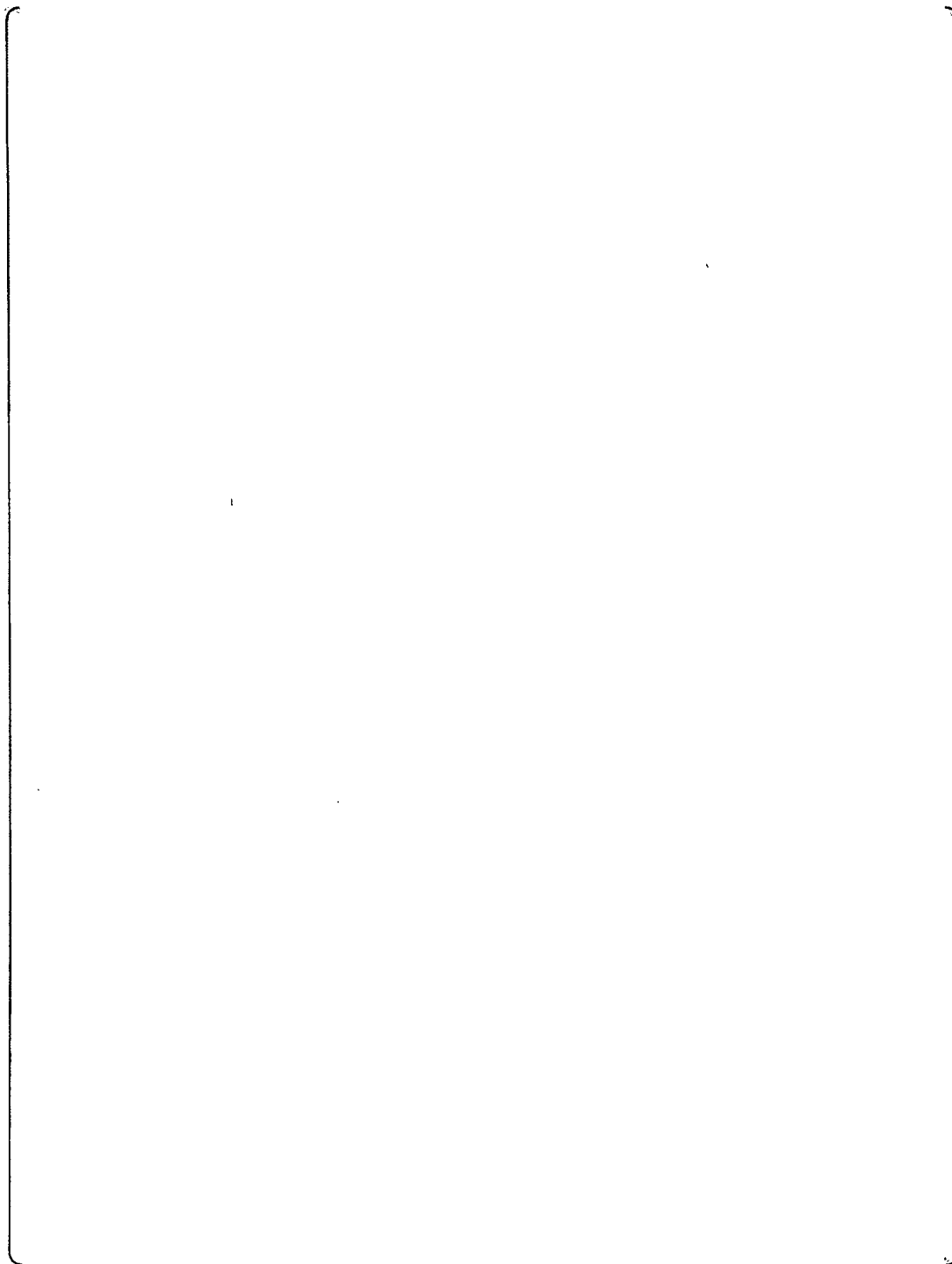


**Figure C.2-7 Axial Geometry for Z3-1**

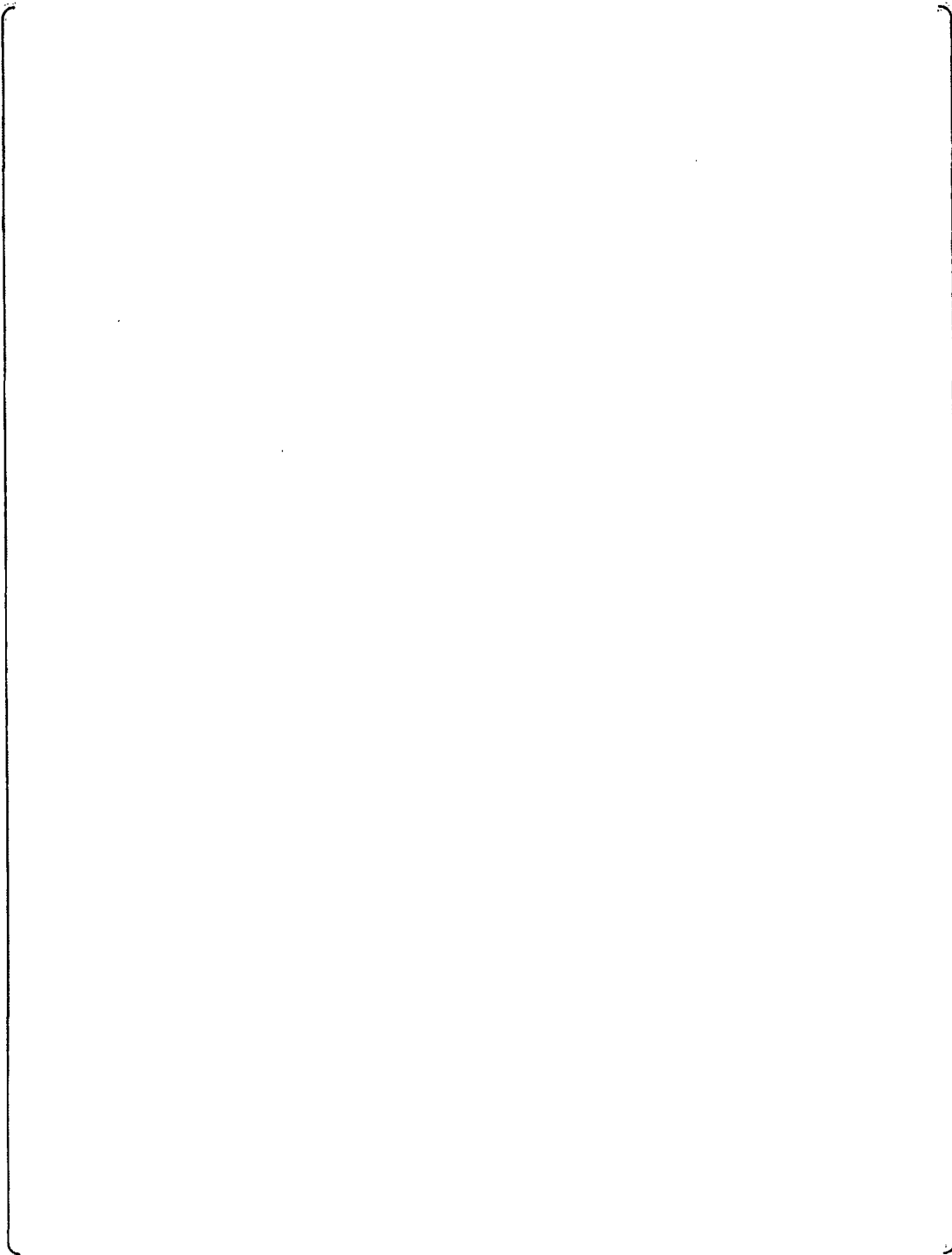


**Figure C.2-8 Axial Geometry for Z3-2**

### C.3 DNB DATA ANALYSES BASED ON WRB-1 AND WRB-2

DNB data analyses based on WRB-1/VIPRE-01M and WRB-2/VIPRE-01M were conducted for both Z2 and Z3 grid spacers. The analysis procedure is corresponding with that in appendix B, i.e., a geometry modeling and model options for calculating void fraction, heat transfer and pressure drop.

#### C.3.1 Statistical Results

Table C.3-1 and C.3-2 show the summary of results for Z2 and Z3 DNB data analyses based on WRB-1. These tables show the number of data points ( $n$ ), the mean of M/P which is the ratio of measured and predicted DNB heat flux ( $m$ ) and the sample standard deviation of M/P ( $s$ ).

Based on the results in Tables C.3-1 and C.3-2, limit DNBR can be evaluated as follows;

$$\text{Limit DNBR}_{(95 \times 95)} = \frac{1}{m - k \cdot S} \quad (\text{C.1})$$

where  $k$  is a one-sided tolerance factor based on 95% confidence level and 95% portion of the population covered, and  $S$  is a modified sample standard deviation of M/P which takes into account the degree of freedom. The detail of statistical procedure to evaluate limit DNBR is shown in Tables C.3-5 and C.3-6. The number of  $k$  can be obtained from Ref.C-1. As a result, it was confirmed that limit DNBRs are [ ] and [ ] for Z2 and Z3 respectively. Therefore, limit DNBR 1.17 can be conservatively applied for the design based on WRB-1/VIPRE-01M.

On the other hand, Tables C.3-3 and C.3-4 show the summary of results for Z2 and Z3 DNB data analyses based on WRB-2. As was evaluated in the above, limit DNBR for Z2 and Z3 were resulted in [ ] and [ ] respectively as shown in Tables C.3-7 and C.3-8. As in the case of WRB-1/VIPRE-01M, limit DNBR 1.17 can be conservatively applied for the design based on WRB-2/VIPRE-01M.

**Table C.3-1 M/P Statistical Result for Z2 based on WRB-1/VIPRE-01M**

Test case	Cell type	Data points (n)	Mean of M/P (m)	Standard deviation of M/P (s)
-----------	-----------	-----------------	-----------------	-------------------------------

**Table C.3-2 M/P Statistical Result for Z3 based on WRB-1/VIPRE-01M**

Test case	Cell type	Data points (n)	Mean of M/P (m)	Standard deviation of M/P (s)
-----------	-----------	-----------------	-----------------	-------------------------------

**Table C.3-3 M/P Statistical Result for Z2 based on WRB-2/VIPRE-01M**

Test case	Cell type	Data points (n)	Mean of M/P (m)	Standard deviation of M/P (s)
-----------	-----------	-----------------	-----------------	-------------------------------

**Table C.3-4 M/P Statistics Result for Z3 based on WRB-2/VIPRE-01M**

Test case	Cell type	Data points (n)	Mean of M/P (m)	Standard deviation of M/P (s)
-----------	-----------	-----------------	-----------------	-------------------------------

**Table C.3-5 Statistical Procedure for Z2 Limit DNBR based on WRB-1**

Number of data	n	
Degree of freedom	N	
Mean of M/P	m	
Standard deviation of M/P	s	
Modified Standard deviation of M/P	S	
Owen's k-factor	k	
Limit DNBR		

\*WRB-1 correlation includes( ) constants.

**Table C.3-6 Statistical Procedure for Z3 Limit DNBR based on WRB-1**

Number of data	n	
Degree of freedom	N	
Mean of M/P	m	
Standard deviation of M/P	s	
Modified Standard deviation of M/P	S	
Owen's k-factor	k	
Limit DNBR		

\*WRB-1 correlation includes( ) constants.

**Table C.3-7 Statistical Procedure for Z2 Limit DNBR based on WRB-2**

Number of data	n	
Degree of freedom	N	
Mean of M/P	m	
Standard deviation of M/P	s	
Modified Standard deviation of M/P	S	
Owen's k-factor	k	
Limit DNBR		

\*WRB-2 correlation includes(    )constants.

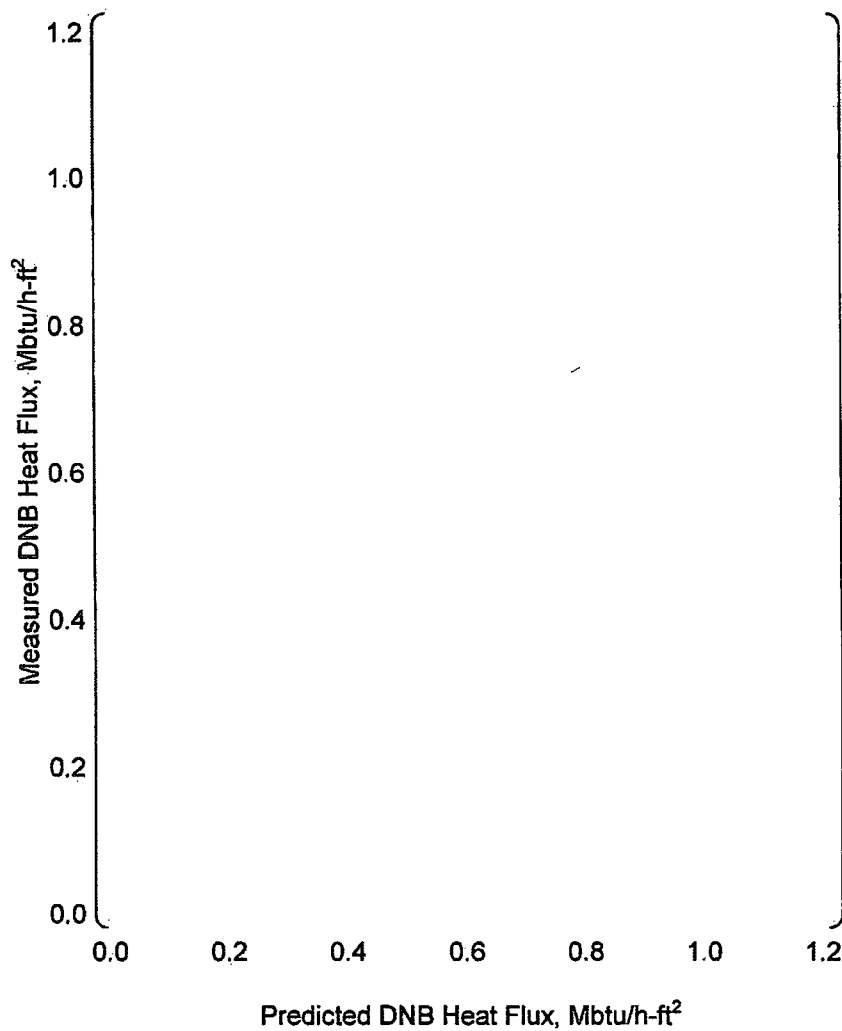
**Table C.3-8 Statistical Procedure for Z3 Limit DNBR based on WRB-2**

Number of data	n	
Degree of freedom	N	
Mean of M/P	m	
Standard deviation of M/P	s	
Modified Standard deviation of M/P	S	
Owen's k-factor	k	
Limit DNBR		

\*WRB-2 correlation includes(    )constants.

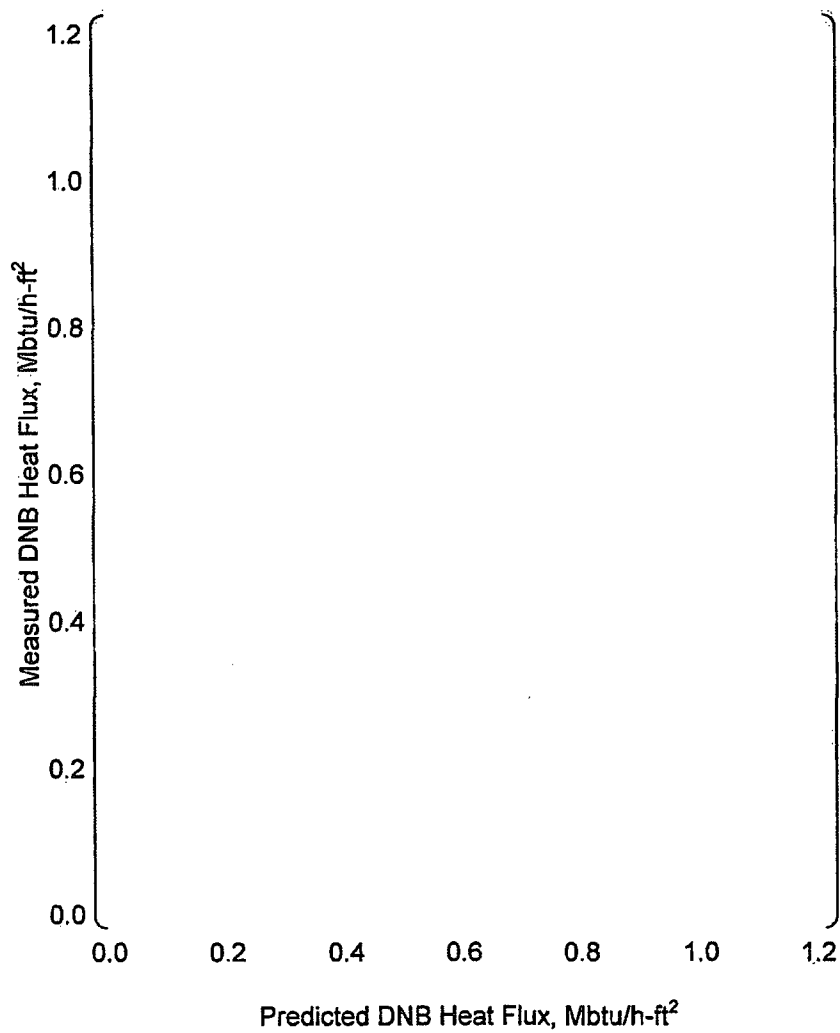
### C.3.2 M/P Data Distribution

Figure C.3-1 to C.3-16 show the data distribution of M/P and the dependency of M/P on local mass flux, system pressure and local quality conditions. Figure C.3-1 to C.3-8 illustrate for data plots based on WRB-1/VIPRE-01M and the others based on WRB-2/VIPRE-01M. These figures show that M/P data plots are uniformly distributed and there is no significant tendency against the fluid conditions. As a result, it was confirmed that both WRB-1 and WRB-2 can well be applied to predict DNB heat fluxes for Z2 and Z3 spacer grids. For reference purposes, DNB data base for Z2 and Z3 are summarized in Attachments C-(a) to C-(d).



**Figure C.3-1 Measured vs. Predicted DNB Heat Flux for Z2 based on WRB-1/VIPRE-01M**





**Figure C.3-2 Measured vs. Predicted DNB Heat Flux for Z3 based on WRB-1/VIPRE-01M**

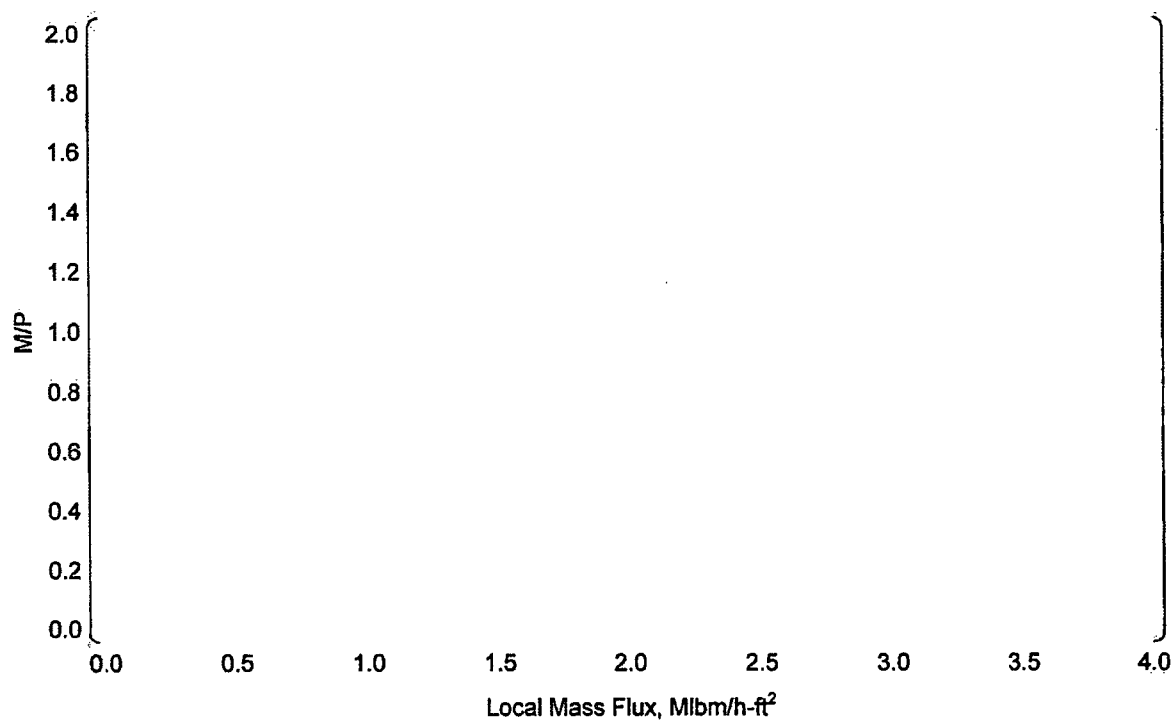


**Figure C.3-3 M/P vs. Local Mass Flux for Z2 based on WRB-1/VIPRE-01M**

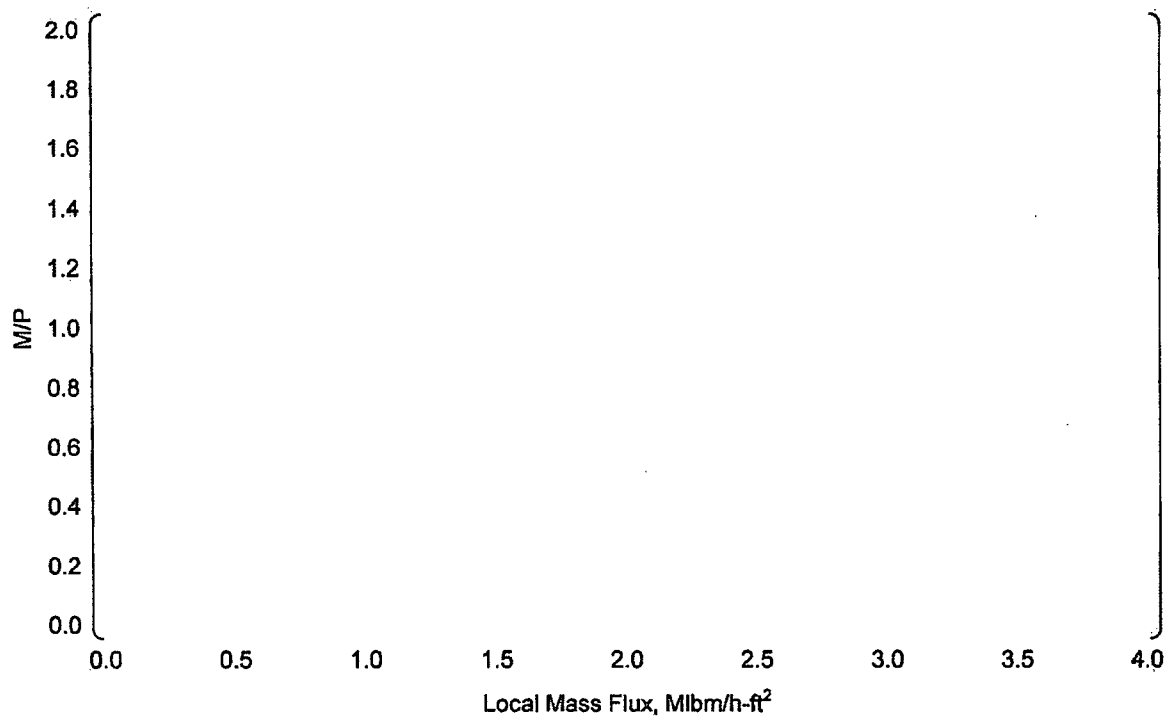


**Figure C.3-4 M/P vs. Local Mass Flux for Z3 based on WRB-1/VIPRE-01M**

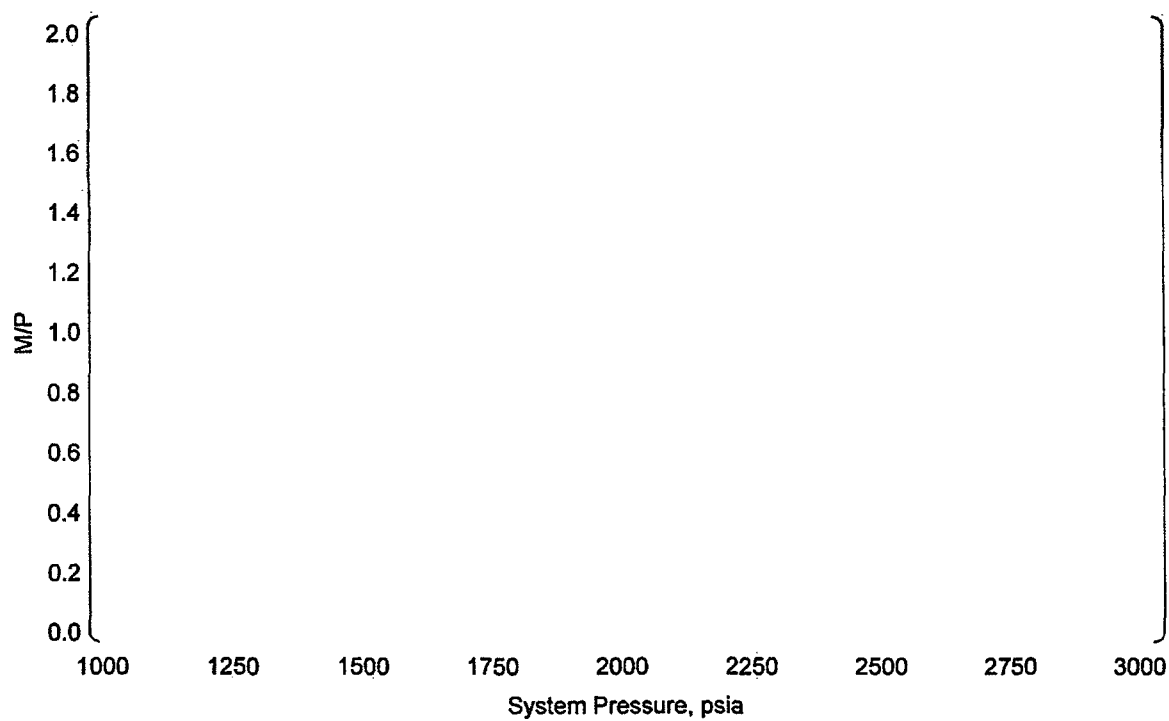


**Figure C.3-5 M/P vs. System Pressure for Z2 based on WRB-1/VIPRE-01M**

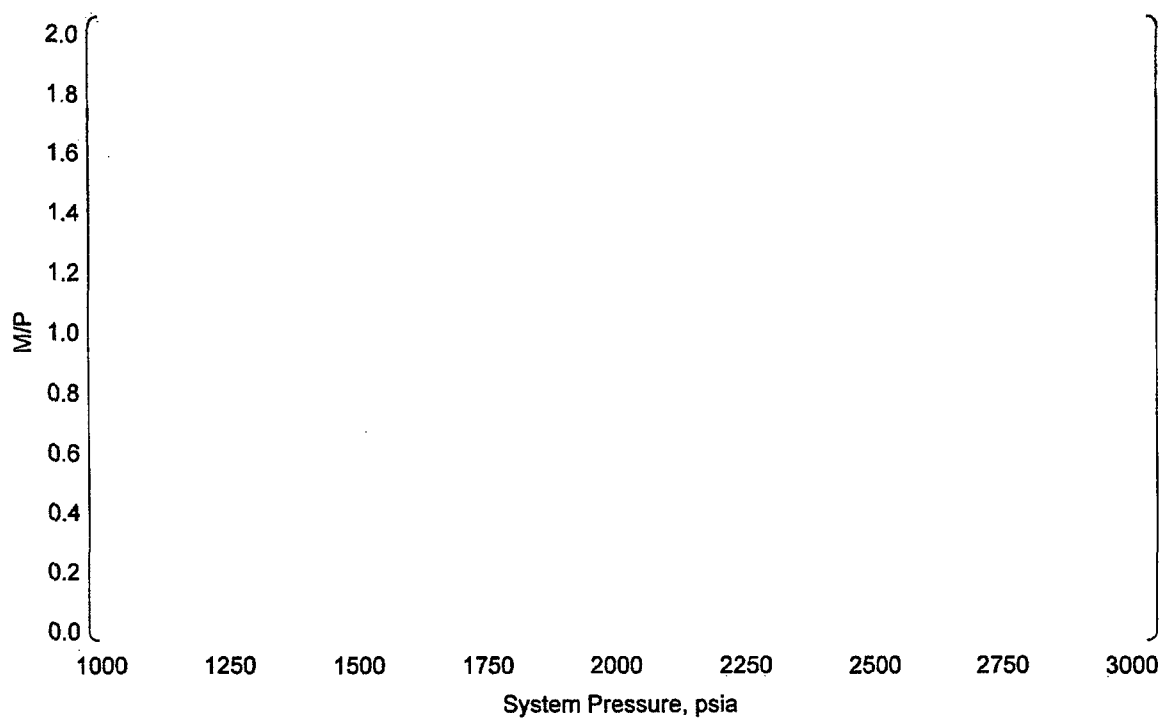


**Figure C.3-6 M/P vs. System Pressure for Z3 based on WRB-1/VIPRE-01M**

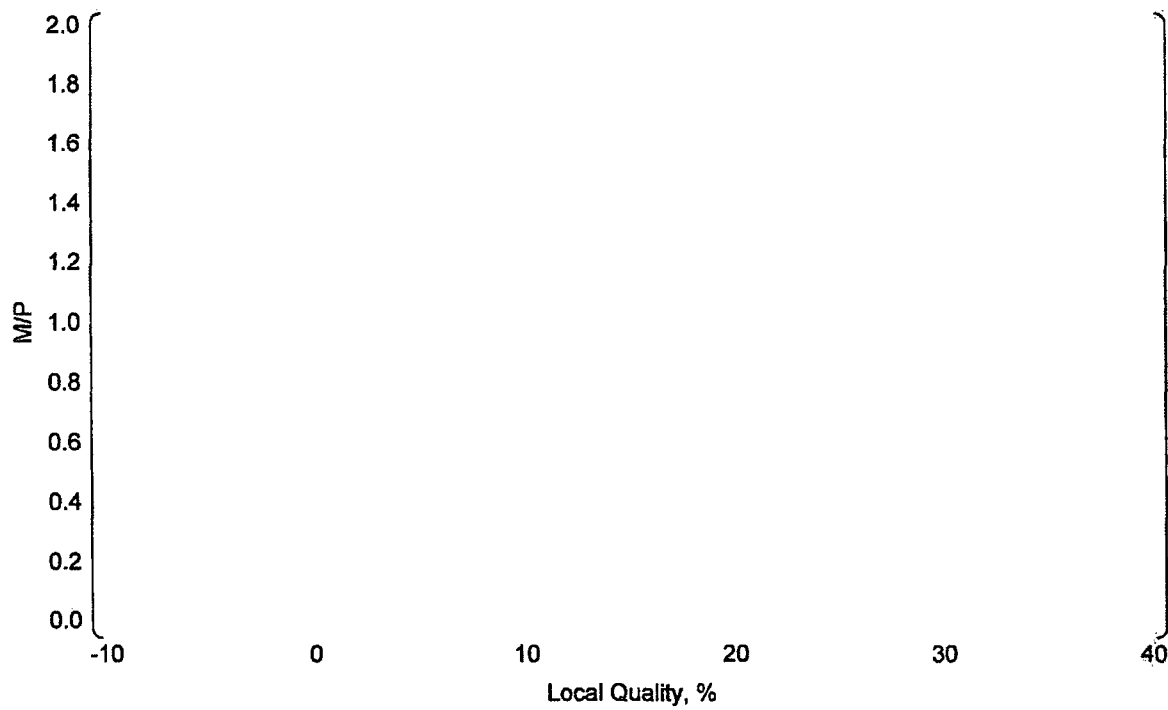


**Figure C.3-7 M/P vs. Local Quality for Z2 based on WRB-1/VIPRE-01M**

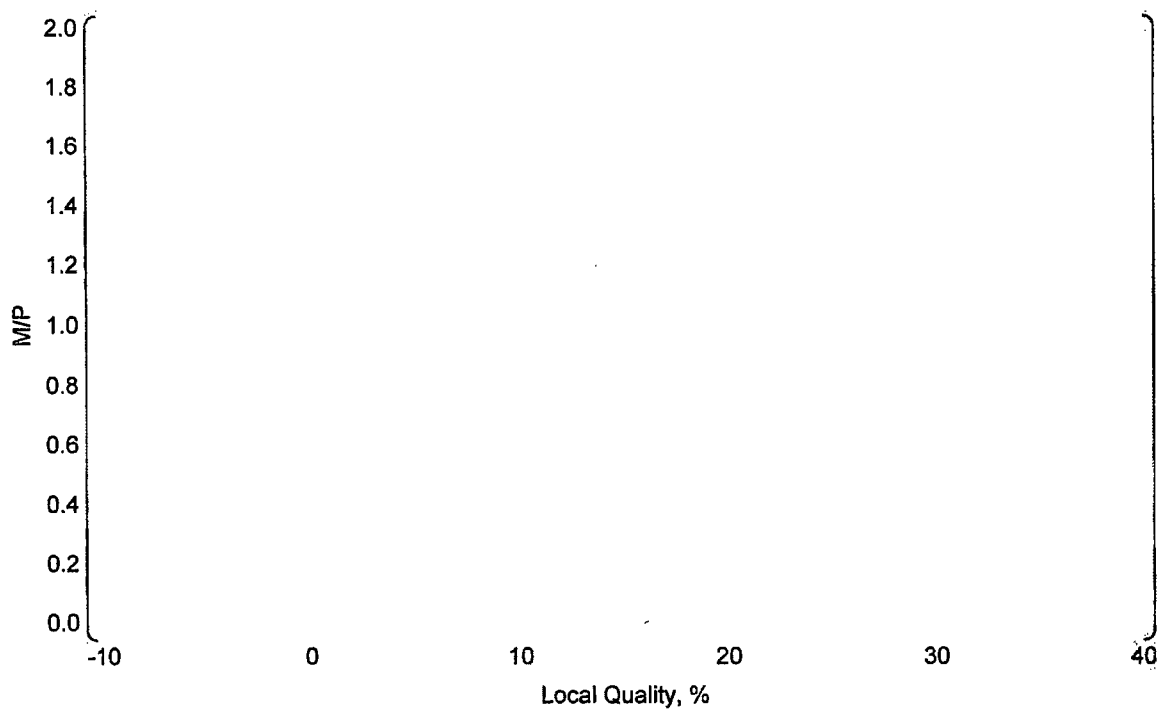


**Figure C.3-8 M/P vs. Local Quality for Z3 based on WRB-1/VIPRE-01M**

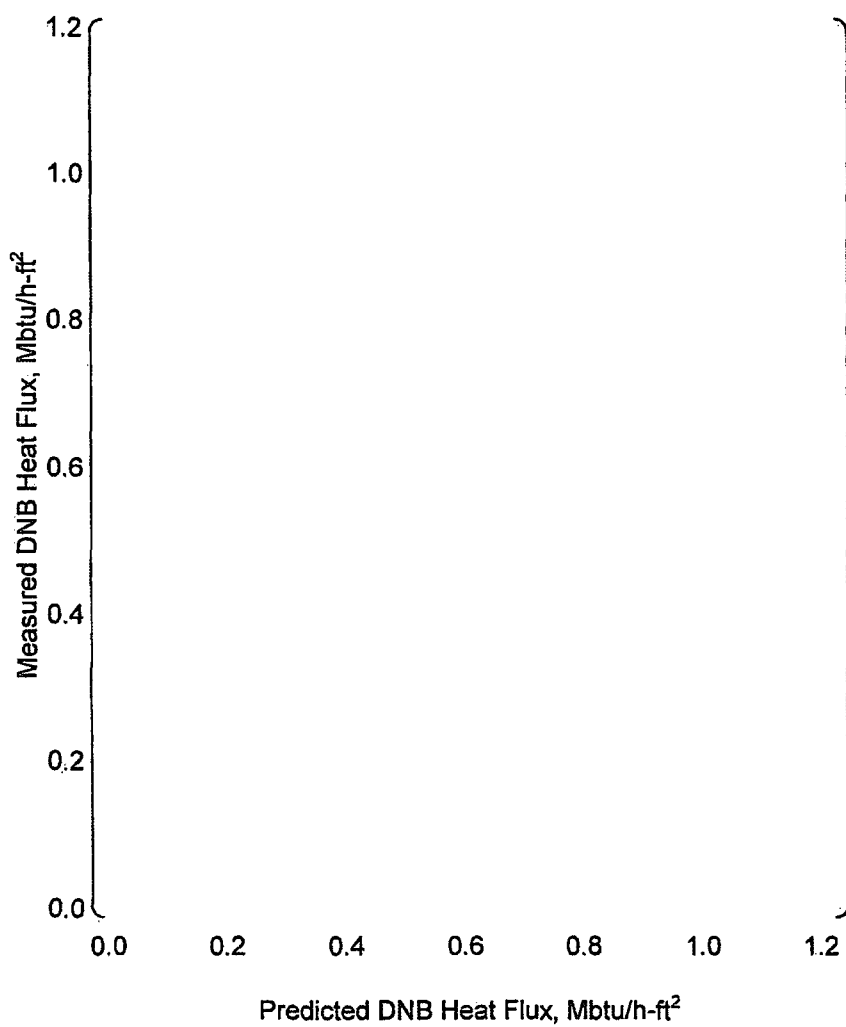
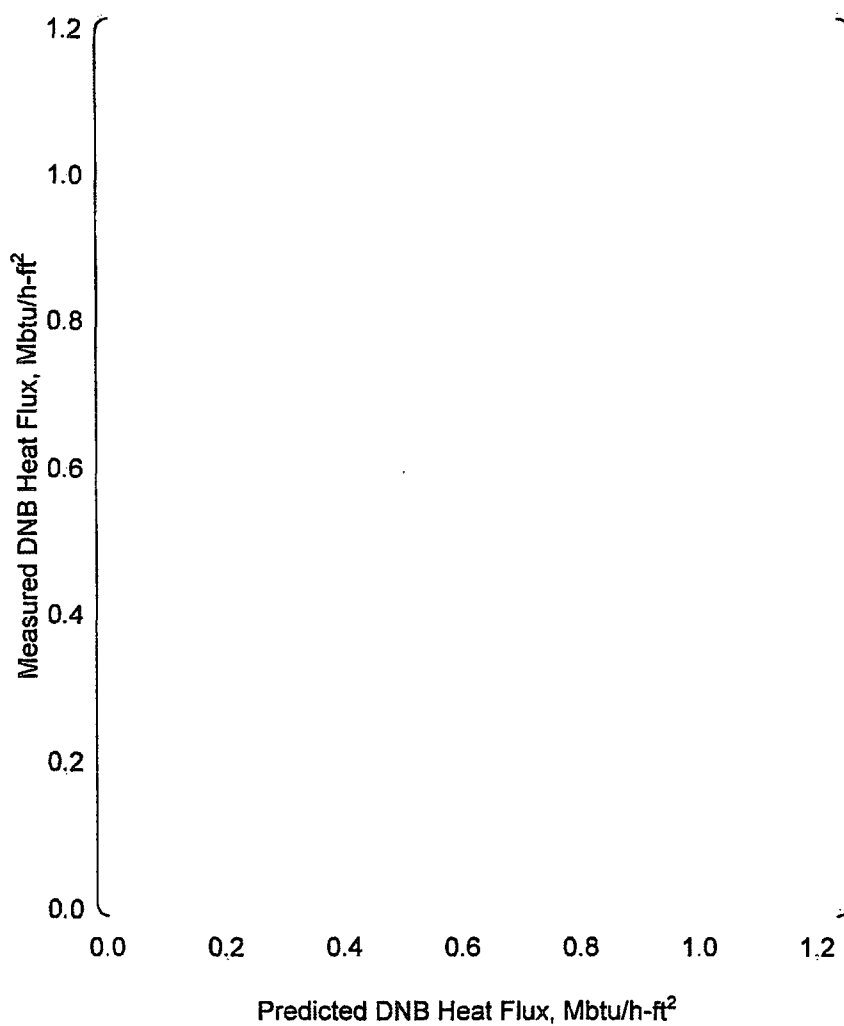
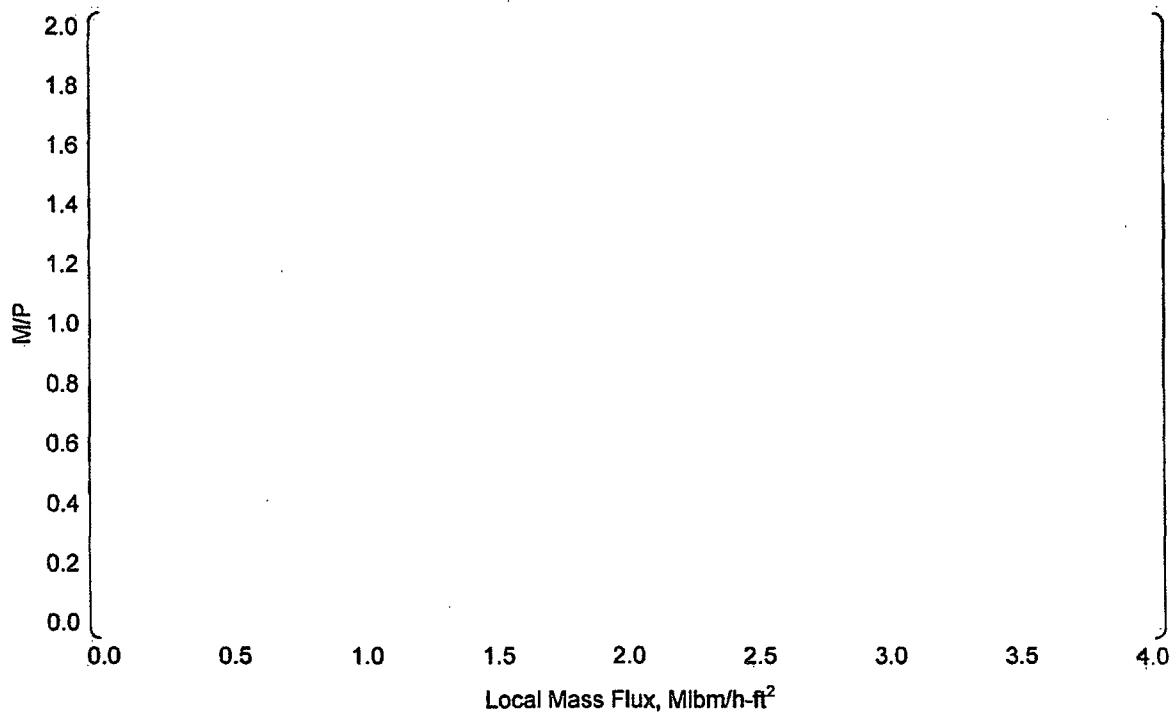


Figure C.3-9 Measured vs. Predicted DNB Heat Flux for Z2 based on WRB-2/VIPRE-01M





**Figure C.3-10 Measured vs. Predicted DNB Heat Flux for Z3 based on WRB-2/VIPRE-01M**



**Figure C.3-11 M/P vs. Local Mass Flux for Z2 based on WRB-2/VIPRE-01M**

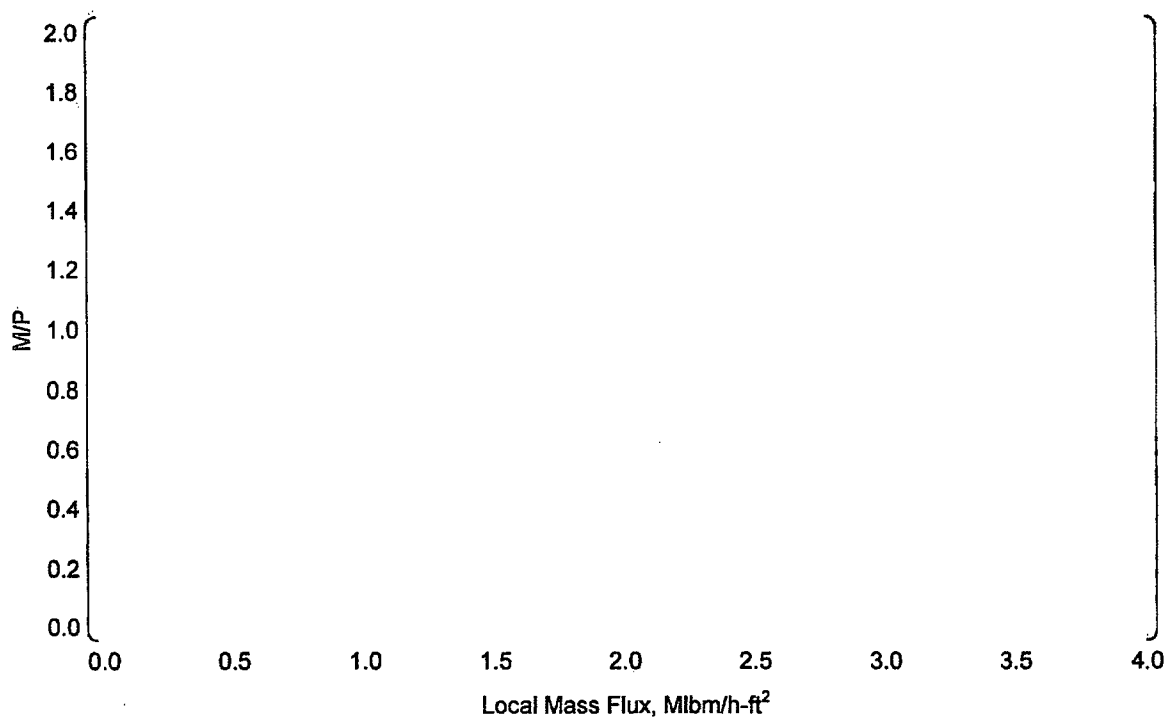


**Figure C.3-12 M/P vs. Local Mass Flux for Z3 based on WRB-2/VIPRE-01M**

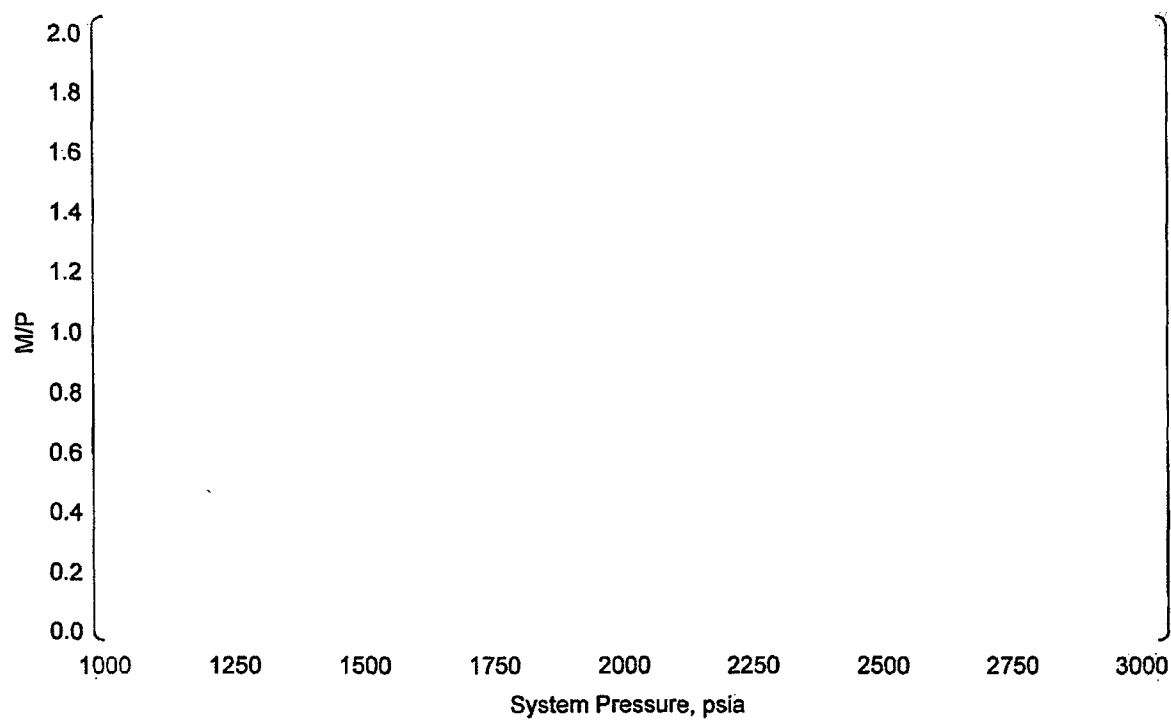


**Figure C.3-13 M/P vs. System Pressure for Z2 based on WRB-2/VIPRE-01M**

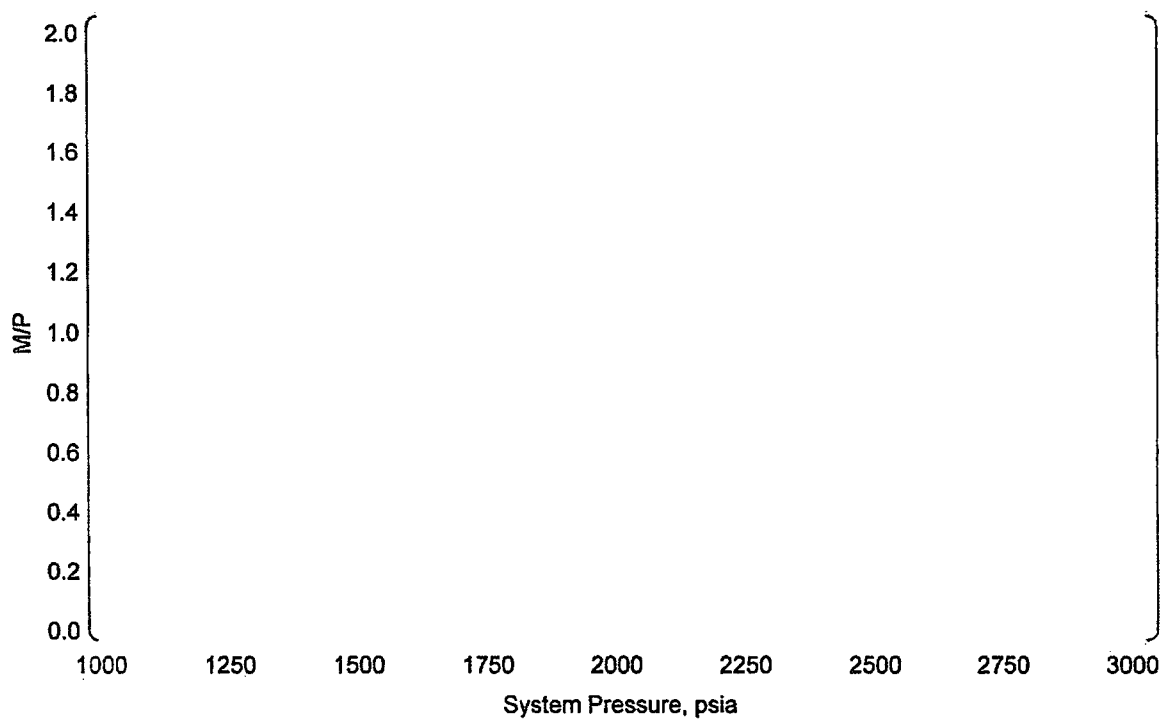


**Figure C.3-14 M/P vs. System Pressure for Z3 based on WRB-2/VIPRE-01M**

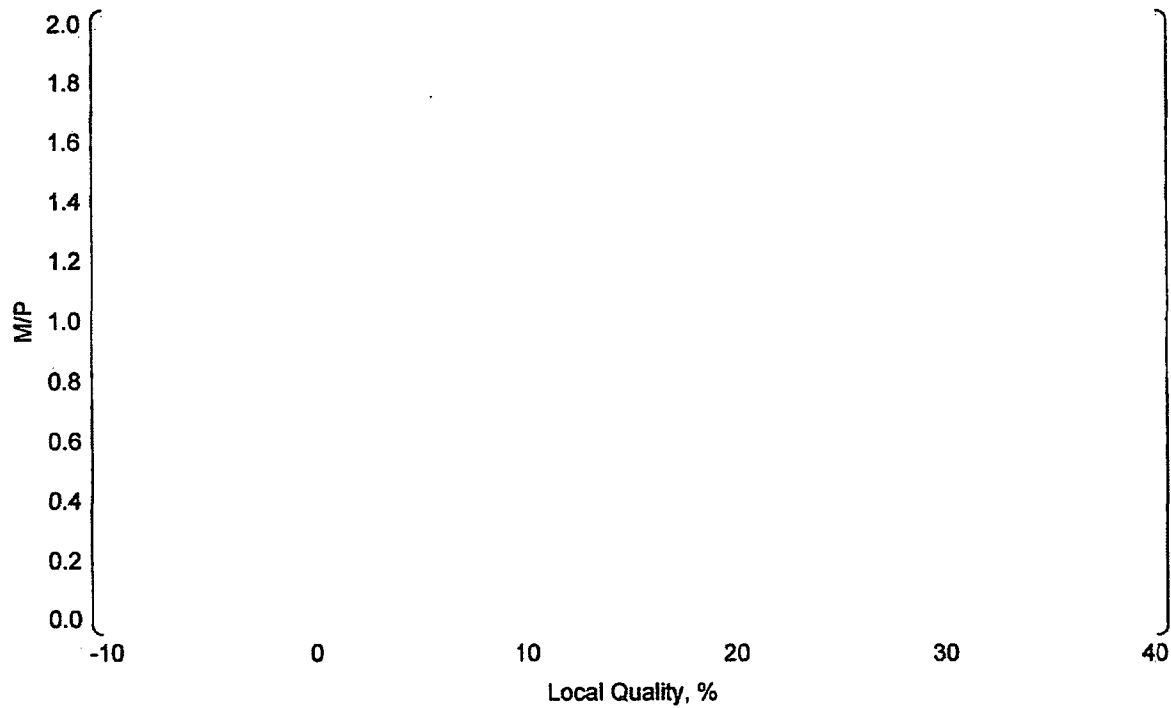


**Figure C.3-15 M/P vs. Local Quality for Z2 based on WRB-2/VIPRE-01M**

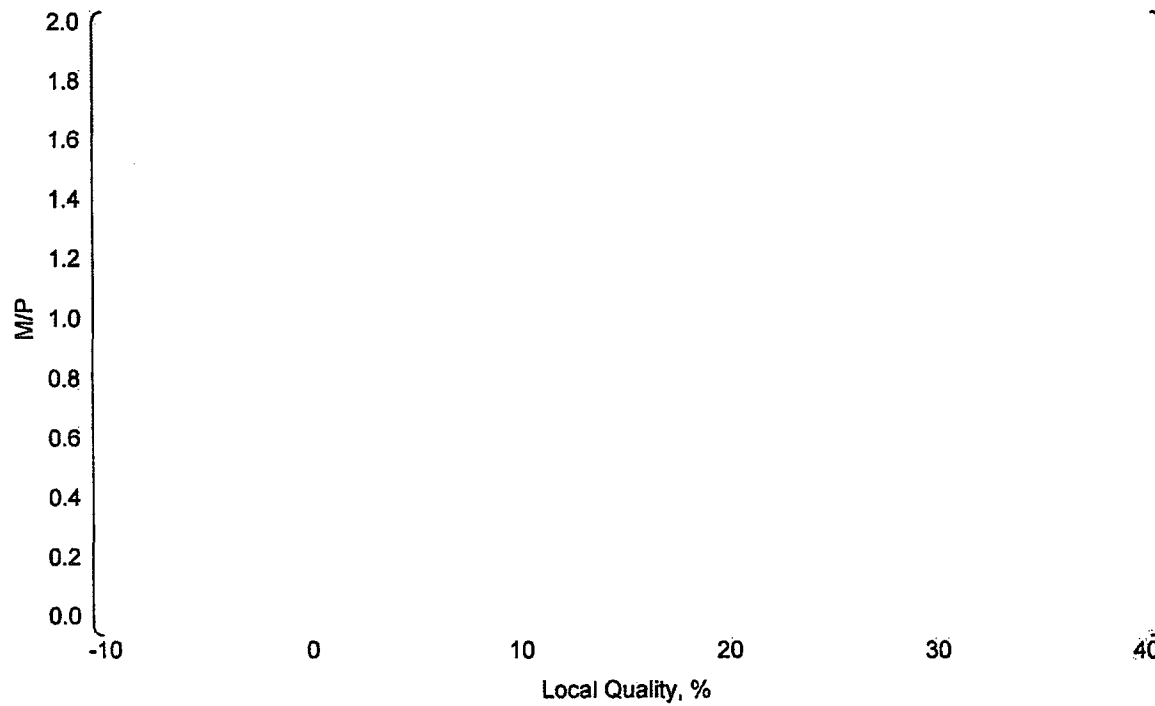


**Figure C.3-16 M/P vs. Local Quality for Z3 based on WRB-2/VIPRE-01M**

---

#### C.4 CONCLUSION

DNB data analyses for Z2 and Z3 were conducted to confirm the applicability of WRB-1 and WRB-2 correlations for the two types of grid spacers. Through the statistical examination, it was confirmed that WRB-1 and WRB-2 can be conservatively applied to predict DNB heat flux for fuel assemblies with either Z2 or Z3 grid spacer using limit DNBR 1.17.

#### C.5 REFERENCE

- C-1. R. E. Odeh & D. B. Owen, "Tables for Nominal Tolerance Limits, Sampling Plans, and Screening", 1980



**ATTACHMENT C-(a) Z2-1 DNB DATA****Table C-(a)-1 Z2-1 DNB DATA BASE (WRB-1/VIPRE-01M)**

Run No.	Outlet Pressure	Inlet Temperature	Inlet Mass Velocity	Local Quality	Local Heat Flux		M/P
-	psia	F	Mlbm/h-ft²	%	Mbtu/h-ft²		-
					Measured	Predicted	

**Table C-(a)-1 (cont.) Z2-1 DNB DATA BASE (WRB-1/VIPRE-01M)**

Run No.	Outlet Pressure	Inlet Temperature	Inlet Mass Velocity	Local Quality	Local Heat Flux		M/P
	psia	F	Mlbm/h-ft <sup>2</sup>	%	Mbtu/h-ft <sup>2</sup>		
					Measured	Predicted	

**Table C-(a)-2 Z2-1 DNB DATA BASE (WRB-2/VIPRE-01M)**

Run No.	Outlet Pressure	Inlet Temperature	Inlet Mass Velocity	Local Quality	Local Heat Flux		M/P
-	psia	F	Mlbm/h-ft <sup>2</sup>	%	Mbtu/h-ft <sup>2</sup>		-
					Measured	Predicted	

**Table C-(a)-2 (cont.) Z2-1 DNB DATA BASE (WRB-2/VIPRE-01M)**

Run No.	Outlet Pressure	Inlet Temperature	Inlet Mass Velocity	Local Quality	Local Heat Flux		M/P
-	psia	F	Mlbm/h-ft <sup>2</sup>	%	Mbtu/h-ft <sup>2</sup>		-
					Measured	Predicted	

**ATTACHMENT C-(b) Z2-2 DNB DATA****Table C-(b)-1 Z2-2 DNB DATA BASE (WRB-1/VIPRE-01M)**

Run No.	Outlet Pressure	Inlet Temperature	Inlet Mass Velocity	Local Quality	Local Heat Flux		M/P
-	psia	F	Mlbm/h-ft <sup>2</sup>	%	Mbtu/h-ft <sup>2</sup>		-
					Measured	Predicted	

**Table C-(b)-1 (cont.) Z2-2 DNB DATA BASE (WRB-1/VIPRE-01M)**

Run No.	Outlet Pressure	Inlet Temperature	Inlet Mass Velocity	Local Quality	Local Heat Flux		M/P
-	psia	F	Mlbm/h-ft <sup>2</sup>	%	Mbtu/h-ft <sup>2</sup>		-
					Measured	Predicted	

Table C-(b)-2 Z2-2 DNB DATA BASE (WRB-2/VIPRE-01M)

Run No.	Outlet Pressure	Inlet Temperature	Inlet Mass Velocity	Local Quality	Local Heat Flux		M/P
-	psia	F	Mlbm/h-ft <sup>2</sup>	%	Mbtu/h-ft <sup>2</sup>		-
					Measured	Predicted	

**Table C-(b)-2 (cont.) Z2-2 DNB DATA BASE (WRB-2/VIPRE-01M)**

Run No.	Outlet Pressure	Inlet Temperature	Inlet Mass Velocity	Local Quality	Local Heat Flux		M/P
-	psia	F	Mlbm/h-ft <sup>2</sup>	%	Mbtu/h-ft <sup>2</sup>		-
					Measured	Predicted	



**ATTACHMENT C-(c) Z3-1 DNB DATA****Table C-(c)-1 Z3-1 DNB DATA BASE (WRB-1/VIPRE-01M)**

Run No.	Outlet Pressure	Inlet Temperature	Inlet Mass Velocity	Local Quality	Local Heat Flux		M/P
-	psia	F	Mibm/h-ft <sup>2</sup>	%	Mbtu/h-ft <sup>2</sup>		-
					Measured	Predicted	

**Table C-(c)-1 (cont.) Z3-1 DNB DATA BASE (WRB-1/VIPRE-01M)**

Run No.	Outlet Pressure	Inlet Temperature	Inlet Mass Velocity	Local Quality	Local Heat Flux		M/P
	psia	F	Mlbm/h-ft <sup>2</sup>	%	Mbtu/h-ft <sup>2</sup>		
					Measured	Predicted	

**Table C-(c)-2 Z3-1 DNB DATA BASE (WRB-2/VIPRE-01M)**

Run No.	Outlet Pressure	Inlet Temperature	Inlet Mass Velocity	Local Quality	Local Heat Flux		M/P
-	psia	F	Mlbm/h-ft <sup>2</sup>	%	Mbtu/h-ft <sup>2</sup>		-
					Measured	Predicted	

**Table C-(c)-2 (cont.) Z3-1 DNB DATA BASE (WRB-2/VIPRE-01M)**

Run No.	Outlet Pressure	Inlet Temperature	Inlet Mass Velocity	Local Quality	Local Heat Flux		M/P
-	psia	F	Mlbm/h-ft <sup>2</sup>	%	Mbtu/h-ft <sup>2</sup>		-
					Measured	Predicted	

**ATTACHMENT C-(d) Z3-2 DNB DATA****Table C-(d)-1 Z3-2 DNB DATA BASE (WRB-1/VIPRE-01M)**

Run No.	Outlet Pressure	Inlet Temperature	Inlet Mass Velocity	Local Quality	Local Heat Flux		M/P
-	psia	F	Mlbm/h-ft <sup>2</sup>	%	Mbtu/h-ft <sup>2</sup>		-
					Measured	Predicted	

Table C-(d)-1 (cont.) Z3-2 DNB DATA BASE (WRB-1/VIPRE-01M)

Run No.	Outlet Pressure	Inlet Temperature	Inlet Mass Velocity	Local Quality	Local Heat Flux		M/P
-	psia	F	Mlbm/h-ft <sup>2</sup>	%	Mbtu/h-ft <sup>2</sup>		-
					Measured	Predicted	

**Table C-(d)-2 Z3-2 DNB DATA BASE (WRB-2/VIPRE-01M)**

Run No.	Outlet Pressure	Inlet Temperature	Inlet Mass Velocity	Local Quality	Local Heat Flux		M/P
-	psia	F	Mlbm/h-ft <sup>2</sup>	%	Mbtu/h-ft <sup>2</sup>		-
					Measured	Predicted	

**Table C-(d)-2 (cont.) Z3-2 DNB DATA BASE (WRB-2/VIPRE-01M)**

Run No.	Outlet Pressure	Inlet Temperature	Inlet Mass Velocity	Local Quality	Local Heat Flux		M/P
-	psia	F	Mlbm/h-ft <sup>2</sup>	%	Mbtu/h-ft <sup>2</sup>		-
					Measured	Predicted	



## APPENDIX D

### FUEL THERMAL PROPERTIES

#### D.1 INTRODUCTION

Fuel thermal properties are important to the determination of initial fuel temperature and transient heat flux in safety analysis. Although VIPRE-01 originally includes thermal properties of  $\text{UO}_2$  and Zircaloy [Ref.D-1], Mitsubishi has introduced the thermal properties used in fuel performance code and other transient analysis codes into VIPRE-01M.

The new thermal property library is mainly based on Westinghouse's standard library for safety analysis [Ref.D-2], and adopts the fuel thermal conductivity of FINE code [Ref.D-3]. It gives almost the same result as that by the original VIPRE-01, except the degradation effect on thermal conductivity of  $\text{UO}_2$  pellet along with burnup. It was verified via the comparisons with FINE code and FACTRAN code.

#### D.2 FUEL PROPERTIES

##### D.2.1 Density

Density of  $\text{UO}_2$  is given as a constant which corresponds to cold dimension, because the VIPRE-01M heat conduction analysis does not consider volume change of fuel caused by thermal expansion and other elastic or plastic deformations.

$$\rho_{\text{UO}_2} |_{\text{VIPRE}} = f_{\text{TD}} \cdot \text{TD}$$

$\rho_{\text{UO}_2}  _{\text{VIPRE}}$	: Density of $\text{UO}_2$ used in VIPRE-01M (lbm/ft <sup>3</sup> )
$f_{\text{TD}}$	: Fraction to theoretical density
TD	: Theoretical density of $\text{UO}_2$ at cold condition (lbm/ft <sup>3</sup> ) = 684 (lbm/ft <sup>3</sup> ) [Ref.D-2]

##### D.2.2 Thermal Conductivity

Thermal conductivity of 95% TD  $\text{UO}_2$  fuel is determined by the following expression. This function is from the FINE code [Ref.D-3]. It takes into consideration the degradation effect with burnup [Ref.D-4].

$$k_{\text{UO}_2 95} = \frac{1}{A + \beta \cdot \text{BU} + B \cdot T} + C \cdot T^3$$

$k_{\text{UO}_2 95}$	: Thermal conductivity for 95% TD fuel (W/cm-K)
BU	: Burnup (MWd/kg $\text{UO}_2$ )

---

$T$	: Temperature (C)
$A$	=11.8
$B$	=0.0238
$C$	= $8.775 \times 10^{-13}$
$\beta$	=0.35

Correction for density is based on Bakker's equation [Ref.D-5].

$$k_{\text{UO}_2} = k_{\text{UO}_2,95} \left( \frac{f_{TD}}{0.95} \right)^{1.7}$$

$k_{\text{UO}_2}$  : Thermal conductivity (W/cm-K)  
 $f_{TD}$  : Fraction to theoretical density

The function is compared with the original function in VIPRE-01 in Figure D.2-1. VIPRE-01M is relatively conservative in high temperature region for fuel temperature analysis.

Burnup and density ( $f_{TD}$ ) for thermal conductivity can be input as a local value for each radial ring of fuel rod analysis. In the surface ring, thermal conductivity of rim region and the remaining region can be evaluated separately using respective density, and then be combined.

### D.2.3 Heat Capacity

Heat capacity of  $\text{UO}_2$  pellet is given in MATPRO-11 [Ref.D-6]. This function is the same as that adopted in VIPRE-01 originally.

$$(\rho C_p)_{\text{UO}_2} |_{\text{VIPRE}} = \rho_{\text{UO}_2} |_{\text{VIPRE}} \left\{ \frac{K_1 \theta^2 \exp(\theta/T)}{T^2 [\exp(\theta/T) - 1]^2} + K_2 T + \frac{K_3 E_D}{RT^2} \exp\left(\frac{-E_D}{RT}\right) \right\}$$

$(\rho C_p)_{\text{UO}_2} |_{\text{VIPRE}}$  : Heat capacity used in VIPRE-01M (J/m<sup>3</sup>-K)  
 $\rho$  : Density (kg/m<sup>3</sup>)  
 $C_p$  : Specific heat (J/kg-K)  
 $R$  : Gas constant (J/mol-K)  
 $K_1$  =296.7 (J/kg-K)  
 $K_2$  = $2.43 \times 10^{-2}$  (J/kg-K<sup>2</sup>),  
 $K_3$  = $8.745 \times 10^7$  (J/kg)  
 $\theta$  =535.285 (K)  
 $E_D$  = $1.577 \times 10^5$  (J/mol)

The function of  $C_p$  is shown in Figure D.2-2.

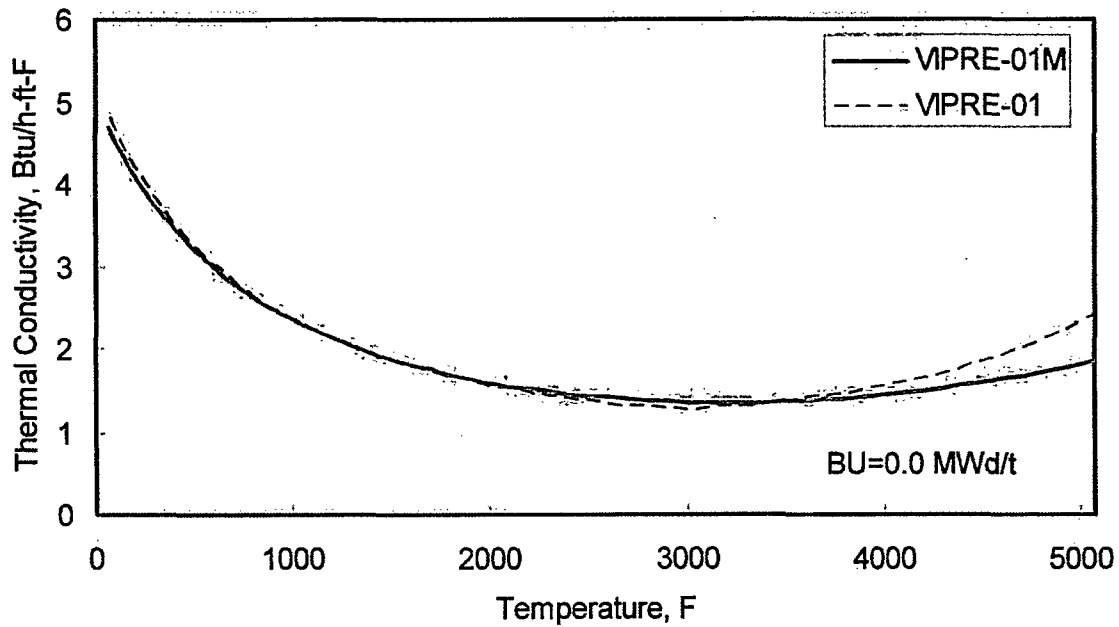


Figure D.2-1 Thermal Conductivity of  $\text{UO}_2$  Fuel

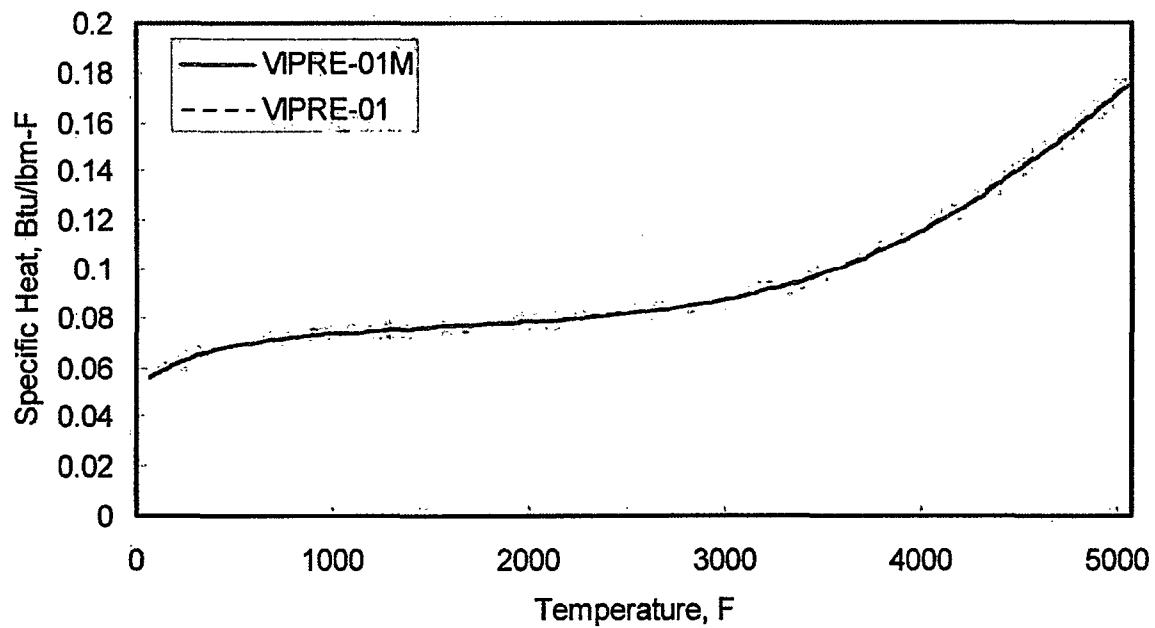


Figure D.2-2 Specific Heat of  $\text{UO}_2$  Fuel

## D.3 CLADDING PROPERTIES

### D.3.1 Density

Density of Zircaloy-4 is given as a constant which corresponds to cold dimension, because the VIPRE-01M heat conduction analysis does not consider volume change of fuel caused by thermal expansion and other elastic or plastic deformations.

The constant density derived [ ] from the equation in Ref.D-2 is used in VIPRE-01M. The value is used also for ZIRLO™ developed by Westinghouse, because ZIRLO™ and Zircaloy-4 have almost same theoretical density and thermal expansion coefficient [Ref.D-7].

$$\rho_{Zr}|_{VIPRE} = \left\{ \frac{410.1}{1 + 9.66 \times 10^{-6} T} \right\}$$

$\rho_{Zr}|_{VIPRE}$  : Density used in VIPRE-01M (lbm/ft<sup>3</sup>)  
 $T$  : Temperature (F)

### D.3.2 Thermal Conductivity

Thermal conductivity of Zircaloy-4 is from Ref.D-2. It can be used also for ZIRLO™ [Ref.D-7].

$$k_{Zr} = \text{Max}\{7.404 + 0.0029T, 5.621 + 0.0053T\}$$

$k_{Zr}$  : Thermal conductivity (Btu/ft-h-F)  
 $T$  : Temperature (F)

Comparison with the original function used in VIPRE-01 is shown in Figure D.3-1. Both expressions give very close result.


### D.3.3 Heat Capacity

Heat capacity of Zircaloy-4 is from Ref.D-2.

$$(\rho C_p)|_{VIPRE} = \left[ \frac{0.00012 T^2 + 0.00012 T + 0.00012}{1 + 9.66 \times 10^{-6} T} \right]$$

$(\rho C_p)|_{VIPRE}$  : Heat capacity used in VIPRE-01M (Btu/ft<sup>3</sup>-F)  
 $\rho|_{VIPRE}$  : Density used in VIPRE-01M (lbm/ft<sup>3</sup>)  
 $C_p$  : Specific heat (Btu/lbm-F)  
 $T$  : Temperature (F)

Regarding ZIRLO™, it has similar property, but phase transformation temperature shows small difference from that of Zircaloy-4 [Ref.D-7].



The original VIPRE-01 function for Zircaloy-4, the VIPRE-01M function for Zircaloy-4 and ZIRLO™ are presented in Figure D.3-2.

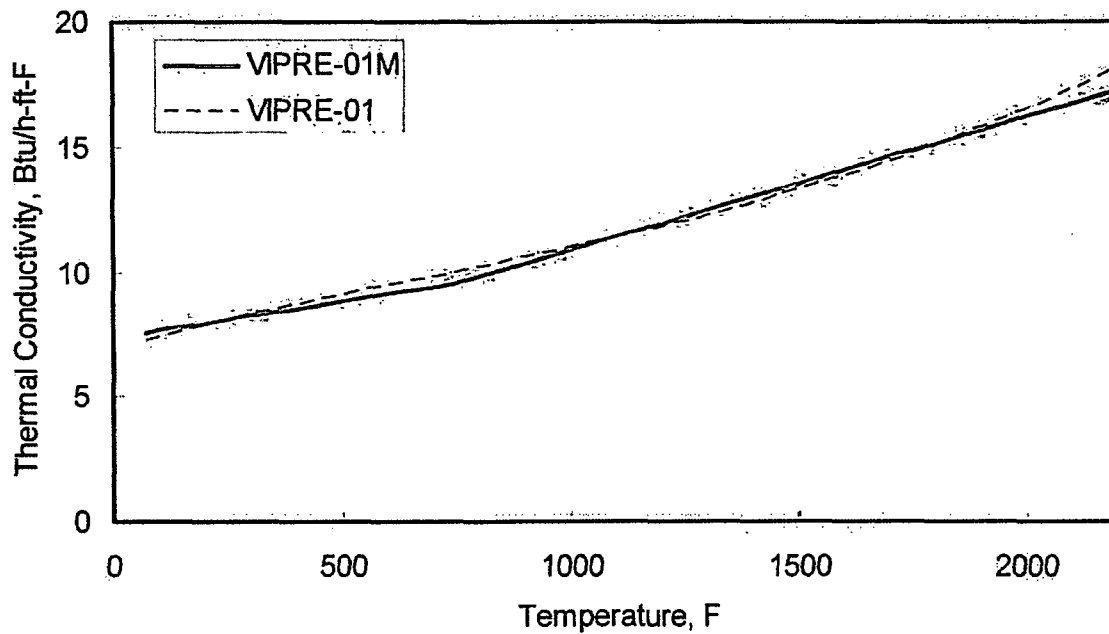


Figure D.3-1 Thermal Conductivity of Zircaloy-4

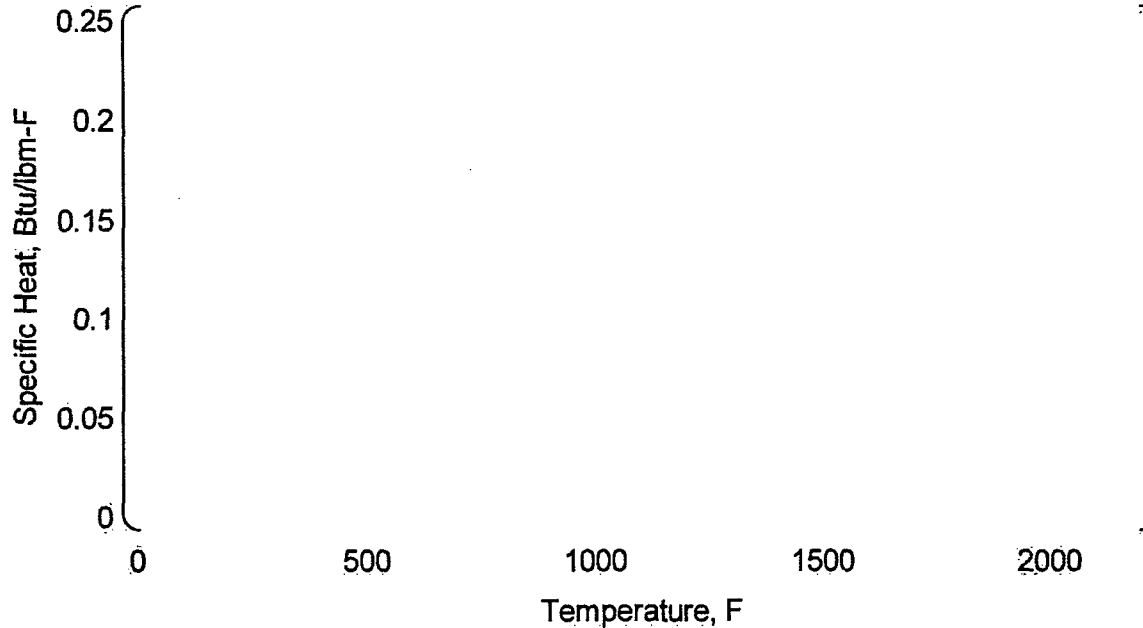


Figure D.3-2 Specific Heat of Zircaloy-4 and ZIRLO™

## D.4 ZrO<sub>2</sub> PROPERTIES

### D.4.1 Density

Density of ZrO<sub>2</sub> is usually given as a constant, because the VIPRE-01M analysis does not consider volume change at any deformation and oxidation.

Density of ZrO<sub>2</sub> is given by Ref.D-2

$$\rho_{ZrO_2} = 347$$

$\rho_{ZrO_2}$  : Density of ZrO<sub>2</sub> (lbm/ft<sup>3</sup>)

However the above value is not used, because VIPRE-01M does not consider the volume change due to a reaction from Zr to ZrO<sub>2</sub>. The above value is used for the correction of thermal conductivity as described in D.4.2.

### D.4.2 Thermal Conductivity

Thermal conductivity of ZrO<sub>2</sub> is given by the following equation in Ref.D-2.

$$k_{ZrO_2} = \left[ \begin{array}{l} \\ k_{ZrO_2} \\ T \end{array} \right]$$

$k_{ZrO_2}$  : Thermal conductivity of ZrO<sub>2</sub> (Btu/ft-h-F)  
 $T$  : Temperature (F)

Shape of the function is illustrated in Figure D.4-1.

### D.4.3 Heat Capacity

Heat capacity of  $ZrO_2$  is from Ref.D-2.

$$\rho C_p_{ZrO_2} \big|_{WPRE} = \left[ \begin{array}{l} \rho \\ C_p \\ T \end{array} \right]$$

$\rho$  : Density (lbm/ft<sup>3</sup>)  
 $C_p$  : Specific heat (Btu/lbm-F)  
 $T$  : Temperature (F)

The specific heat function is illustrated in Figure D.4-2.



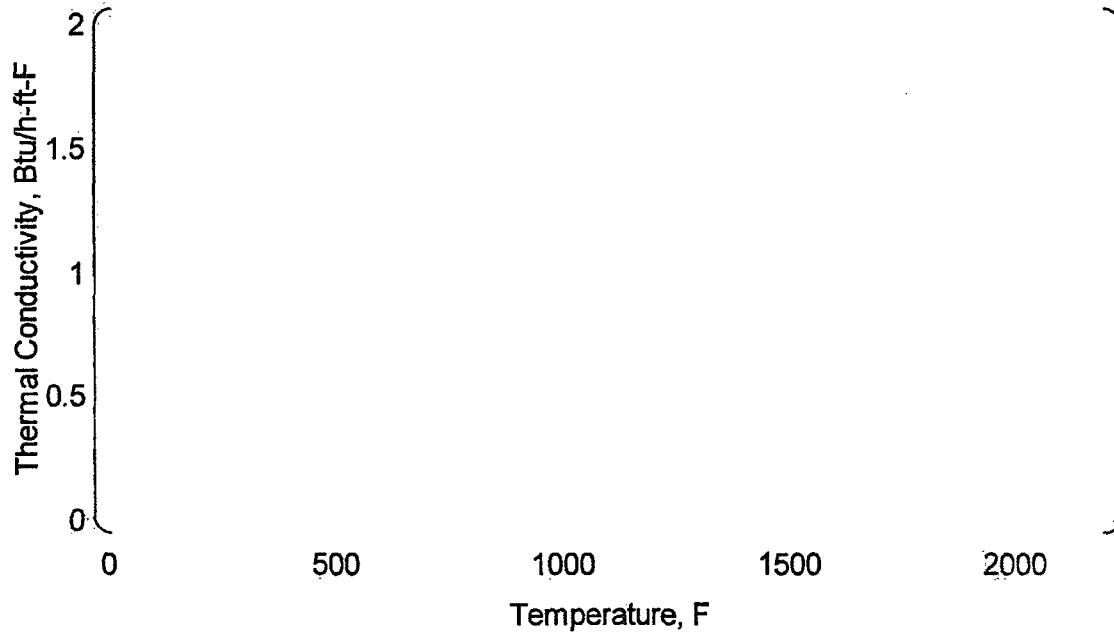


Figure D.4-1 Thermal Conductivity of  $ZrO_2$

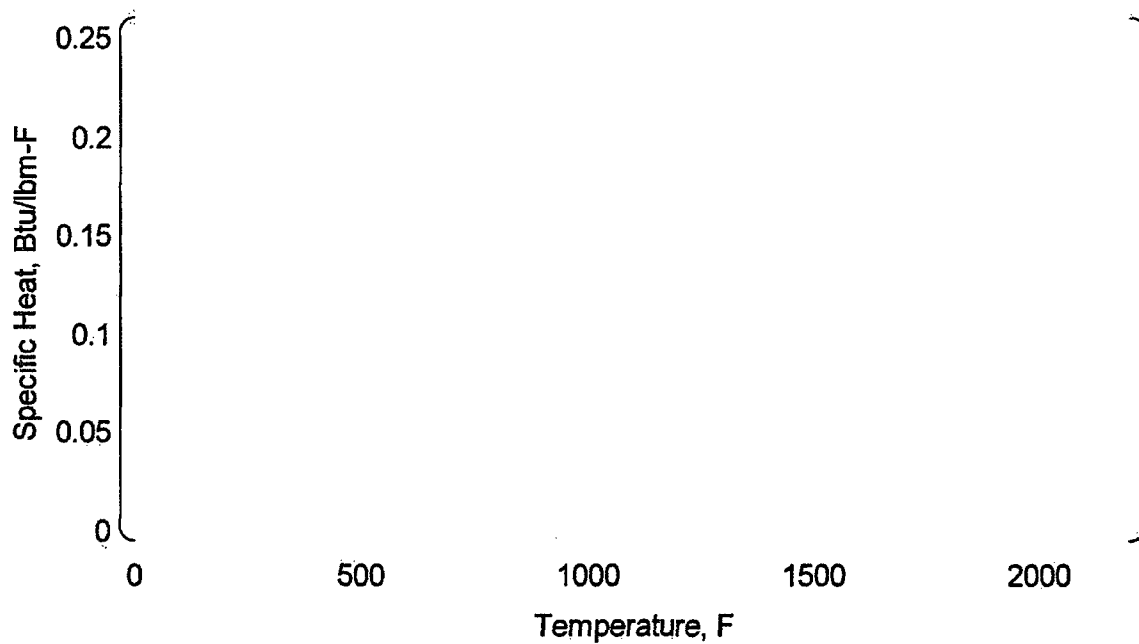


Figure D.4-2 Specific Heat of  $ZrO_2$

## D.5 REFERENCES

- D-1. C. W. Stewart, et al., "VIPRE-01: A Thermal-Hydraulic Code for Reactor Cores, Volume 1 (Revision 4): Mathematical Modeling", NP-2511-CCM-A, Electric Power Research Institute (EPRI), February 2001.
- D-2. F. M. Bordelon, et al., "LOCTA-IV Program: Loss-of-coolant Transient Analysis", WCAP-8301, June 1974
- D-3. T. Shimomura, et al., "Fuel System Design Criteria and Methodology", MUAP-07008-P, Mitsubishi Heavy Industries, 2007
- D-4. W. Wiesenack, "Assessment of  $\text{UO}_2$  Conductivity Degradation Based on In-Pile Temperature Data", ANS 1997 International Topical Meeting on LWR Fuel Performance, March 1997, Portland, Oregon
- D-5. K. Bakker et al., "Determination of a Porosity Correction Factor for the Thermal Conductivity of Irradiated  $\text{UO}_2$  Fuel by Means of the Finite Element Method", Journal of Nuclear Materials, 226, 1995, pp.128-143
- D-6. D. L. Hagarman, G. A. Reymann and R. E. Mason, "MATPRO - Version 11 (Revision 2): A Handbook of Material Properties for Use in the Analysis of Light Water Reactor Fuel Rod Behavior", NUREG/CR-0497 TREE-1280, Revision 2, Idaho National Engineering Laboratories, August 1980
- D-7. S. L. Davidson and D.L.Nuhfer, "VANTAGE+ Fuel Assembly Reference Core Report", WCAP-12610, June 1990